AD NUMBER: AD0823654

LIMITATION CHANGES

TO:

Approved for public release; distribution is unlimited.

FROM:

Distribution authorized to U.S. Defense agencies only; Administrative/Operational Use; 31 DEC 1960. Other requests shall be referred to the Army Office of the Chief of Engineers, Military Construction, Washington, DC 20315

AUTHORITY

OCE, D/A LTR, 24 MAR 1975

AD

OCE NEMP PROGRAM

Development of Criteria for Protection of NIKE-X Power Plant and Facilities Electrical Systems Against Nuclear Electromagnetic Pulse Effects

MAGNETICALLY INDUCED VOLTAGES ON CONDUCTORS WITHIN CONDUITS AND CABLES

3 November 1967

Submitted by:

E. R. UHLIG

Placed by:

Military Construction
Office of the Chief of Engineers
Department of the Army
Washington, D.C. 20315

The findings in this report are not to be construed as an official Department of the Army position unless so designated by other authorized documents.

CONTRACT NUMBER DA-49-129-ENG-543

GENERAL ELECTRIC COMPANY
PITTSFIELD, MASS.

Unclassified
Security Classification

DOCUMENT CONTROL DATA - R&D
(Security classification of title, body of abstract and indexing annotation must be entered when the overall report is classified)

1. ORIGINATING ACTIVITY (Corporate author)
General Electric Company
100 Woodlawn Avenue
Pittsfield, Massachusetts 01201

2a. REPORT SECURITY CLASSIFICATION
Unclassified

2b. GROUP

3. REPORT TITLE OCE NEMP Program, Development of Criteria for Protection of NIKE-X Power Plant and Facilities Electrical Systems Against Nuclear Electromagnetic Pulse Effects, Magnetically Induced Voltages on Conductors within Conduits and Cables

4. DESCRIPTIVE NOTES *(Type of report and inclusive dates)*
Final Report, 5 August 1965 - 1 September 1967

5. AUTHOR(S) *(Last name, first name, initial)*
Brustle, H. H.
Walko, L. C.

6. REPORT DATE	7a. TOTAL NO. OF PAGES	7b. NO. OF REFS
3 November 1967	104	3

8a. CONTRACT OR GRANT NO.	9a. ORIGINATOR'S REPORT NUMBER(S)
DA-49-129-ENG-543	67U10
b. PROJECT NO.	
c.	9b. OTHER REPORT NO(S) *(Any other numbers that may be assigned this report)* None
d.	

10. AVAILABILITY/LIMITATION NOTICES
Each transmittal of this document outside the Department of Defense must have prior approval of Millitary Construction, Office of the Chief of Engineers, Department of the Army, Washington, D. C. 20315

11. SUPPLEMENTARY NOTES	12. SPONSORING MILITARY ACTIVITY
None	Military Construction, OCE Department of the Army Washington, D. C. 20315

13. ABSTRACT

This document describes a series of tests to determine the magnetically induced voltages on conductors within conduit as influenced by such parameters as conductor position, conduit joints, bends, diameter, wall thickness, length, material, etc.

Other raceways such as flexible conduit, armor sheathed power cable, flexible couplings were also evaluated for shielding effectiveness.

DD FORM 1 JAN 64 1473

Unclassified
Security Classification

KEY WORDS	LINK A		LINK B		LINK C	
	ROLE	WT	ROLE	WT	ROLE	WT
EMP Effects Shielding Power Systems Protection						

INSTRUCTIONS

1. ORIGINATING ACTIVITY: Enter the name and address of the contractor, subcontractor, grantee, Department of Defense activity or other organization *(corporate author)* issuing the report.

2a. REPORT SECURITY CLASSIFICATION: Enter the overall security classification of the report. Indicate whether "Restricted Data" is included. Marking is to be in accordance with appropriate security regulations.

2b. GROUP: Automatic downgrading is specified in DoD Directive 5200.10 and Armed Forces Industrial Manual. Enter the group number. Also, when applicable, show that optional markings have been used for Group 3 and Group 4 as authorized.

3. REPORT TITLE: Enter the complete report title in all capital letters. Titles in all cases should be unclassified. If a meaningful title cannot be selected without classification, show title classification in all capitals in parenthesis immediately following the title.

4. DESCRIPTIVE NOTES: If appropriate, enter the type of report, e.g., interim, progress, summary, annual, or final. Give the inclusive dates when a specific reporting period is covered.

5. AUTHOR(S): Enter the name(s) of author(s) as shown on or in the report. Enter last name, first name, middle initial. If military, show rank and branch of service. The name of the principal author is an absolute minimum requirement.

6. REPORT DATE: Enter the date of the report as day, month, year; or month, year. If more than one date appears on the report, use date of publication.

7a. TOTAL NUMBER OF PAGES: The total page count should follow normal pagination procedures, i.e., enter the number of pages containing information.

7b. NUMBER OF REFERENCES: Enter the total number of references cited in the report.

8a. CONTRACT OR GRANT NUMBER: If appropriate, enter the applicable number of the contract or grant under which the report was written.

8b, 8c, & 8d. PROJECT NUMBER: Enter the appropriate military department identification, such as project number, subproject number, system numbers, task number, etc.

9a. ORIGINATOR'S REPORT NUMBER(S): Enter the official report number by which the document will be identified and controlled by the originating activity. This number must be unique to this report.

9b. OTHER REPORT NUMBER(S): If the report has been assigned any other report numbers *(either by the originator or by the sponsor)*, also enter this number(s).

10. AVAILABILITY/LIMITATION NOTICES: Enter any limitations on further dissemination of the report, other than those imposed by security classification, using standard statements such as:

(1) "Qualified requesters may obtain copies of this report from DDC."

(2) "Foreign announcement and dissemination of this report by DDC is not authorized."

(3) "U. S. Government agencies may obtain copies of this report directly from DDC. Other qualified DDC users shall request through _____."

(4) "U. S. military agencies may obtain copies of this report directly from DDC. Other qualified users shall request through _____."

(5) "All distribution of this report is controlled. Qualified DDC users shall request through _____."

If the report has been furnished to the Office of Technical Services, Department of Commerce, for sale to the public, indicate this fact and enter the price, if known.

11. SUPPLEMENTARY NOTES: Use for additional explanatory notes.

12. SPONSORING MILITARY ACTIVITY: Enter the name of the departmental project office or laboratory sponsoring *(paying for)* the research and development. Include address.

13. ABSTRACT: Enter an abstract giving a brief and factual summary of the document indicative of the report, even though it may also appear elsewhere in the body of the technical report. If additional space is required, a continuation sheet shall be attached.

It is highly desirable that the abstract of classified reports be unclassified. Each paragraph of the abstract shall end with an indication of the military security classification of the information in the paragraph, represented as *(TS)*, *(S)*, *(C)*, or *(U)*.

There is no limitation on the length of the abstract. However, the suggested length is from 150 to 225 words.

14. KEY WORDS: Key words are technically meaningful terms or short phrases that characterize a report and may be used as index entries for cataloging the report. Key words must be selected so that no security classification is required. Identifiers, such as equipment model designation, trade name, military project code name, geographic location, may be used as key words but will be followed by an indication of technical context. The assignment of links, rules, and weights is optional.

Report No. 67U10

OCE NEMP PROGRAM

Development of Criteria for Protection of NIKE-X Power Plant and Facilities Electrical Systems Against Nuclear Electromagnetic Pulse Effects

MAGNETICALLY INDUCED VOLTAGES ON CONDUCTORS WITHIN CONDUITS AND CABLES

3 November 1967

Report by:

H. H. BRUSTLE L. C. WALKO

Submitted by:

E. R. UHLIG

Placed by:

Military Construction
Office of the Chief of Engineers
Department of the Army
Washington, D.C. 20315

CONTRACT NUMBER DA-49-129-ENG-543

GENERAL ELECTRIC COMPANY
PITTSFIELD, MASS.

TABLE OF CONTENTS

Table of Contents
- 2 -

LIST OF ILLUSTRATIONS

List of Illustrations

List of Illustrations
- 3 -

LIST OF TABLES

1.0 INTRODUCTION AND OBJECT OF REPORT

The OCE program to develop design criteria for protection of NIKE-X power plant and facilities against NEMP has entailed a diverse testing program in support of the criteria effort. One phase of this testing effort entailed the evaluation of the shielding effectiveness of various metal raceways for electrical wiring such as conduits, etc. This report will summarize the pertinent results of this phase of the testing program which have direct applicability in the 31 March 1967 Status Report.

The material for this summary report has been taken from three sources: "Conductor Voltages Caused by Pulse Currents Flowing in a Steel Conduit, Part I" dated 5 August 1965; Part II of this series reported 5 January 1966; and a Technical Memorandum on the same subject reported 30 June 1967.

2.0 EXPERIMENT OBJECTIVES

The purposes of these experiments were:

a. to obtain data on the relationship between the pulse current flowing in a conduit and the resultant pulse voltage generated on wiring within the conduit,

b. to compare the time response wave form of the applied current to the resultant voltage time response wave form measured on the conductors,

c. to determine the influence of such factors as conduit joints, bends, diameter, wall thickness, length, material, etc. on induced conductor voltages within the conduit,

d. to determine the degradation in shielding effectiveness of rigid steel conduit when used in conjunction with flexible bellows,

e. to determine the comparative shielding effectiveness between aluminum armored power cable and rigid steel conduit,

f. to correlate the induced voltage wave forms from injected pulse current in conduit and H-field produced pulse current.

3.0 TEST AREA AND SETUP

The tests described in this report were made in two different test areas. One area was unshielded requiring the instrumentation to be housed in a shielded cage. The other area was completely shielded with the instrumentation outside the shielded area. The instrumentation noise level of the two testing techniques was similar because in either case the measuring system shielding is similar. The measurement system and its shielding is shown in Figure 1 and Figure 2. For conductor-to-conduit tests the measuring impedance was 75 ohms; for conductor-to-conductor tests the measuring impedance between conductors was 100 ohms.

3.1 Injected Current Tests

For these tests the current generator was directly connected to the conduit configuration under tests and the pulse current was forced to flow on the conduit to ground. The generator-to-conduit connection was made by several pieces of braid fastened more or less uniformly around the conduit to equalize the current distribution around the conduit at the point of injection. At the ground end of the conduit, a metal connection box was inserted for ease in changing conductor connections. The conduit was grounded in an area several inches above the connection box by several pieces of braid connected to a metal ground plane (for some tests copper; for others aluminum) which was in turn connected to the building counterpoise system. The metal ground plane covered the complete test area. The various conduit configurations used to the injected current tests are shown in Figures 3 and 7. Figure 7 is described later in the report.

3.2 H-field Tests

For these tests a conduit loop was placed in an H-field environment causing an induced current to flow on the conduit. The resultant induced voltage developed on conductors inside the conduit was measured. The test setup is shown in Figure 4.

The actual H-field inside and outside the radiating loop was measured by means of an H-field transducer. The transducer and its connecting circuitry are shown in Figure 5.

3.3 Current Wave Shapes

3.3.1 Pulse Current

In all tests where the pulse current was supplied by the pulse current generator, an applied pulse current wave having rise times between 0.9 and 1.3 microseconds and tail times between 30 and 35 μsec was used. The current wave measurement was made with a 0.036 ohm shunt in series with the conduit and all other grounds removed. Typical oscillograms are shown in Figure 6. The current throughout the tests was monitored by means of a current transformer.

3.3.2 Quasi-Unit Function

These current waves were generated by connecting a 12-volt battery through a suitable series resistance to the conduit under test. Typical oscillograms depicting the waves used are shown in the Appendix of this report.

4.0 INJECTED CURRENT TESTS

4.1 Effect of Conductor Location

The effect of conductor location on the conductor-to-conduit induced voltage was evaluated early in the testing program. For this test an L-shaped test setup was erected as shown in Figure 7. Also in Figure 7 is shown the position of the conductors being measured, one conductor (light green) being placed next to the conduit wall and the other (red) centered by insulating spacers throughout the conduit length. Both conductors were electrically connected to the conduit at the generator end. At the measurement end the measurement system was terminated in 76 ohms. The measured conductor-to-conduit induced voltages for these widely separated conductors is shown in Figure 8 and tabulated in Table 1.

TABLE 1

EFFECT OF CONDUCTOR LOCATION ON CONDUCTOR-TO-CONDUIT INDUCED VOLTAGES

Applied Pulse Current - 1755 amperes

	First Peak		Second Peak		Third Peak	
Conductor	Ampl.	Time	Ampl.	Time	Ampl.	Time
Light Green (at wall)	540 MV	0.5 μs	40 MV	300 μs	30 MV	3500 μs
Red (at center)	730 MV	0.5 μs	40 MV	300 μs	30 MV	3500 μs

The data clearly shows that the conductor at the center of the conduit develops the higher initial crest (first peak) voltage but the increase is only 1.3 times the conductor-to-conduit voltage of the conductor adjacent to the wall. This is probably due to the very non-uniform peripheral current distribution at the condulet corner. Due to this relatively small change in induced voltage with respect to conductor location, experiments using randomly located conductors will result in valid data. It should be noted that two other voltage peaks occur, one at 300 μsec and one at 3500 μsec. The induced voltage at 3500 μsec is a result of the IR voltage drop from one end of the conduit to the other and the phenomenon which causes this voltage is explained in the Appendix. The second induced voltage peak is probably the IR induced voltage due to the condulet material which is cast or malleable iron and has a lower permeability than the steel conduit. Also another factor which may influence this peak is the thickness of condulet cover.

4.2 Effects of Changing Relative Permeability of Conduit Due to Repetitive Applications of a Unidirectional Pulse Current

In dealing with permeable materials, evaluations must necessarily take into consideration the fact that the relative permeability may change with application of unidirectional pulse currents. This is known as the saturation effect. To determine whether, in fact, a saturation effect would take place, the same 40 foot length of conduit as described in 4.1 and shown in

Figure 7 was used. Measurements of the induced voltage between the light green conductor and conduit were made at the measurement end of the conduit. At the generator end the conductor was electrically connected to the conduit. The wave shapes are shown in Figure 9 and the results tabulated in Table 2.

TABLE 2

EFFECT OF CONDUIT SATURATION ON THE CONDUCTOR-TO-CONDUIT INDUCED VOLTAGE IN TWO INCH RIGID STEEL CONDUIT

Applied Pulse Current - 1755 amperes

Number of Applied Waves and Polarity	IR Peak Induced Voltage	
	Amplitude	Time
20 Negative	22.5 MV	3500 μs
1 Positive	5.0 MV	3500 μs
3 Positive	15.0 MV	3500 μs
10 Positive	28.0 MV	3500 μs
20 Positive	32.0 MV	3500 μs
50 Positive	33.0 MV	3500 μs

The IR induced voltage amplitude increases with increasing numbers of applied unidirectional waves until saturation is reached. Between the first positive applied wave and the twentieth which is considered to be the saturated condition, an induced voltage change of about 6:1 occurred. Therefore, to avoid the comparison of data from material at different degrees of saturation, all data taken throughout the series of tests reported in this report are values with the material in the saturated condition.

Upon closer inspection of the wave shapes, it can be seen that the second peak occurring at about 300 μsec experiences a similar amplitude change. This second peak has been attributed to the condulet material. Substantiating evidence is given later in the report.

4.3 Effect of Conductor Terminating Impedance on Conductor-to-Conduit Induced Voltages

The tests described in 4.1 were repeated with the light green and red conductors in the same position except that the measurement terminating impedance was reduced from 76 and 75 ohms to 1.5 ohms. The results were quite interesting and are shown in Figure 10 and a comparison tabulation is given in Table 3. (The 75 ohms wave shapes are not shown in Figure 10.)

TABLE 3

EFFECT OF CONDUCTOR TERMINATING IMPEDANCE
Conductor-to-Conduit Induced Voltages
Applied Pulse Current - 1755 amperes

Conductor	Cable Term.	First Peak		Additional Peak		Second Peak		Third Peak	
		Ampl.	Time	Ampl.	Time	Ampl.	Time	Ampl.	Time
Lt. green	76 ohms	540 MV	0.5 μs			40 MV	300 μs	30 MV	3500 μs
Lt. green	75 ohms	480 MV	0.5 μs			40 MV	300 μs	33 MV	3500 μs
Lt. green	1.5 ohms	-55 MV	0.3 μs	145 MV	10 μs	27 MV	400 μs	22 MV	3500 μs
Red	76 ohms	730 MV	0.5 μs			40 MV	300 μs	30 MV	3500 μs
Red	1.5 ohms	-100 MV	0.3 μs	150 MV	10 μs	27 MV	400 μs	22 MV	3500 μs

Immediately apparent is the initial crest voltage of opposite polarity when the measuring system terminating impedance is a low resistance. If we analyze the initial crest voltages for the 75 and 1.5 ohm terminations as shown in Figure 11, we find that the difference voltage is initially about the same magnitude but of opposite polarity. This infers that for the low impedance termination there is an initial flow of current in the conductor in the opposite direction from that when the higher impedance termination is used. This is probably due to the fact that the conduit ground at the measurement end assumes a transient impedance which is substantially higher than 1.5 ohms.

It should be also noted that the IR peak voltage occurring at 3500 μsec in the 75 ohm tests also occurred at the same time in the 1.5 ohm tests, but was somewhat lower in magnitude. This indicates that the current on the conductor is higher at the longer times when the conductor is terminated in 1.5 ohms. For the 1.5 ohm tests, however, an additional peak voltage was measured at 10 μs on both the wall and center conductors which in effect made the second peak move to a slightly longer time and resulted in a lower measured voltage.

It is apparent then that the induced conductor-to-conduit voltages measured are influenced somewhat by the effective measuring system terminating impedance. However, the 75 ohm measuring system results are worst case and can safely be used for design purposes.

4.4 Conductor-to-Conductor Induced Voltages from Twisted Pair and Parallel Pair Conductors

For these measurements the test setup was again as described in 4.1, except that a parallel pair of wires were pulled through the conduit as well as a twisted pair of conductors. Their relative positions are shown in Figure 7. Measurements were made with both the twisted pair and parallel pair wires connected together and to the conduit at the generator end. The measuring impedance between conductors was 100 ohms. The wave shapes are shown in Figure 12 and the pertinent data is tabulated in Table 4.

TABLE 4

CONDUCTOR-TO-CONDUCTOR INDUCED VOLTAGE ON PARALLEL AND TWISTED WIRE PAIRS

Applied Pulse Current - 1755 amperes

	First Peak	
Conductors	Amplitude	Time
Parallel pair	170 MV	0.3 μs
Twisted pair	30 MV	0.3 μs

It should be noted that the conductor-to-conductor, unlike the conductor-to-conduit, case exhibits only an initial crest voltage of short time duration. The voltage measured for the twisted pair is less than that measured for the parallel pair. This is what might be expected because the parallel pair, even though taped together at one foot intervals, are not necessarily always adjacent to each other and thus the leakage component of the wave would not be equal on each conductor and thus a small difference voltage would develop. In the case of twisted pairs the voltage cancellation phenomenon is well known.

The long time IR voltage has nothing to do with the changing initial flux phenomenon. At times long after the current wave has reduced to zero, the IR voltage on each conductor of the pair is essentially equal resulting in no difference in voltage between conductors in a pair.

4.5 Effect of Openings in Conduit

In any conduit system utilizing condulets, it is possible to inadvertently leave off one or several condulet covers. To determine the shielding degradation caused by removal of condulet covers, a test simulating this condition was made. The test setup was again the L-shaped configuration shown in Figure 7, which contained three condulets. Both the red and light green conductors were used and were electrically connected to the conduit at the generator end. The wave shapes showing the effect of removing one, two, and three covers is shown in Figure 13 and tabulated in Table 5.

TABLE 5

CONDUCTOR-TO-CONDUIT AND CONDUCTOR TO CONDUCTOR INDUCED VOLTAGE SHOWING EFFECT OF OPENINGS IN CONDUIT SYSTEM

Applied Pulse Current - 1755 amperes

Test Condition	First Peak Induced Voltages		
	Lt. green to conduit	Red to conduit	Lt. green to red
1. All condulet covers in place	580 MV	800 MV	0.23 V
2. Generator end condulet cover off	-2.1, 1.1 V	-1.1, +1.5 V	2.1 V
3. Measurement end condulet cover off	3.4 V	4.3 V	825 V
4. Corner condulet cover off	11.0 V	18.5 V	6.5 V
5. Corner and measurement end condulet cover off	15.9 V	21.0 V	5.25 V

An opening in a conduit system such as a condulet cover removed will, in general, only effect the flux leakage induced voltage. This first peak voltage induced on the conductors will depend to a large extent on the wire position as it goes by the opening.

Analyzing the data, it appears that the largest induced voltage for a single condulet cover removed resulted when the corner or 90° condulet cover was taken off. This indicates an additional effect is taking place and for want of a better term will be called a corner effect.

It is interesting to note that the measured conductor-to-conductor voltages are, in general, equal to the difference between the individual measured conductor-to-conduit voltages for each of the various cover conditions. The exception was the case where the cover was removed at the generator end.

4.6 Conductor-to-Conduit Induced Voltages Comparing Couplings, Bends, and Condulets in Two Inch Conduit System

The L-shaped configuration used in test experiments described in

Sections 4.1 through 4.5 always had condulets in the conduit system and it was suspected that condulets obscured other effects which may be of interest. Therefore, a series of tests was made using the conduit systems shown in Figure 3; namely, 1) a conduit system with couplings only, 2) a conduit system with couplings and a 90° elbow, and 3) a conduit system with couplings and two 90° elbows. A single conductor was randomly placed within the conduit and electrically connected to the conduit at the generator end. All joints were clean and threaded. The wave shapes are shown in Figure 14 and the results tabulated in Table 6.

TABLE 6

CONDUCTOR-TO-CONDUIT INDUCED VOLTAGES
COMPARING THE EFFECT OF BENDS AND COUPLINGS
Applied Pulse Current - 1755 amperes

	First Peak		Second Peak	
Test Setup	Amplitude	Time	Amplitude	Time
Couplings only	22.5 MV	0.5 μs	22.5 MV	3500 μs
Couplings and one 90° elbow	60 MV	0.4 μs	22.5 MV	3500 μs
Couplings and two 90° elbows	95 MV	0.5 μs	25 MV	3500 μs

When adding a bend to straight run conduit systems, it is necessary to add an additional coupling to install the bend. Therefore, it is difficult to make a direct comparison between bends and couplings. Making the comparison with this in mind, the addition of one bend to a straight run conduit system increased the initial peak induced voltage by 2.7 times. The addition of two bends increased the induced voltage about 4.2 times.

It should be noted that the measured wave shape for the straight run conduit containing no condulets exhibited only an initial peak occurring in less than 1 μsecond and a long time peak at 3500 μseconds. The intermediate peak occurring at 300 μseconds measured in the conduit system with condulets was not present. The different permeability of the condulet material accounts for this additional peak.

An interesting comparison can be made by noting the induced voltages measured for the conduit system containing a 90° condulet (Table 3) and the conduit system containing one 90° elbow. Even though the two conduit systems were slightly different, that is 6 threaded joints versus 8 threaded joints, this would not account for the larger difference in first peak voltage measured. The results are tabulated in Table 7.

TABLE 7

CONDUCTOR-TO-CONDUIT INDUCED VOLTAGES IN TWO INCH RIGID STEEL CONDUIT SYSTEM SHOWING DIFFERENCE BETWEEN ONE 90° CONDULET AND ONE 90° ELBOW

Applied Pulse Current - 1755 amperes

	First Peak		Condulet IR Peak		Conduit IR Peak	
Test Setup	Amplitude	Time	Amplitude	Time	Amplitude	Time
40' conduit system with 90° condulet	480 MV	0.5 μs	40 MV	300 μs	33 MV	3500 μs
30' conduit system with 90° elbow	60 MV	0.5 μs			22.5 MV	3500 μs

Note that the conductor-to-conduit long time IR peak induced voltage is higher for the 40 foot conduit run, as it should be, since the resistance of this conduit run is higher.

4.7 Effect of Loose Joints on the Conductor-to-Conduit Induced Voltages in a Two Inch Conduit System

For these tests the two inch conduit system containing the two 90° elbows as used in Section 4.6 was assembled so that one coupling joint was loosely connected by only a few threads. The remainder of the conduit system was tightly threaded. The resulting wave shapes are shown in Figure 15 and the results tabulated in Table 8.

TABLE 8

CONDUCTOR-TO-CONDUIT INDUCED VOLTAGES IN TWO INCH CONDUIT SYSTEM SHOWING THE EFFECT OF A LOOSE JOINT

Applied Pulse Current - 1755 amperes

Test Setup	First Peak Amplitude	First Peak Time
1. 30 Foot conduit run and two 90° elbows	95 MV	0.5 μs
2. Same as one, except one loose joint	32 V	0.4 μs

The data shows that a conductor-to-conduit induced voltage increase of over 300 times can occur when a conduit system contains a very loose joint. The magnitude of the voltage measured with a loose joint becomes a significant amount of the rated voltage for a 120 or 480 volt system, to say nothing of low level control circuits. This test clearly points out the importance of tightly made joints.

4.8 Effect of Pulse Current Amplitude on the Conductor-to-Conduit Voltages in a Two Inch Rigid Steel Conduit Having Only Threaded Couplings

Extrapolation of the data to larger currents is a necessity since the test facilities used were not capable of producing larger currents. Therefore, to determine the relationship between applied pulse current and induced voltage measured on conductors within a conduit system, the 30 foot straight conduit run was pulsed at 600 and 1200 amperes in addition to the 1755 amperes which was previously used for tests described in Section 4.6. The wave shapes are shown in Figure 16 and the results tabulated in Table 9.

TABLE 9

CONDUCTOR-TO-CONDUIT INDUCED VOLTAGES IN TWO INCH RIGID STEEL CONDUIT AS INFLUENCED BY INJECTED PULSE CURRENT MAGNITUDE

Applied Current (amperes)	First Peak Amplitude	First Peak Time	IR Peak Amplitude	IR Peak Time
600	7.5 MV	< 1 μs	8.5 MV	3500 μs
1200	15.0 MV	< 1 μs	17.0 MV	3500 μs
1755	22.5 MV	< 1 μs	22.5 MV	3500 μs

The data indicates for a fixed current wave shape that a linear relationship exists for the first peak (leakage flux) for this conduit system containing only couplings. The linearity of the second peak is, of course, expected since this voltage peak is directly proportional to the current.

4.9 Effect of Threaded or Welded Joints on the Conductor-to-Conduit Voltages in Two Inch Rigid Steel Conduit

For these tests a different 30 foot straight conduit system containing only couplings was set up in the test area. First, conductor-to-conduit voltages were measured with all joints threaded. Then the joints were completely welded around the circumference of the conduit. The conductor within the conduit was a #20 flamenol insulated wire electrically connected to the conduit at the generator end. The measured wave shapes are shown in Figure 17 and the results are tabulated in Table 10.

TABLE 10

CONDUCTOR-TO-CONDUIT INDUCED VOLTAGES MEASURED IN A TWO INCH CONDUIT SYSTEM COMPARING THREADED VERSUS WELDED JOINTS

	First Peak		Second Peak	
Test Setup	Amplitude	Time	Amplitude	Time
Threaded joints	68 MV	0.5 μs	16 MV	3500 μs
Welded joints	8.5 MV	0.6 μs	19 MV	3500 μs

Notice that the first peak induced voltage measured for this threaded joint conduit system is approximately three times higher than that for a similar 30 foot threaded conduit system measured earlier (Table 6). This may indicate the normal variation in flux leakage voltage which could be measured in threaded conduit systems. Welding the joints reduced the flux leakage (first peak) induced voltage eight times or approximately 18 dB. It is interesting to note, however, that welding of this 30 foot conduit run resulted in only an 8.5 dB improvement in shielding effectiveness when compared to the previously tested threaded conduit run, thus indicating

some variability in tightness of the unwelded threaded joints.

The small difference in IR induced voltage is probably due, in part, to the difference in conduit resistance. For the threaded conduit, the resistance was 0.00182 ohms; for the welded conduit the resistance was 0.00176 ohms.

4.10 Effect of Conduit Wall Thickness on the Conductor-to-Conduit Induced Voltage

For these tests a 1-inch rigid steel, 30 foot straight conduit run having only welded joints was used. The test setup was similar to the 30 foot straight welded conduit run described in Section 4.9 except for conduit thickness. The resulting wave shapes are shown in Figure 18 and the pertinent data are tabulated in Table 11. The applied pulse current in the case of the two tests was slightly different. Therefore, the data given in Table 11 has been normalized for the current amplitude used in two inch rigid steel conduit tests.

TABLE 11

CONDUCTOR-TO-CONDUIT INDUCED VOLTAGES
COMPARING EFFECT OF CONDUIT WALL THICKNESS
Applied Pulse Current - 1755 amperes

	First Peak		Second Peak	
	Amplitude	Time	Amplitude	Time
One inch rigid steel conduit (measured wall thickness - 0.1207")	8.1 MV	0.7 μs	39.4 MV	3500 μs
Two inch rigid steel conduit (measured wall thickness - 0.1335")	8.5 MV	0.7 μs	19 MV	3050 μs

The data points out that the conduit wall thickness essentially influences the long time IR induced voltage peak and does not influence the flux leakage voltage peak or its wave shape. As shown in the Appendix, the time for current to diffuse through the conduit wall is a function of the

thickness squared. Assuming the resistivity and permeability of both conduits to be the same, the ratio of squared wall thicknesses should equal the ratio of the measured current diffusion times. The calculation as follows shows a reasonable check:

Let Z and Z_1 represent the wall thickness of 2" rigid and 1" rigid conduit, respectively, then

$$\frac{(Z)^2}{(Z_1)^2} = \frac{.0179}{.0146} = 1.22$$

and let T and T_1 represent the diffusion times of the 2" and 1" rigid conduit, respectively, then

$$\frac{T}{T_1} = \frac{3500}{3050} = 1.15$$

The measured difference in the IR induced voltage is a function of both resistance and current. The IR ratio of both conduits should equal the ratio of the measured voltages. The resistance of the two inch rigid welded conduit measured 0.00176 ohms and resistance for the one inch rigid welded conduit measured 0.00355 ohms. Therefore,

$$\frac{IR_{(2\ inch)}}{IR_{(1\ inch)}} = \frac{1755 \times 0.00176}{1660 \times 0.00355} = 0.523$$

The ratio of the measured IR voltage peaks checks reasonably close, being 0.485.

4.11 Induced Voltages on Conductors within Two Inch Rigid Conduit Comparing Wrought Iron and Steel

Wrought iron conduit with its reported good corrosion resistance qualities may be considered for mechanical protection of buried electrical circuits. Therefore, an electrical shielding evaluation of this material for comparative purposes with steel was made.

The evaluation was made by the injected current method using the test setup shown in Figure 3a. A twisted pair of #20 flamenol insulated wires

was inserted in the total 30 foot length of 2-inch diameter conduit. The twisted pair was electrically connected to the conduit at the generator end for all tests.

The induced voltages measured on conductors in wrought iron are shown in Figure 19. For comparison induced voltages measured previously in 2-inch rigid steel conduit are shown also in Figure 19. It will be noted that the current pulse peak value used in the steel conduit tests was higher than that used for the wrought iron test. The current pulse wave shape, however, was approximately the same. Therefore, these voltages are approximately a linear function of the peak current. Normalizing the voltages measured to the pulse current value used for the wrought iron tests results in the comparison shown in Table 12.

TABLE 12

COMPARISON OF INDUCED CONDUCTOR VOLTAGES
IN TWO INCH RIGID STEEL AND WROUGHT IRON CONDUIT
Applied Peak Current Pulse - 1420 amperes

	First Peak		Second Peak		(IR) Peak	
	Amplitude	Time	Amplitude	Time	Amplitude	Time
Wrought Iron						
C - C	< 6 MV*	1.05 μs	< 2 MV*	22.5 μs	None	
C - G	52 MV	1.3 μs	68 MV	27 μs	38 MV	1200 μs
Steel (rigid)						
C - C	< 1.6 MV*	0.5 μs	None		None	
C - G	54 MV	0.5 μs	None		13 MV	3500 μs

* Essentially the noise level of the measuring system

C - C denotes conductor-to-conductor measurement

C - G denotes conductor-to-conduit measurement

As can be noted from the above table, the conductor-to-conduit induced voltage for wrought iron exhibits two flux leakage peaks nearly similar in magnitude but occurring at different times. The first occurs at 1.3 μsec

which was the approximate time to crest of the applied current wave. The induced voltage on the conductor in the steel conduit also exhibited this characteristic. The second peak occurring at 27 μsec, however, was not exhibited by the conductor in the steel conduit and probably this is due to the coupling material. The magnitudes of these first two peaks are similar in magnitude to those measured on conductors in the steel conduit. The long time IR voltage peak measured on conductors in wrought iron occurred at a much shorter time (1200 μsec) than for similar measurements made with steel conduit (3500 μsec). Since the resistivity of these two materials differs only by a factor of 1.2, the measured difference in the IR crest time must be due to the permeability of the two materials, the wrought iron having a permeability approximately one third that of steel for this current pulse application. This comparison was made with both conduits in the saturated condition. (Saturation is defined as that point in the application of current pulse waves where no further increase in induced conductor-to-conduit voltage is noted. For steel this was 20 applied waves; for wrought iron this was 35 applied waves.)

Experiments have shown (see Appendix) that the peak conductor-to-ground IR voltage is related to the time constant of the current diffusion through the conduit wall thickness and the resistance of the conduit material. For the case of the wrought iron and steel conduits used in this experiment, the wall thicknesses were equal and the resistance varied only by a factor of 1.2. Therefore, it appears that the 3 to 1 difference in the voltage magnitude is also directly related to the 3 to 1 difference in permeability.

The significance of the test data from both steel and wrought iron tests in terms of application is that both conduit materials have considerable shielding effectiveness when the conduit runs have properly-made tight joints.

The principal difference between the two types of materials is that the

wrought iron exhibits a greater resistance to permeability change (i.e. saturation) from exposure to magnetic fields. Literature describing wrought iron states also that the permeability of the material is less affected by working, handling, welding, etc. than that of steel. Since the application information for conduit is based on experimental data obtained from magnetically saturated conditions, which is a worst case condition, differences in unsaturated values of permeability for both wrought iron and steel become relatively unimportant.

4.12 Induced Voltages on Conductors in Two Inch Rigid Steel Conduit Sectioned by a One Foot Long Corrugated Flexible Steel Tubing

The purpose of this experiment was to evaluate the possible degradation in shielding effectiveness which could occur by the insertion of a corrugated flexible tubing in a two inch rigid steel conduit run. Application of such short flexible tubing could occur at building and conduit interfaces where displacement between building and conduit may change over a period of years or wherever vibration isolation is needed.

The test setup for this experiment was similar to that shown in Figure 3a. except that the one foot long flexible corrugated tubing was inserted between two of the three 10 foot conduit lengths. All joints were made up tight with threaded couplings.

Three types of corrugated tubing (bellows) were tested; one made of carbon steel, one made of stainless steel (321 alloy), and one made of stainless steel armored with one layer of stainless steel wire braid. These are shown in Figure 20.

The induced conductor voltage wave shapes are similar to those measured without the corrugated tubing. These are shown in Figures 21, 22, and 23. Comparing these with data in Table 12 on steel conduit having no bellows results in the comparison shown in Table 13.

The measured resistances of the 30 foot rigid steel conduit with and without a one foot length of corrugated tubing using threaded joints was as

TABLE 13

COMPARISON OF INDUCED CONDUCTOR VOLTAGES

(30 Feet of Two Inch Steel Conduit Containing
a One Foot Length of Corrugated Flexible Tubing
between Two 10 Foot Conduit Lengths - Threaded Joints)

Applied Peak Current Pulse - 1420 amps

	First Peak		Second Peak		IR Peak	
	Amplitude	Time	Amplitude	Time	Amplitude	Time
One Foot Stainless Steel Tubing, R = .01054 Ω						
C - C	200 MV	0.5 μs	None		None	
C - G	17.5 V	1 μs	None		22 MV	3500 μs
One Foot Stainless Steel Tubing with Braid, R = .00335 Ω						
C - C	< 5 MV*	0.6 μs	3 MV	2.4 μs	None	
C - G	5.6 V	4 μs	None		22 MV	3500 μs
One Foot Carbon Steel Tubing, R = .00305 Ω						
C - C	10 MV	0.7 μs	6.5 MV	3.5 μs	None	
C - G	350 MV	1.4 μs	1400 MV	49 μs	22 MV	3500 μs
Steel Conduit (No Corrugated Tubing)						
C - C	< 1.6 MV*	0.5 μs	None		None	
C - G	54 MV	0.5 μs	None		13 MV	3500 μs

* Essentially noise level of measuring system

follows:

Resistances of 30 foot rigid steel two inch electrical trade size conduit,

With no flexible section - 0.00182 ohm

With 321 stainless bellows - 0.0122 ohm

With 321 stainless bellows and braid armor - 0.00498 ohm

With carbon steel bellows - 0.0057 ohm

In previous discussion it was pointed out that the IR peak voltage was a function of the time of the current diffusion through the conduit wall and the resistance of the material. The time required for the current to diffuse through the material is proportional to the thickness squared and permeability and inversely proportional to resistance. From analysis of the data in Table 13, it appears that the corrugated tubing had very little effect on the IR peak magnitude or response time of the conduit, even though the one foot of corrugated tubing causes considerable changes in the parameters just mentioned. A probable reason for this could be that the one foot length of flexible tubing has its own response time and its IR peak occurs at a much different time than that of the conduit. We can examine what the diffusion time of the tubing might be on a proportional basis since we know what the diffusion time for the conduit is for this particular wave shape. For example:

$$TC_{conduit} \propto \frac{(Z)^2 \mu_s}{\rho_s} = \frac{(0.3)^2 \mu_s}{\rho_s} = \frac{0.09\ \mu_s}{\rho_s}$$

$$TC_{ss\ conduit} \propto \frac{(Z)^2 \mu_{ss}}{\rho_{ss}} = \frac{(0.060)^2 \mu_{ss}}{\rho_{ss}} = \frac{0.0036\ \mu_{ss}}{\rho_{ss}}$$

(μ_s and μ_{ss} are the relative permeability of steel and stainless steel respectively.)

Since ρ_s and ρ_{ss} vary much less than 2 to 1 and we assume that μ_s for steel is 100 and μ_{ss} for stainless steel is 1, then the ratio of the two diffusion

times becomes

$$\frac{0.009 \times 100}{0.0036 \times 1} = 2500$$

The diffusion time for the conduit was measured at 3500 μsec. Therefore, the diffusion time for the stainless steel tubing can be estimated to be

$$\frac{3500 \text{ μsec}}{2500} = 1.4 \text{ μsec}$$

Referring back to Table 13, the measured induced voltage from the conduit run containing the stainless steel tubing indicated only a flux leakage peak at 1 μs and an IR peak at 3500 μs. The calculations indicate that the IR peak of the tubing is so short it occurs at approximately the same time as the flux leakage peak. Analyzing the magnitude of the first peak voltage measured from the stainless steel and carbon steel bellows, the carbon steel initial peak induced voltage was only 350 MV as compared with 17.5 volts for the stainless steel bellows. The carbon steel first peak is truly a flux leakage peak voltage since its IR peak occurs at 49 μseconds. Since there should be very little difference in flux leakage induced voltage between the stainless steel and carbon steel bellows, the high first peak voltage measured for the stainless steel is mainly an IR voltage. This can be checked by calculation since the current is known at the time of occurrence of the first peak. The applied current (Figure 6) at approximately 1.2 μseconds is 1420 amperes and the resistance of the stainless steel bellows measured 0.0122 ohm, resulting in a calculated IR voltage of 17.2 volts. This checks the 17.5 volts measured and confirms that the initial voltage measured is proportional to the resistance of the non-magnetic bellows material and the current through it.

The IR voltage for the carbon steel bellows occurring at 49 μseconds can also be checked by calculation. The applied current at 49 μseconds was approximately 490 amperes. The resistance of the carbon steel bellows measured 0.00305 ohm. Therefore, the calculated IR voltage is 1.5 volts which

approximates the 1.4 volts measured. Note the IR voltage of the conduit was still present at 3500 μseconds.

The initial conductor-to-conduit peak voltages measured from both stainless steel flexible tubings (with and without braid covering) were from 100 to 300 times higher than the induced voltage that was measured from flux leakages in the conduit run with threaded joints and no flexible tubing. Use of the carbon steel flexible corrugated tube in place of the stainless steel tube reduced the conductor-to-conduit voltage by a factor of about 12. Compared to rigid steel conduit with no flexible tube, the one foot carbon steel flexible tube increased the conductor-to-conduit voltage about 25 times.

4.13 Induced Voltages on Conductors in Two Inch Flexible Steel Conduit - Standard Grade and Sealtite®

There may be situations which require the use of flexible conduit rather than rigid steel conduit. Therefore, two types of flexible conduit measuring 25 feet in length were evaluated. One was standard grade flexible conduit, the other was a flexible conduit commercially called Sealtite®. The main difference between the two flexible conduits was the looseness or tightness of the interlocking steel strip.

The test setup was again similar to that shown in Figure 3a. with twisted pair wires within the flexible conduit.

The measured induced voltages from both flexible conduits are listed in Table 14. The measured wave shapes are shown in Figures 24 and 25.

® Trademark of Anaconda Metal Hose Company

TABLE 14

COMPARISON OF INDUCED CONDUCTOR VOLTAGES ON CONDUCTORS IN 25 FEET OF TWO INCH FLEXIBLE STEEL CONDUIT

(Standard and Sealtite®)

Applied Peak Current Pulse - 1420 amps

	First Peak		Second Peak	
	Amplitude	Time	Amplitude	Time
Standard				
C - C	9 V	0.8 μs	None	
C - G	1450 V	0.6 μs	None	
Sealtite®				
C - C	1.6 V	0.5 μs	None	
C - G	68 V	0.6 μs	54 V	20 μs

The data significantly reveals the higher induced short time voltages which occur from these types of conduits. The standard flexible steel conduit, especially, acted as practically no shield at all, the induced voltage being approximately 25,000 times higher than that from conductors in rigid steel conduit. Because of the leaky open construction, no long-time voltage indicating flux diffusion through the metal wall was exhibited. The Sealtite® conduit, which is tightly wound and has metal continuously overlapped, did exhibit a second IR peak at 20 μseconds. At 20 μseconds the current, from the applied current wave shown in Figure 6, is approximately 930 amps. The IR voltage at 20 μseconds is 930 amps times the resistance of the conduit which measured 0.055 ohm. Therefore, the IR voltage calculated to be 51 volts which checks the measured value of 54 volts quite closely. The conductor-to-ground flux leakage peak induced voltage of Sealtite® conduit was approximately 1250 times higher than that measured from conductors in rigid steel conduit.

4.14 Induced Voltages on Conductors within 30 Feet of Three-Phase Aluminum Armored Power Cable Rated 15,000 Volts

The basic objective of this experiment was to determine the shielding effectiveness of commercial type power cable. The cable construction is shown in Figure 26. Note that the cable selected for test has two shields as far as each conductor is concerned. One is the outer aluminum armor and the other is the individual copper shielding tape wrapped over each conductor insulation.

The physical test setup was similar to that shown in Figure 3a. Tests were made with the cable conductors, conductor shields, ground wires, and armor connected in relation to each other in four basically different ways. These are shown diagrammatically in the four sketches in Figure 27. To simplify identification of parts, numbers were assigned to the various elements of the cable as follows:

1, 2, 3 - phase conductors
4 - all neutral ground wires connected together
5, 6, 7 - phase conductor copper shielding tapes
8 - aluminum armor

For ease of presentation and analysis, the wave shapes and comparisons in tables will be listed by test connection. Figure 28 and Table 15 present the data of induced voltages from Test Connection 1. Figures 29 through 33 and Table 15 present the data of induced voltages from Test Connection 2. Figures 34 through 36 and Table 15 present the data of induced voltages from Test Connection 3. Figures 37 and 38 and Table 15 present data of induced voltages from Test Connection 4.

4.14.1 Significance of the Four Test Connections

The type of cable tested is normally used in indoor installations such as central stations and substations, industrial plants, and similar locations. Test Connection 4 has probably the most significance as far as usage is concerned since the neutral ground wires, phase conductor shields, and outer

TABLE 15

INDUCED CONDUCTOR VOLTAGES ON CONDUCTORS
IN A 15 kV ALUMINUM ARMORED, 3-PHASE POWER CABLE

Applied Peak Current Pulse - 1420 amps

Measurement Points	First Peak		Second Peak	
	Amplitude	Time	Amplitude	Time
	Test Connection #1			
4 - 8	9.0 V	0.6 µs	12.0 V	4.5 µs
	Test Connection #2			
4 - 8	9.0 V	0.7 µs	12.0 V	4.5 µs
5 - 8	9.0 V	0.6 µs	12.0 V	4.5 µs
1 - 8	2.2 V	0.5 µs	None	
1 - 5	12.0 V	0.7 µs	15.0 V	4.6 µs
1 - 2	0.34 V	0.6 µs	None	
	Test Connection #3			
4 - 8	5.5 V	0.7 µs	7.0 V	4.4 µs
1 - 8	4.8 V	0.7 µs	6.6 V	5.2 µs
1 - 2	0.46 V	1.4 µs	None	
	Test Connection #4			
1 - 8	3.6 V	0.7 µs	4.6 V	3.9 µs
1 - 2	0.46 V	1.4 µs	None	

armor are all connected to ground. The results, however, would be termed "worst case", since the load impedance usually found in actual service conditions is $\frac{1}{100}$ or less than that of the measuring system impedance used.

The purpose of the four test connections was to allow determination of the shielding effectiveness of both the outer armor and the phase conductor shields with current flowing in 1) the armor only, 2) in both the armor and the neutral wires, and 3) in the armor, neutral wires and the phase conductor shields as well.

4.14.2 Analysis of Cable Test Data

The first significant fact which is immediately apparent is that the long-time IR induced voltage peak on the conductors in aluminum armor cable occurs at about 5 μseconds which is a much shorter time than the 100 μsec exhibited by conductors in rigid aluminum conduit. (Aluminum conduit data is given later in the report under H-field tests.) Also the peak IR induced voltage magnitude of the phase conductor is approximately 15 times higher than that on conductors in rigid aluminum conduit and approximately 300 times higher than conductor-to-conduit voltages induced on conductors in rigid steel conduit.

In terms of induced conductor-to-conduit flux leakage voltages, the aluminum armor cable allows about 30 times more flux penetration than does threaded rigid aluminum conduit and about 90 times more than threaded rigid steel conduit in much the same configuration. The conductor-to-conductor flux leakage induced voltage for the aluminum armored cable was negligible as was rigid aluminum and steel conduit.

The difference in shielding effectiveness of the cable with the shields, armor, and neutral wires carrying pulse current compared to the condition of the armor only carrying current is shown in Table 16.

TABLE 16

INDUCED CONDUCTOR VOLTAGE

Applied Peak Current Pulse - 1420 amps

Measurement Points	Pulse Current Carried by Armor and Shields				Pulse Current Carried by Armor, Shields, and Neutral Wire			
	First Peak		Second Peak		First Peak		Second Peak	
	Ampl.	Time	Ampl.	Time	Ampl.	Time	Ampl.	Time
1 - 8	4.8 V	0.7 μs	6.6 V	5.2 μs	3.6 V	0.7 μs	4.6 V	3.9 μs
1 - 2	.46 V	1.4 μs	None		.46 V	1.4 μs	None	

As can be noted, the shielding effectiveness of the cable is improved only 3 dB by also allowing the neutral wire to carry pulse current. Therefore, it would make little difference from a pulse current point of view whether the neutral wires were connected at both ends of a conduit run or not connected. In the case of steel armoring, the neutral wire may have more significance because of the larger difference in resistance between the steel armor and the copper shielding tape.

4.14.3 Variation in Cable Experiment

The armored power cable used in this experiment could, in service, be mounted along metal bulkheads and walls. Therefore, the cable was reoriented in position as shown in Figure 39. The grounds were made from aluminum foil connected at three points to the aluminum ground plane floor of the shielded room. Except for cable orientation, all other conditions of the experiment were the same. Measurements were made with the cable in Test Connection 3, as given in Figure 27. The data comparing the induced voltages for conditions of various ground connections is given in Table 17.

TABLE 17

COMPARISON OF INDUCED CONDUCTOR VOLTAGES
FOR VARIOUS ARMOR SHEATH GROUND CONNECTIONS
Applied Peak Current Pulse - 1420 amps
Test Connection #3

Conductor Connection	First Peak		Second Peak		Ground Connection
	Amplitude	Time	Amplitude	Time	
4 - 8	9.2 V	0.8 μs	10.6 V	3.2 μs	1
	9.0 V	0.9 μs	9.8 V	2.9 μs	1 and 2
	8.0 V	0.8 μs	8.6 V	1.2 μs	1, 2, 3
	7.6 V	0.7 μs	8.4 V	1.2 μs	1 and 3
1 - 8	8.2 V	0.9 μs	9.2 V	3.7 μs	1
	8.0 V	0.9 μs	8.4 V	3.3 μs	1 and 2
	7.2 V	0.9 μs	7.4 V	1.2 μs	1, 2, 3
	7.0 V	0.9 μs	7.2 V	1.2 μs	1 and 3
1 - 2	.34 V	1.4 μs	None		1
	.40 V	1.1 μs	None		1 and 2
	.36 V	1.2 μs	None		1, 2, 3
	.34 V	1.3 μs	None		1 and 3

As can be noted by comparing Tables 16 and 17, placing 20 feet of cable four inches from the floor in the manner shown in Figure 13 has degraded the conductor-to-conduit shielding effectiveness of the cable by about 4.5 dB. This is no doubt due to the more non-uniform peripheral current distribution which occurs both at the bend in the cable armor and along the surface of the armor spaced four inches from the ground plane. The conductor-to-conductor induced voltages, as would be expected, were not affected by the change in cable location.

The affect of the additional ground connections was to divert the current flowing in the armor to ground at points along the cable. In an actual

installation engulfed by an H-field, these multiple grounds would serve to shorten conductor loops which could in effect limit the current and induced voltages developed in these loops.

5.0 H-FIELD TESTS

The current which will flow on a conduit system in an NEMP environment will be an induced current resulting from the changing H-field flux linking the conduit. In the injected current tests only an injected current flow on the conduit was considered and the conduit was not simultaneously engulfed by a changing magnetic field. To determine whether the injected current tests have simulation validity, a series of tests were made which allowed measurement of the induced voltages on conductors within conduit when the conduit was both carrying pulse current and engulfed by a varying H-field.

The general test setup showing the radiating loop and the conduit loop was shown in Figure 4. Current measurements in both the radiating and conduit loops were measured with a 0.03664 ohm shunt. For monitoring the current while making induced voltage measurements on conductors within the conduit, a toroidal current transformer which clamped around the conduit was used.

The measurement system was the same as that used for the injected current tests. The current wave shape applied to the radiating loop was similar to that applied in the injected current tests. The induced current wave shape as measured from the conduit loop was similar to the applied current wave shape. Figure 40 shows the comparison of wave shapes of the applied radiator current measured with both the current shunt and the transducer and the conduit loop induced current measured with the current transducer only. Note the similarity of the applied and induced wave shape.

5.1 H-Field Measurements

It was recognized that the H-field generated by the radiating loop and surrounding the conduit loop would be a function of the magnitude of the

induced current in the conduit loop as well as the current being injected in the radiating loop. The intensity of this field near the conduit is of interest since the conduit traverses this field. Therefore, the H-field surrounding the conduit loop was measured for two conditions, 1) with the conduit loop carrying an induced current which will be used in all tests and 2) the conduit loop open and carrying no current at all. The H-field plots were made with the probe shown in Figure 5. Figure 41 gives the H-field intensities with the conduit loop open and with a pulse current of 1755 amperes applied to the radiating loop. Figure 42 shows the H-field intensities with induced current flowing in the conduit loop. Analyzing these plots, two things are immediately apparent. One, the H-field within the conduit loop in the vicinity of the ground plane undergoes a considerable change both in magnitude and polarity when the conduit loop has current induced in it and two, because of transformer action, the shorted conduit loop loads the current generating circuit resulting in a lower current crest of 1690 amperes. The 1690 amperes flowing in the radiating loop resulted in 490 amperes induced in the conduit loop.

5.2 Conductor-to-Conduit Induced Voltages Measured in Conduit Loop Systems Carrying Induced Currents

Many of the conduit systems tested by current injection such as those containing 90° elbows, condulets, and couplings as well as conduit systems of other sizes and materials were tested by the H-field method. Because of the disparity in H-field intensity surrounding the top and bottom lengths of the conduit loop, the conductor within the conduit loop was electrically connected to the conduit in the upper corner opposite the conduit loop ground connection. This in effect resulted in two L-shaped conduit sections carrying the same current but traversing different H-field intensities.

Using this same conduit and conductor configuration, the following was evaluated:

induced current in the conduit loop as well as the current being injected in the radiating loop. The intensity of this field near the conduit is of interest since the conduit traverses this field. Therefore, the H-field surrounding the conduit loop was measured for two conditions, 1) with the conduit loop carrying an induced current which will be used in all tests and 2) the conduit loop open and carrying no current at all. The H-field plots were made with the probe shown in Figure 5. Figure 41 gives the H-field intensities with the conduit loop open and with a pulse current of 1755 amperes applied to the radiating loop. Figure 42 shows the H-field intensities with induced current flowing in the conduit loop. Analyzing these plots, two things are immediately apparent. One, the H-field within the conduit loop in the vicinity of the ground plane undergoes a considerable change both in magnitude and polarity when the conduit loop has current induced in it and two, because of transformer action, the shorted conduit loop loads the current generating circuit resulting in a lower current crest of 1690 amperes. The 1690 amperes flowing in the radiating loop resulted in 490 amperes induced in the conduit loop.

5.2 Conductor-to-Conduit Induced Voltages Measured in Conduit Loop Systems Carrying Induced Currents

Many of the conduit systems tested by current injection such as those containing 90° elbows, condulets, and couplings as well as conduit systems of other sizes and materials were tested by the H-field method. Because of the disparity in H-field intensity surrounding the top and bottom lengths of the conduit loop, the conductor within the conduit loop was electrically connected to the conduit in the upper corner opposite the conduit loop ground connection. This in effect resulted in two L-shaped conduit sections carrying the same current but traversing different H-field intensities.

Using this same conduit and conductor configuration, the following was evaluated:

Traversing the smaller H-field

1. 2 inch rigid steel conduit - one 90° elbow
2. 1 inch rigid steel conduit - one 90° elbow
3. 1 inch steel thin wall - one 90° elbow
4. 2 inch aluminum conduit - one 90° elbow
5. 2 inch rigid steel conduit - one condulet

Traversing the larger H-field

1. 2 inch rigid steel conduit - two 90° elbows
2. 1 inch rigid steel conduit - two 90° elbows
3. 1 inch steel thin wall - two 90° elbows
4. 2 inch aluminum conduit - two 90° elbows
5. 2 inch rigid steel conduit - two condulets

The wave shapes resulting from each of these tests are shown in Figures 43, 44, 45, and 46. The pertinent data is tabulated in Table 18.

TABLE 18

COMPARISON OF INDUCED CONDUCTOR TO CONDUIT INDUCED VOLTAGES FROM TOP AND BOTTOM OF A CONDUIT LOOP HAVING VARIED CONSTRUCTIONAL HARDWARE

Conductor Measured	Conductor-to-Conduit Voltages				
	Steel Conduit				Al Conduit
	2" Condulets	2" Elbows	1" Elbows	1" Thin Wall	2" Elbows
	First Peak				
Top-to-Conduit	44 MV	240 MV	160 MV	125 MV	125 MV
Bottom-to-Conduit	88 MV	105 MV	110 MV	110 MV	60 MV
	IR Peak				
Top-to-Conduit	2.8 MV	3.5 MV	5 MV	135 MV	105 MV
Bottom-to-Conduit	3.6 MV	3.8 MV	6.5 MV	135 MV	145 MV

Note: Top conduit traverses larger H-field.

While it is difficult to make direct comparisons between the top and bottom conduit systems (the top conduit system consisted of 11 threaded joints and two 90° devices, either condulets or elbows; the bottom conduit system contained 10 threaded joints and one 90° device, either condulet or elbow), some interesting observations can be made. First, the top half conduit system had the higher induced flux leakage voltage. This is to be expected, since the H-field surrounding the top half conduit was higher. (The top half conduit experienced an H-field approaching 500 amperes/meter.) Secondly, the magnitude of the induced flux leakage voltages measured in both halves are somewhat higher for the induced current tests than they were for the injected current tests. (The conduit system with condulets was the only exception.) For example, from Section 4.6, Table 6, an injected current of 1755 amperes on a two inch rigid steel conduit system containing one elbow produced a conductor-to-conduit induced voltage of 60 MV. At 490 amperes injected, the induced voltage would have been approximately 17 MV which is considerably less than the induced voltages measured and given in Table 18.

When comparing the IR peak induced voltages resulting from the induced current and injected current tests, the reverse is true. The injected current tests gave the higher IR induced voltages. This is probably due to the current reversal of the induced current on the conduit resulting in a varying saturation of the steel conduit.

From a conduit system design standpoint, "worst case" design for the overall conduit system can be obtained by using the injected current test results since extrapolation of the data to longer lengths involving the IR induced voltages will be a controlling factor in the design.

6.0 SUMMARY

1. Conduits exposed to a pulsed H-field environment will result in induced currents flowing on the conduits. These currents produce a magnetic field in addition to the driving H-field which can couple electrical

wiring within the conduit. The magnetic flux which couples the electrical wiring causes transient voltages to be induced on the wiring.

2. The H-field induced conduit current and the resultant induced voltages on electrical wiring within the conduit can be simulated by injecting a current pulse of similar wave shape directly on the conduit.
3. The wave shapes of the induced conductor-to-conduit voltages on wiring resulting from the simulated pulse currents applied show an initial peak cresting at the time of the maximum di/dt of the applied current wave and a second peak cresting long after the current wave has reached zero. The first peak is the result of flux leakages at joints, bends, or other openings; the second peak is related to the rate of current diffusion through the conduit wall. Wave shapes of induced voltages between a pair of conductors do not show the presence of the second peak.

   Both first peak and second peak magnitudes, for design purposes, will scale linearly with pulse current amplitude.
4. The rate of current diffusion through the conduit wall is a function of the conduit wall thickness, relative permeability, and resistivity:

$$\text{Diffusion Time} \propto \frac{(t)^2 \mu_r}{\rho}$$

   This infers that the best shielding against NEMP can be achieved by use of conduit having a high permeability, a large wall thickness, and a low resistivity. This assumes, of course, that the conduit system has properly made tight joints.
5. A two inch rigid steel conduit system with tightly made, clean, threaded joints and containing no condulets will provide at least 60 dB of shielding for the electrical wiring within it. Welded joints can improve the shielding effectiveness of the conduit by about 8 dB.
6. The use of condulets in a two inch rigid steel conduit system can degrade the shielding effectiveness by 20 dB.

7. Openings such as condulet covers removed or very loose threaded joints can degrade the shielding effectiveness of a two inch rigid steel conduit system by 40 dB.
8. The use of a one inch rigid steel conduit for protection of electrical wiring against NEMP increases the IR induced voltage by a factor of 2 over that resulting from wiring in a two inch rigid steel conduit system.
9. In terms of the voltage induced between conductors in electrical circuitry due to pulse current on the conduit, twisted pair wiring has a 5:1 advantage over parallel pair wiring.
10. From an NEMP point of view, wrought iron conduit has no advantage over rigid steel conduit and either type is suitable for shielding open wiring.
11. The use of a short section of flexible bellows at building entrances or other locations requiring flexibility would not seriously degrade the shielding effectiveness of a long steel conduit run. Caution should be exercised in their use for wiring from circuits which are extremely critical.
12. The use of standard grade flexible steel conduit is not recommended for use, since it provides practically no shielding. Sealtite® flexible conduit, while providing greater shielding than the standard grade, is also not recommended for general use. Application information for using this material with power circuits within buildings is being developed.
13. Aluminum or steel armored power cable should only be used within buildings or rooms.

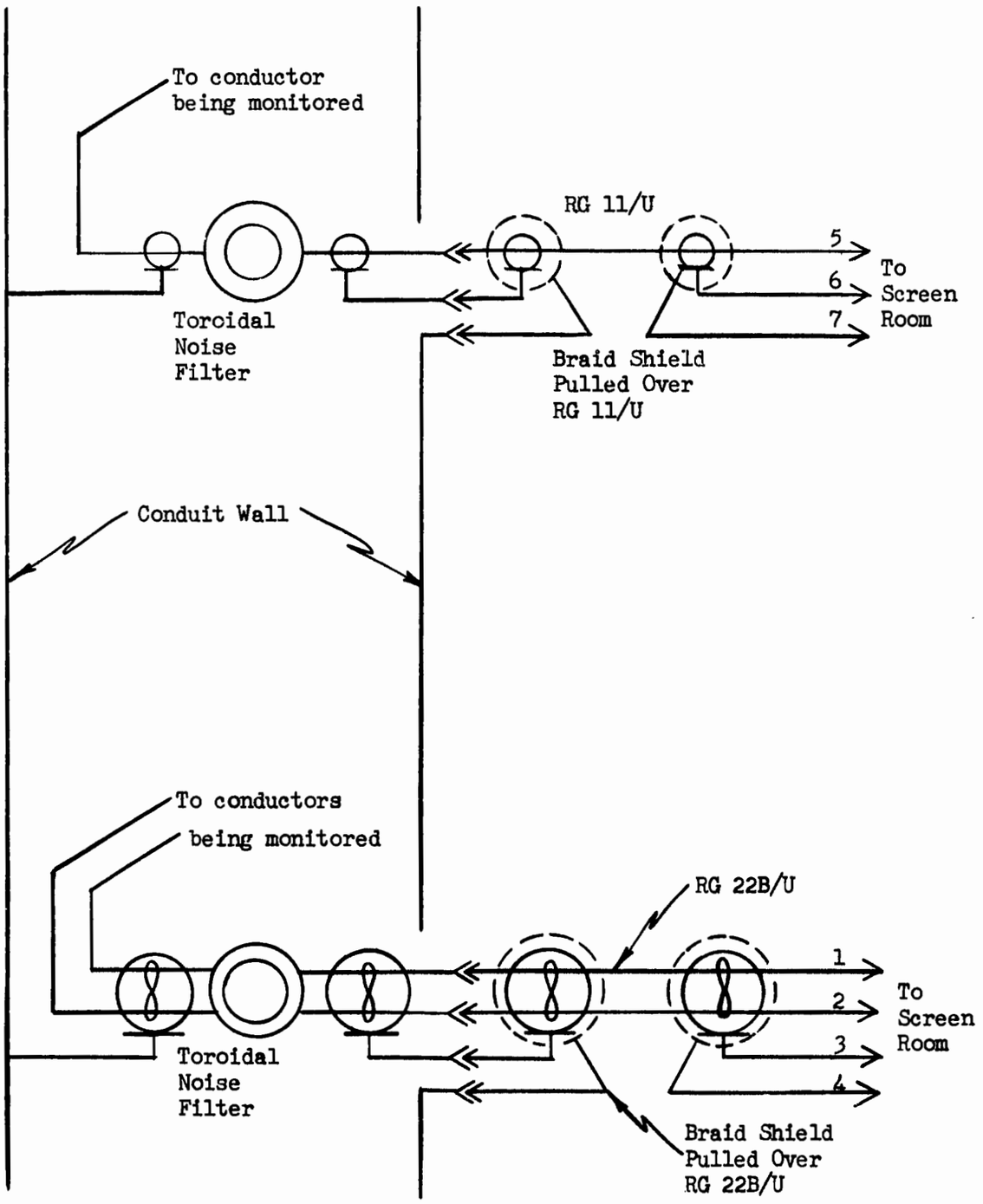

FIGURE 1 Conductor-to-Conduit and Conductor-to-Conductor Measurement System (conduit end)

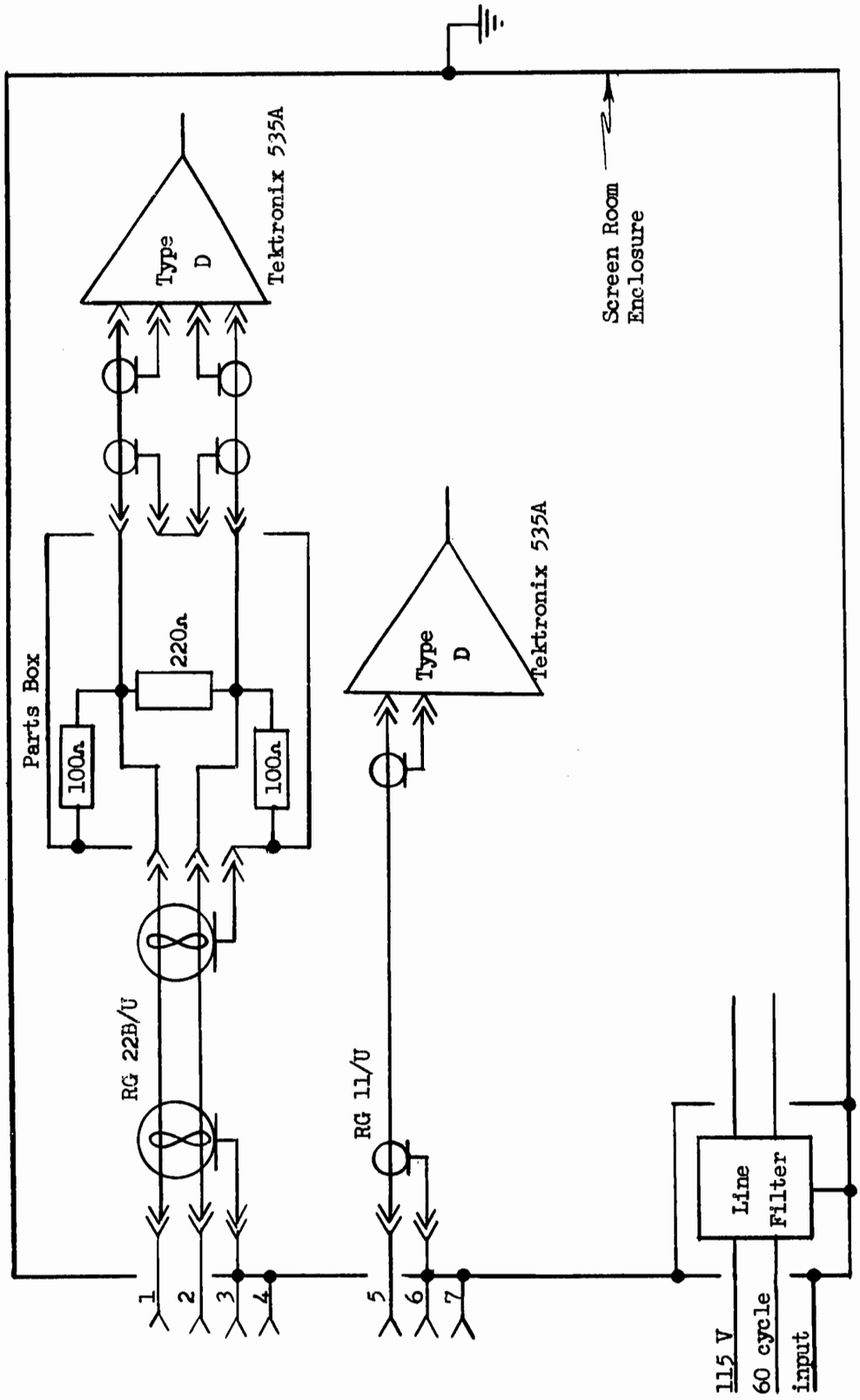

FIGURE 2 Conductor-to-Conduit and Conductor-to-Conductor Measurement System (instrumentation end)

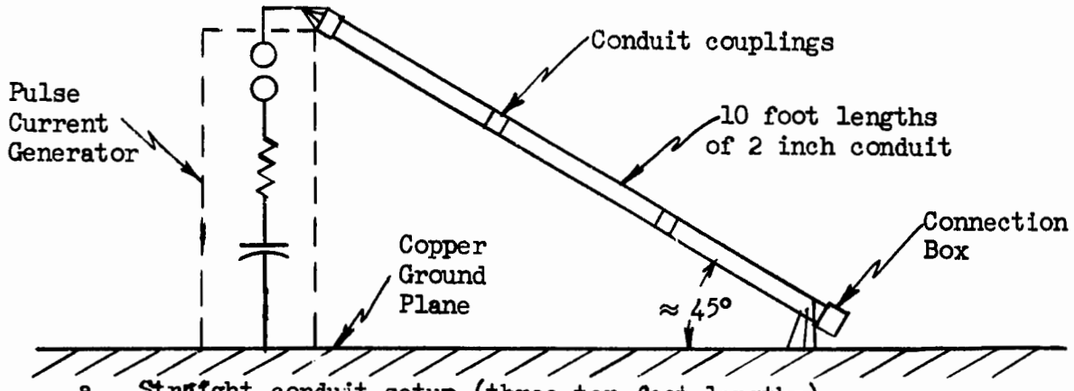

a. Straight conduit setup (three ten foot lengths)

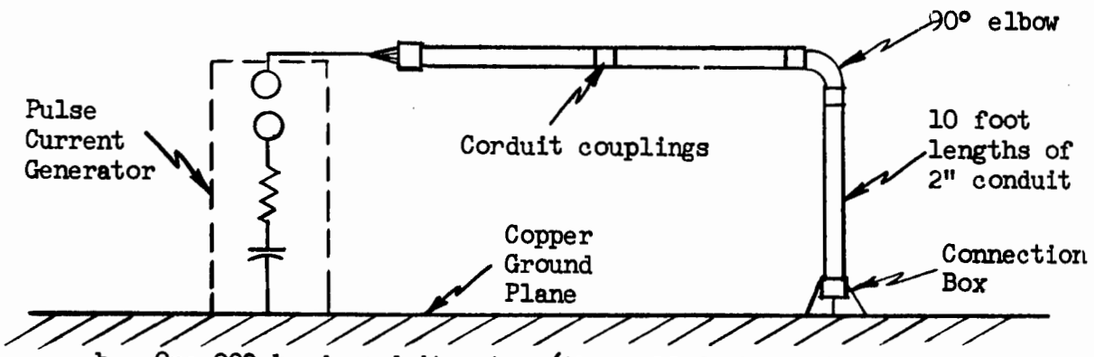

b. One 90° bend conduit setup (three 10 foot lengths and one 90° elbow)

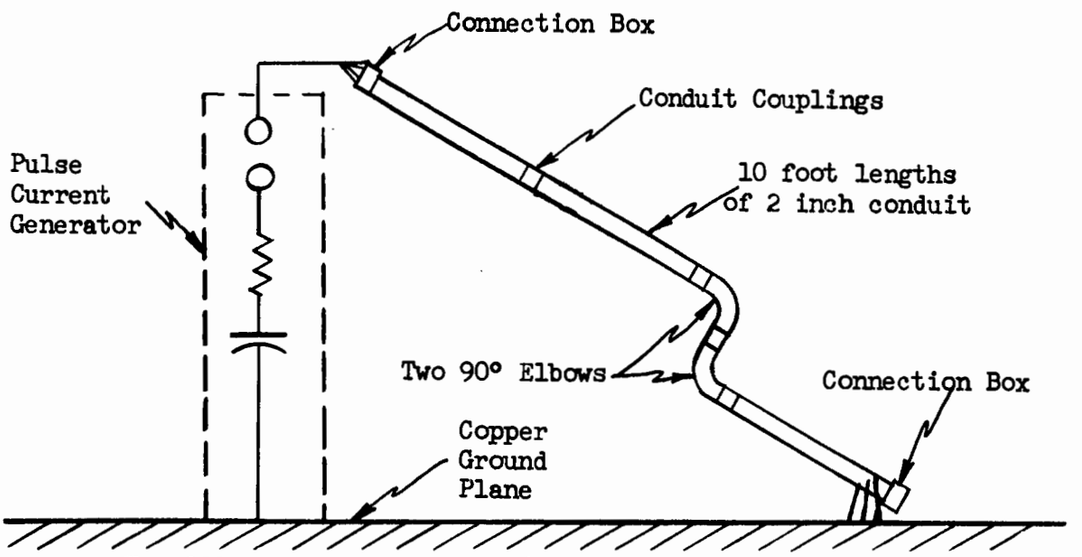

c. Two 90° bend conduit setup (three 10 foot lengths and two 90° elbows)

FIGURE 3 Various Conduit Test Configurations

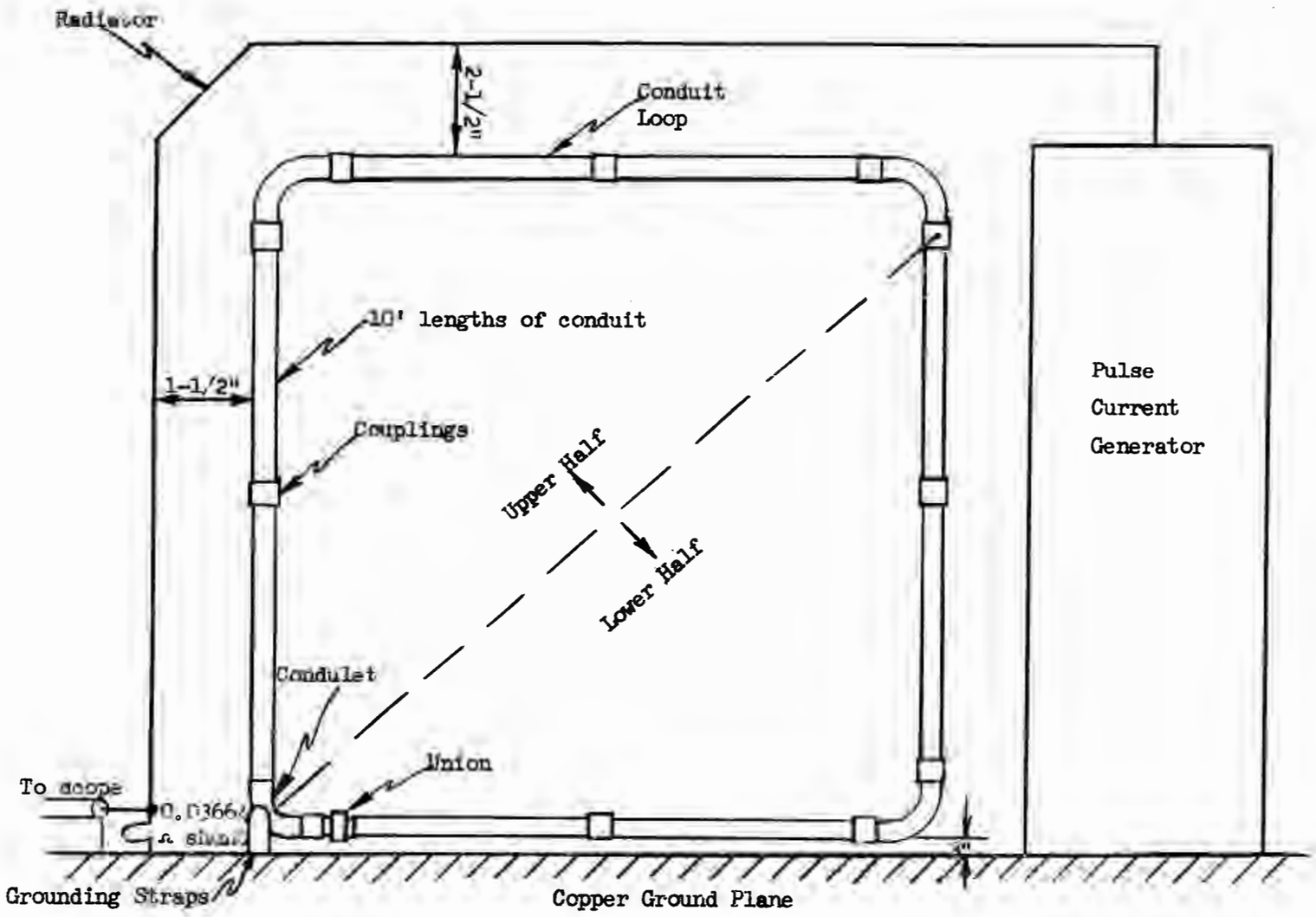

FIGURE 4 Configuration for Currents Induced in Conduit Loop

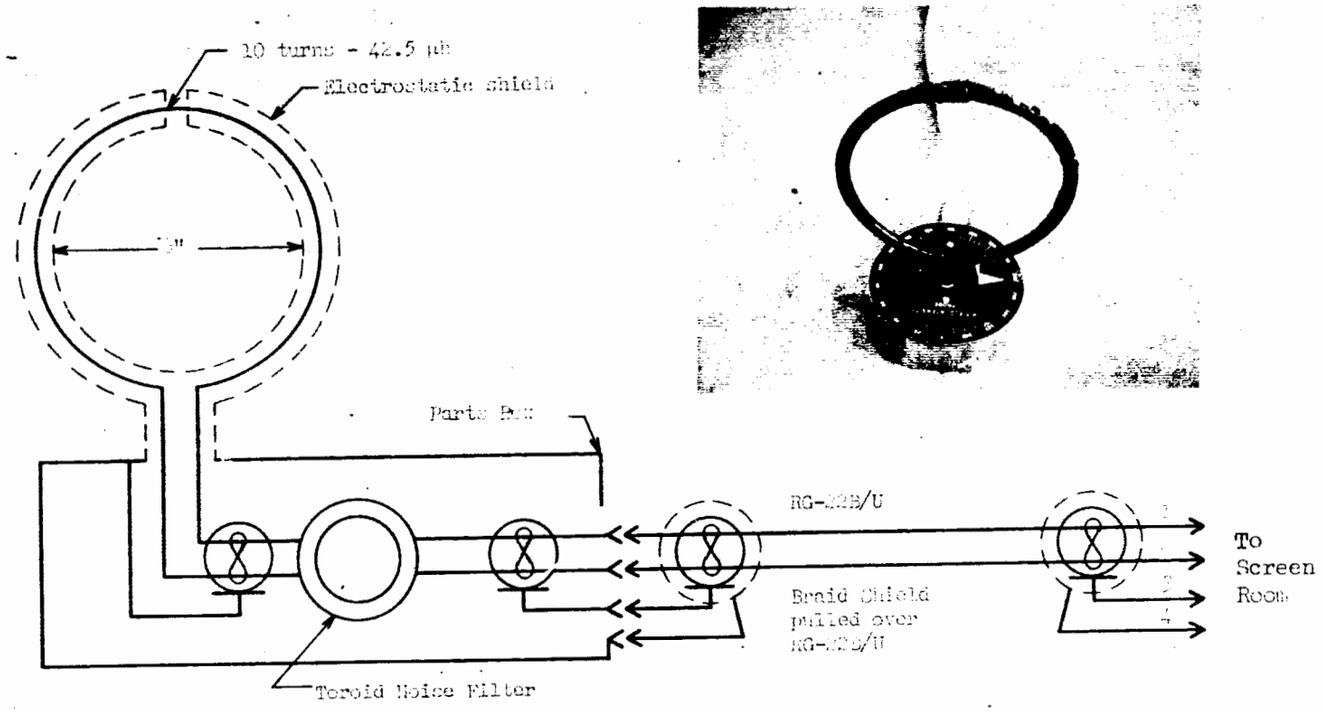

Fig. 5 H-Field Transducer

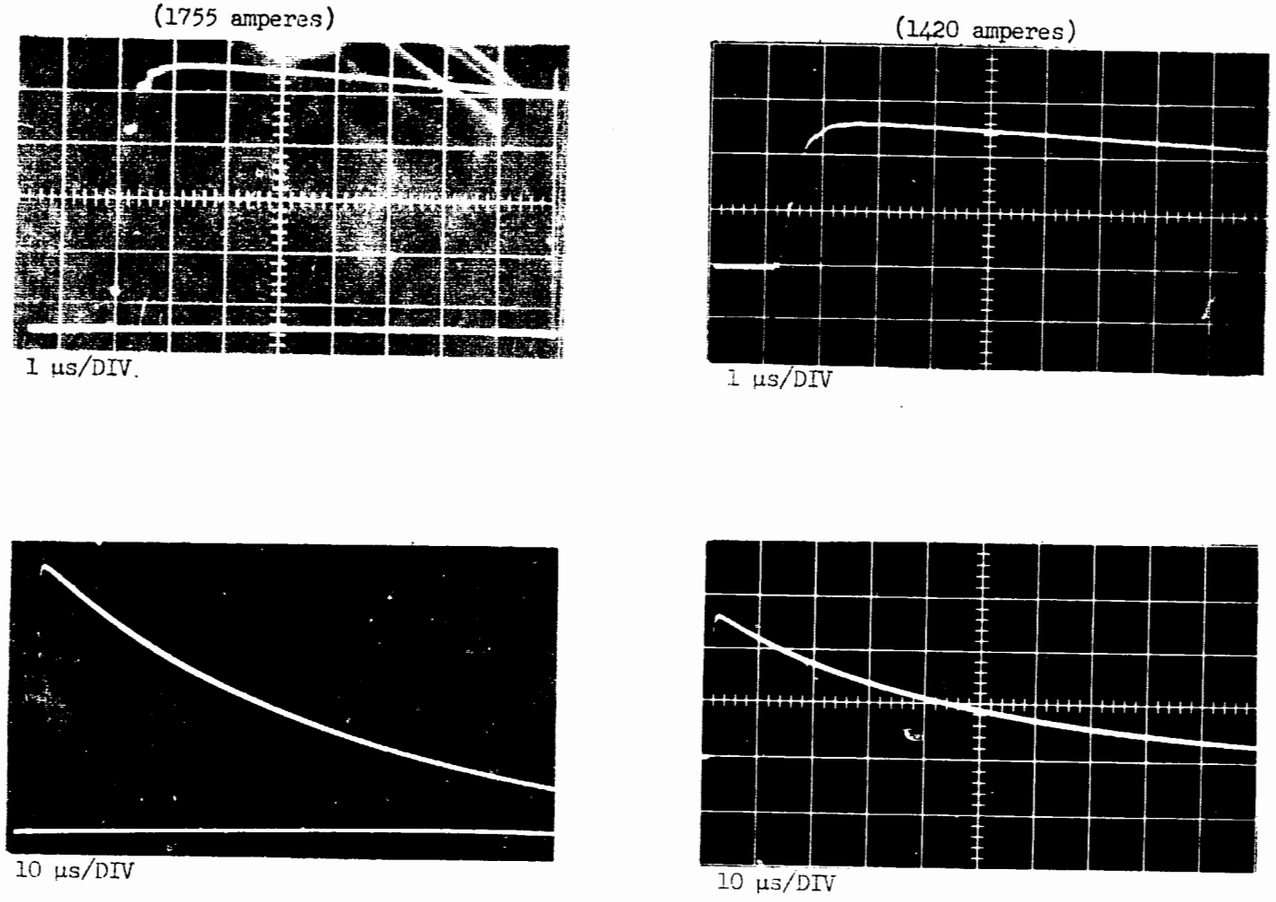

FIGURE 6 Pulse Current Wave Shapes for Injected Current Tests

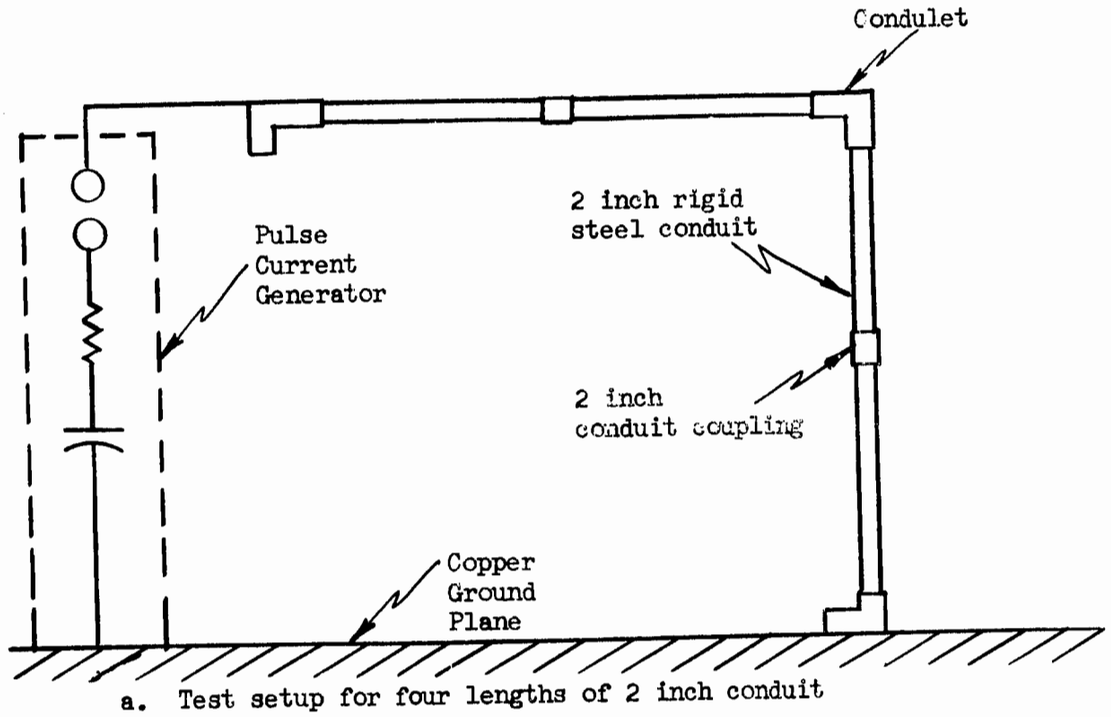

a. Test setup for four lengths of 2 inch conduit

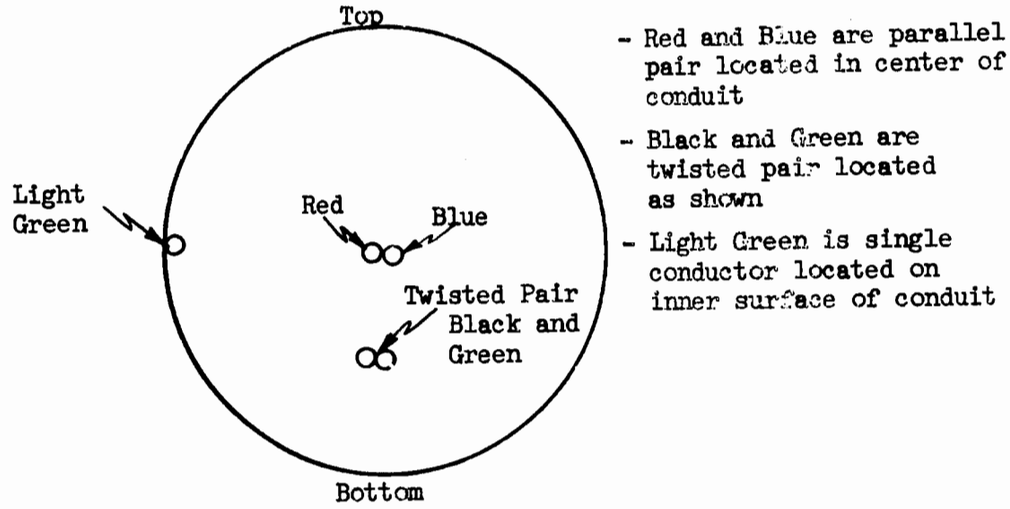

b. Conductor arrangement within the conduit cross section

FIGURE 7 L-Shaped Conduit Test Configuration

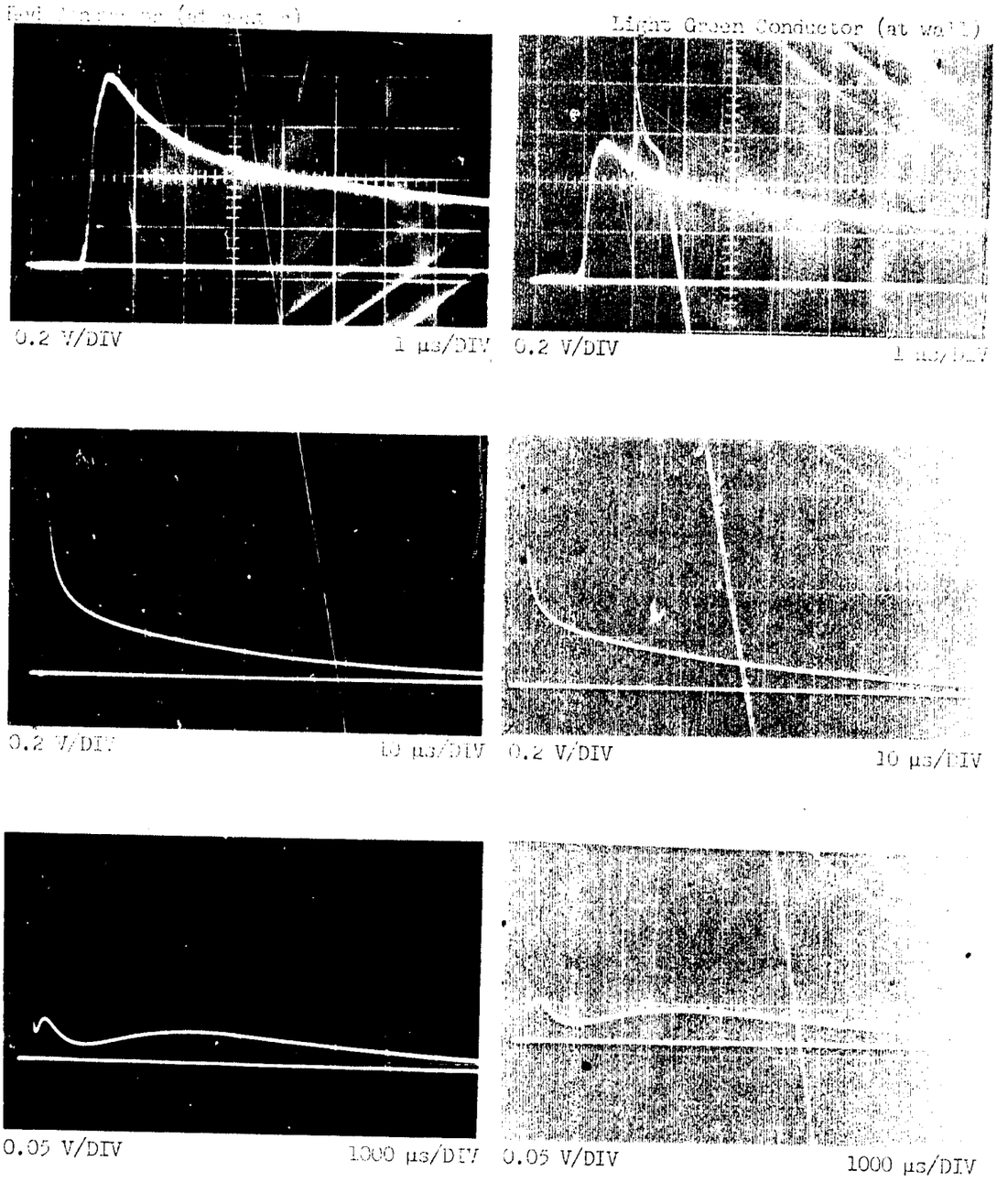

FIGURE 8 Wave Shape of Induced Conductor-to-Conduit Voltages Showing Effect of Conductor Location.
Applied Pulse Current - 1755 amperes

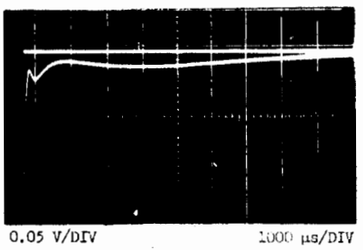

Induced voltage measured during application of 20th negative polarity wave

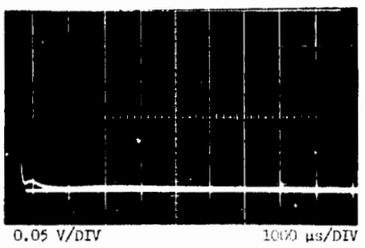

Induced voltage measured during application of first positive polarity wave after the 20th negative polarity wave

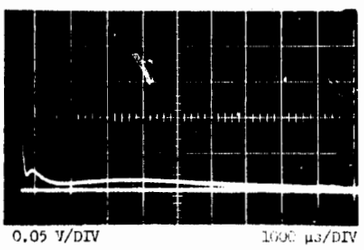

Induced voltage measured during application of third positive polarity wave

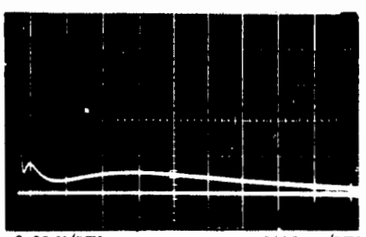

Induced voltage measured during application of tenth positive polarity wave

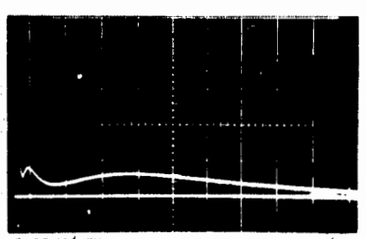

Induced voltage measured during application of 20th positive polarity wave

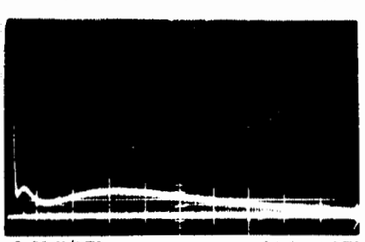

Induced voltage measured during application of 50th positive polarity wave

FIGURE 9 Wave Shapes of Conductor-to-Conduit Induced Voltages Showing Effect of Conduit Saturation. Applied Pulse Current - 1755 amperes

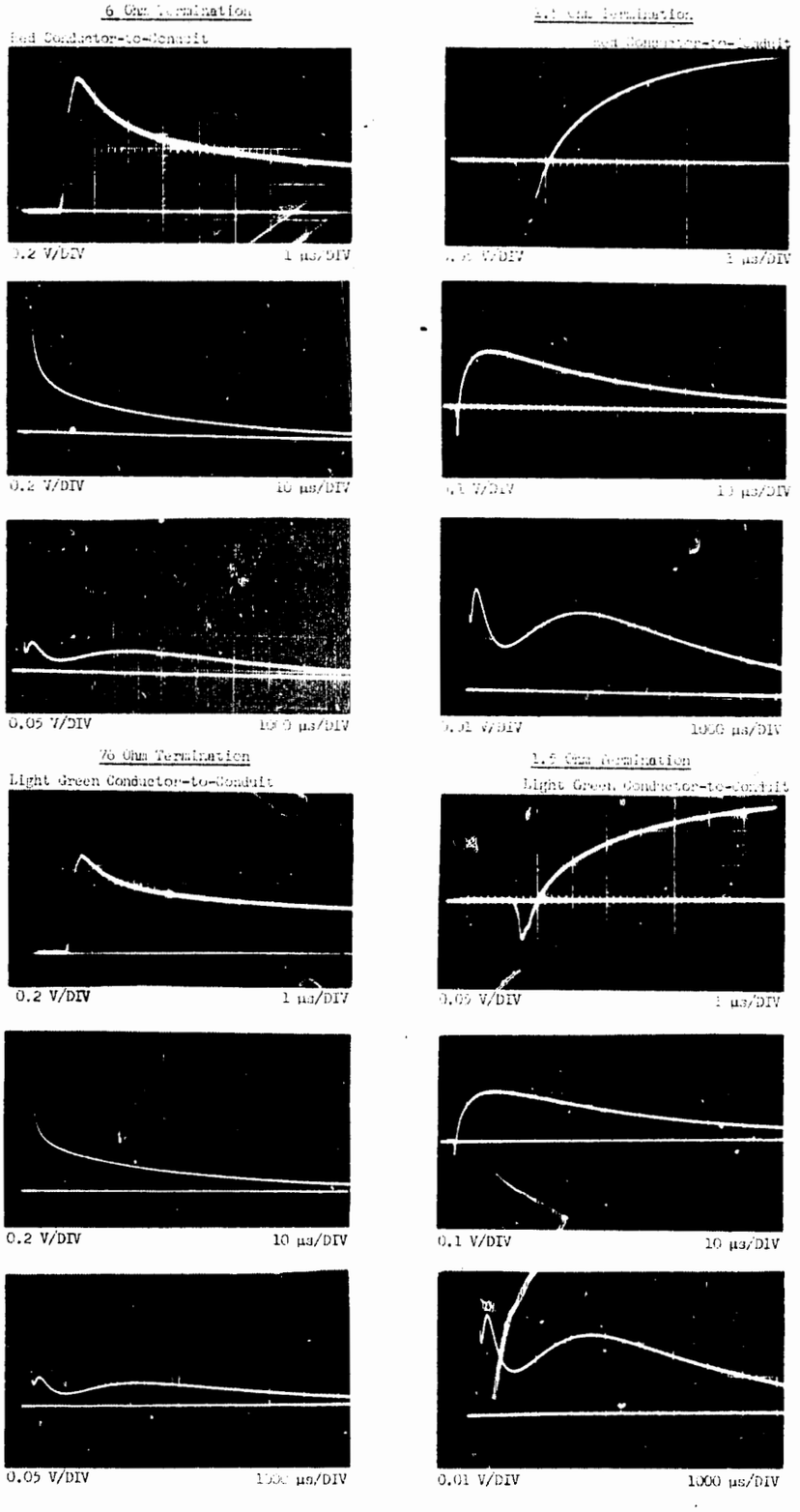

FIGURE 10 Wave Shapes of Conductor-to-Conduit Induced Voltages Showing Effects of Terminating Impedance. Applied Pulse Current - 1755 amperes

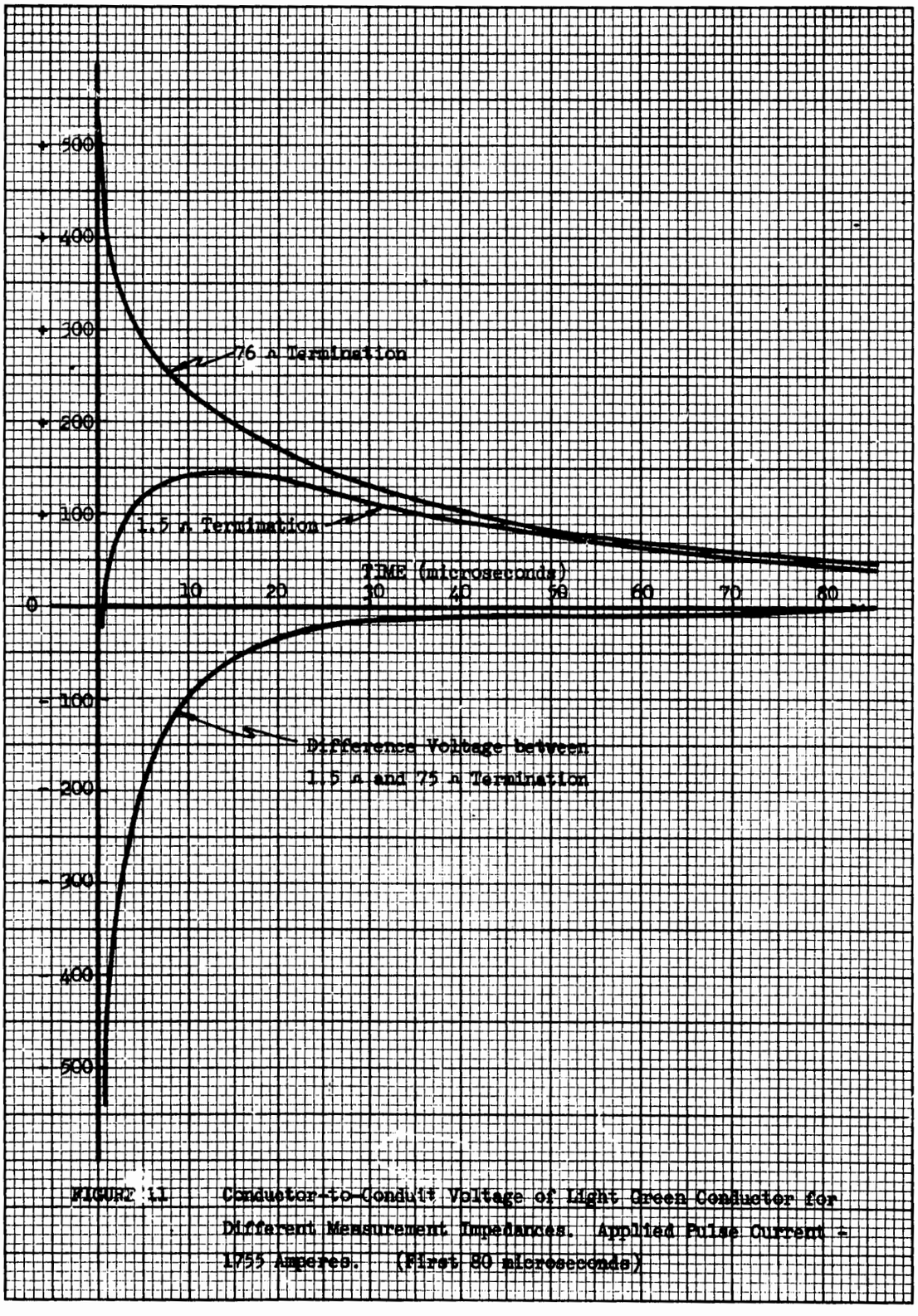

FIGURE 11 Conductor-to-Conduit Voltage of Light Green Conductor for Different Measurement Impedances. Applied Pulse Current = 1755 Amperes. (First 80 microseconds)

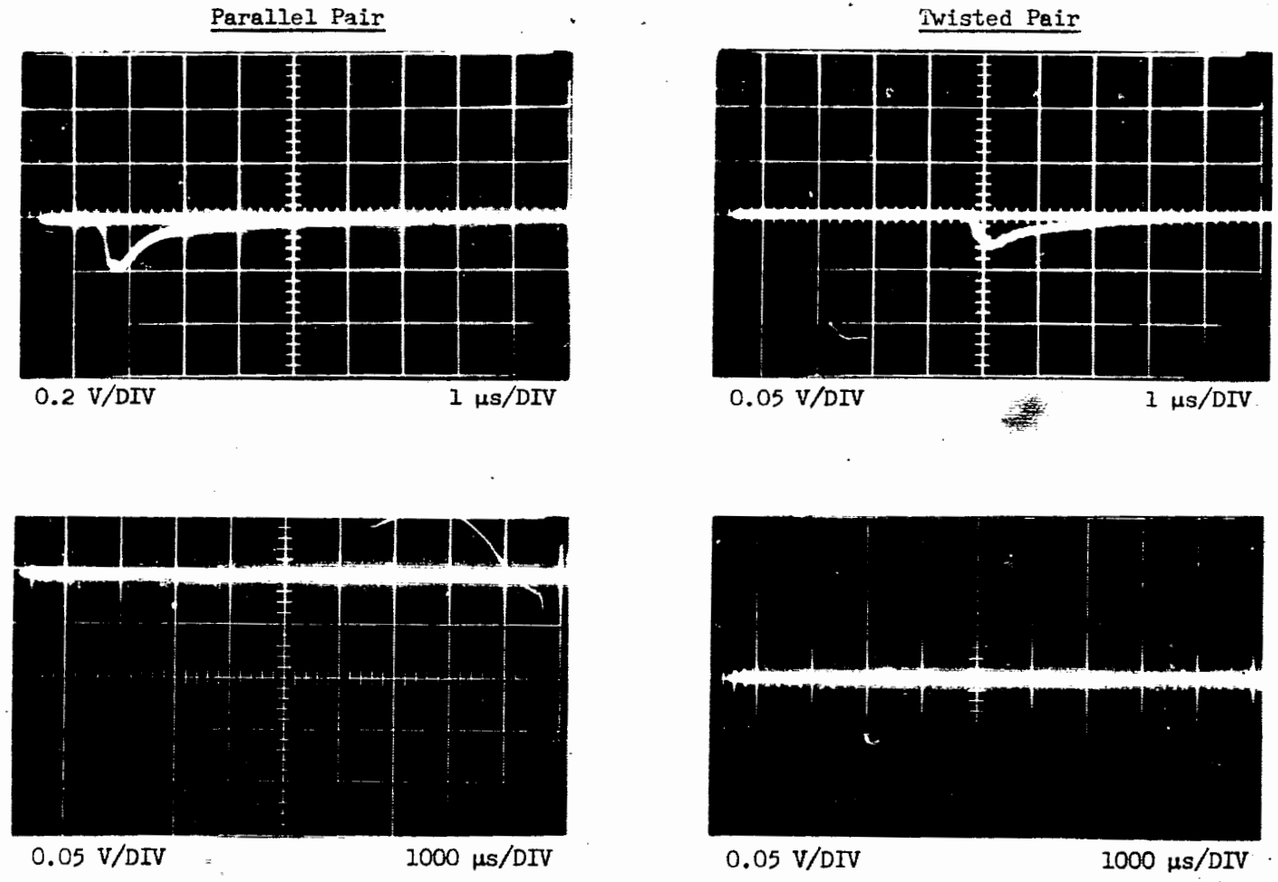

FIGURE 12 Wave Shapes of Conductor-to-Conductor Induced Voltages on Twisted Pair and Parallel Pair Conductors. Applied Pulse Current - 1755 amps

1. All Condulet Covers in Place

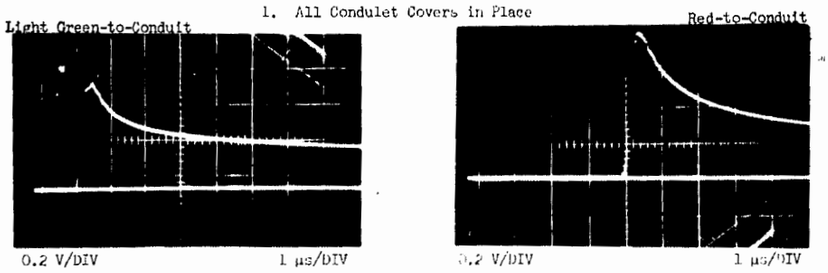

2. Generator End Condulet Cover Off

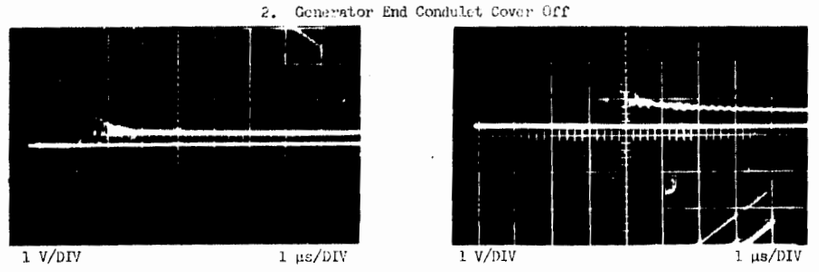

3. Measurement End Condulet Cover Off

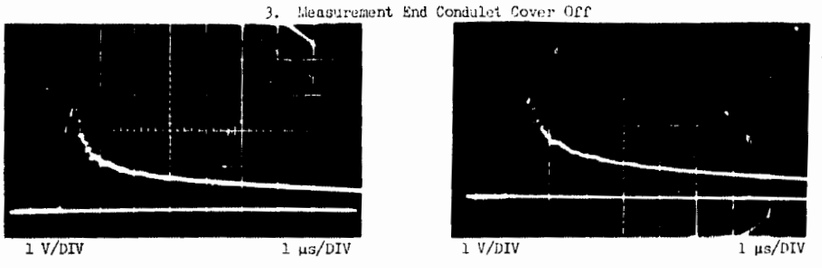

4. Corner Condulet Cover Off

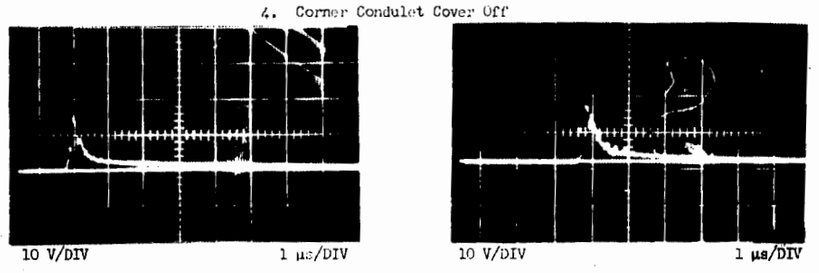

5. Corner and Measurement End Condulet Cover Off

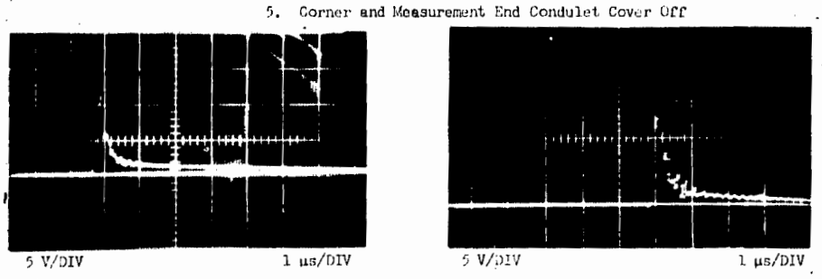

FIGURE 13 Wave Shape of Induced Conductor-to-Conduit Voltage Showing Effect of Openings in the Conduit System. Applied Pulse Current - 1755 amperes

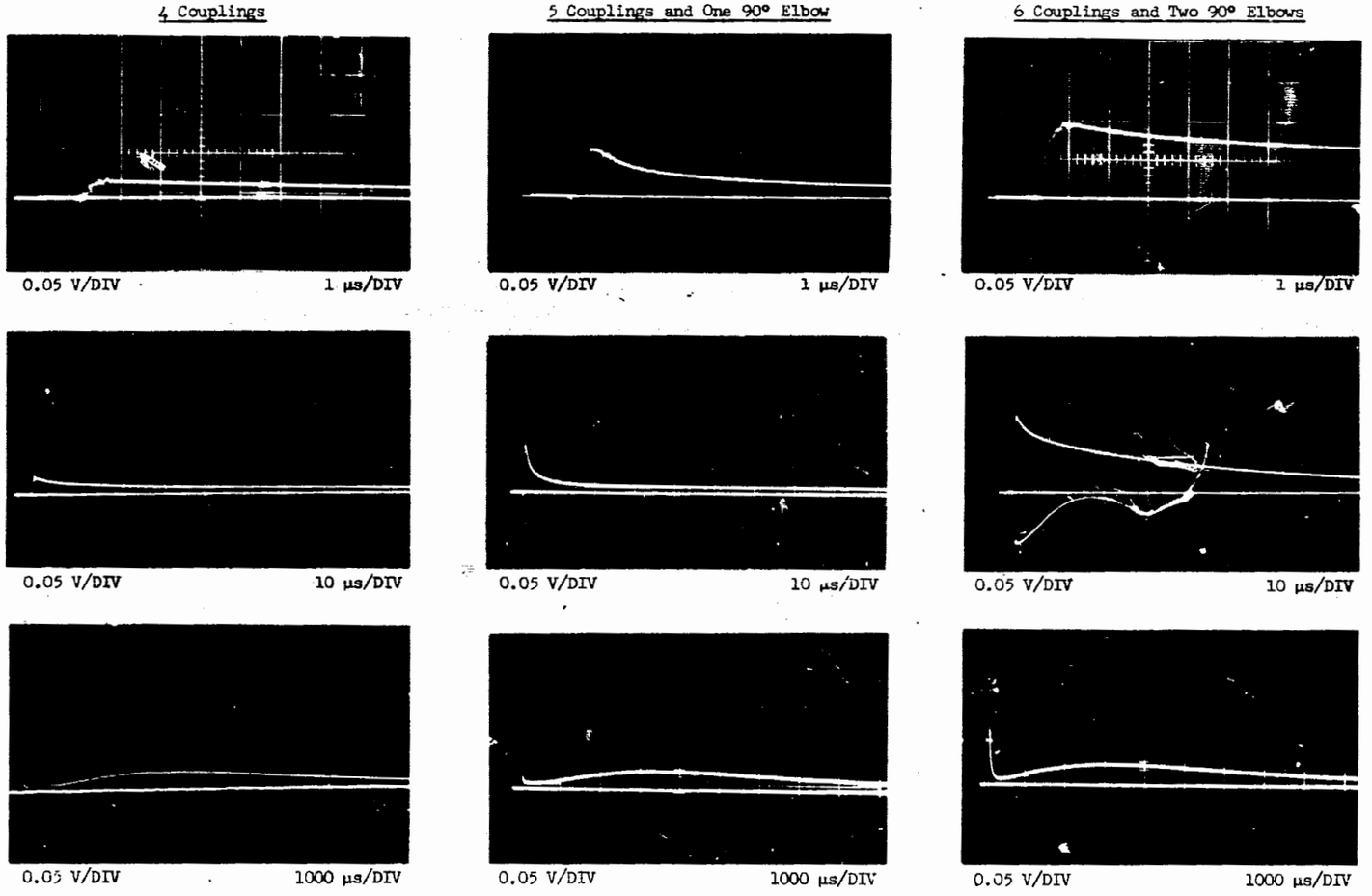

FIGURE 14 Wave Shapes of Induced Conductor-to-Conduit Voltages Showing Effect of Couplings and 90° Elbows. Applied Pulse Current - 1755 amperes

(Tight Joints)

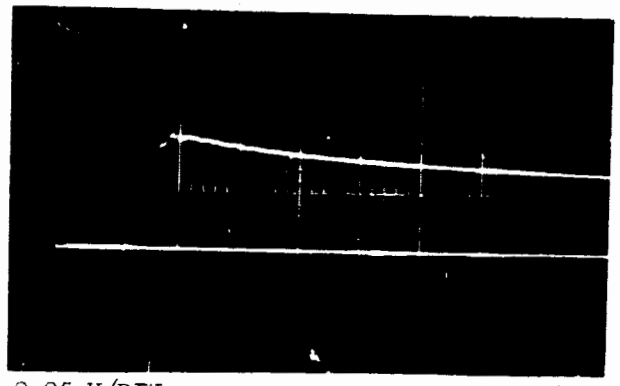

0.05 V/DIV 1 μs/DIV

(Loose Joints)

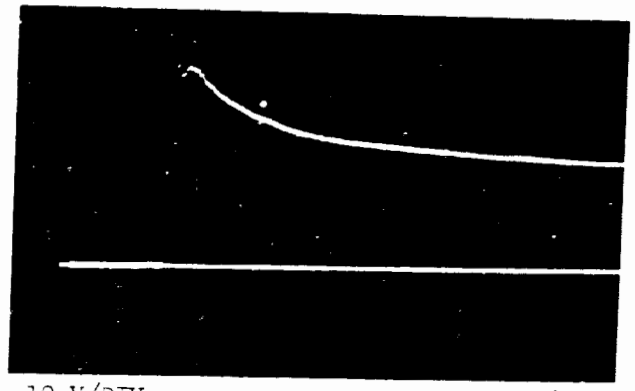

10 V/DIV 1 μs/DIV

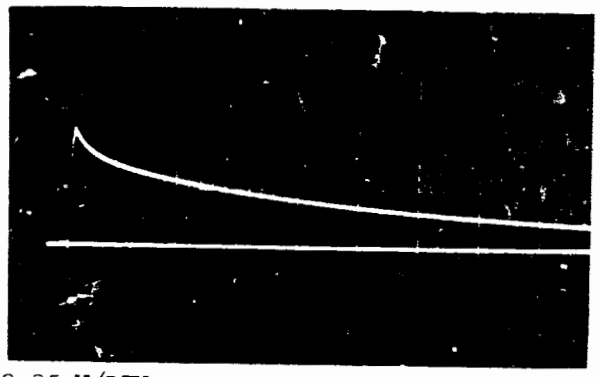

0.05 V/DIV 10 μs/DIV

10 V/DIV 10 μs/DIV

FIGURE 15 Wave Shapes of Induced Conductor-to-Conduit Voltages in Two Inch Conduit System Showing Effect of a Very Loose Joint

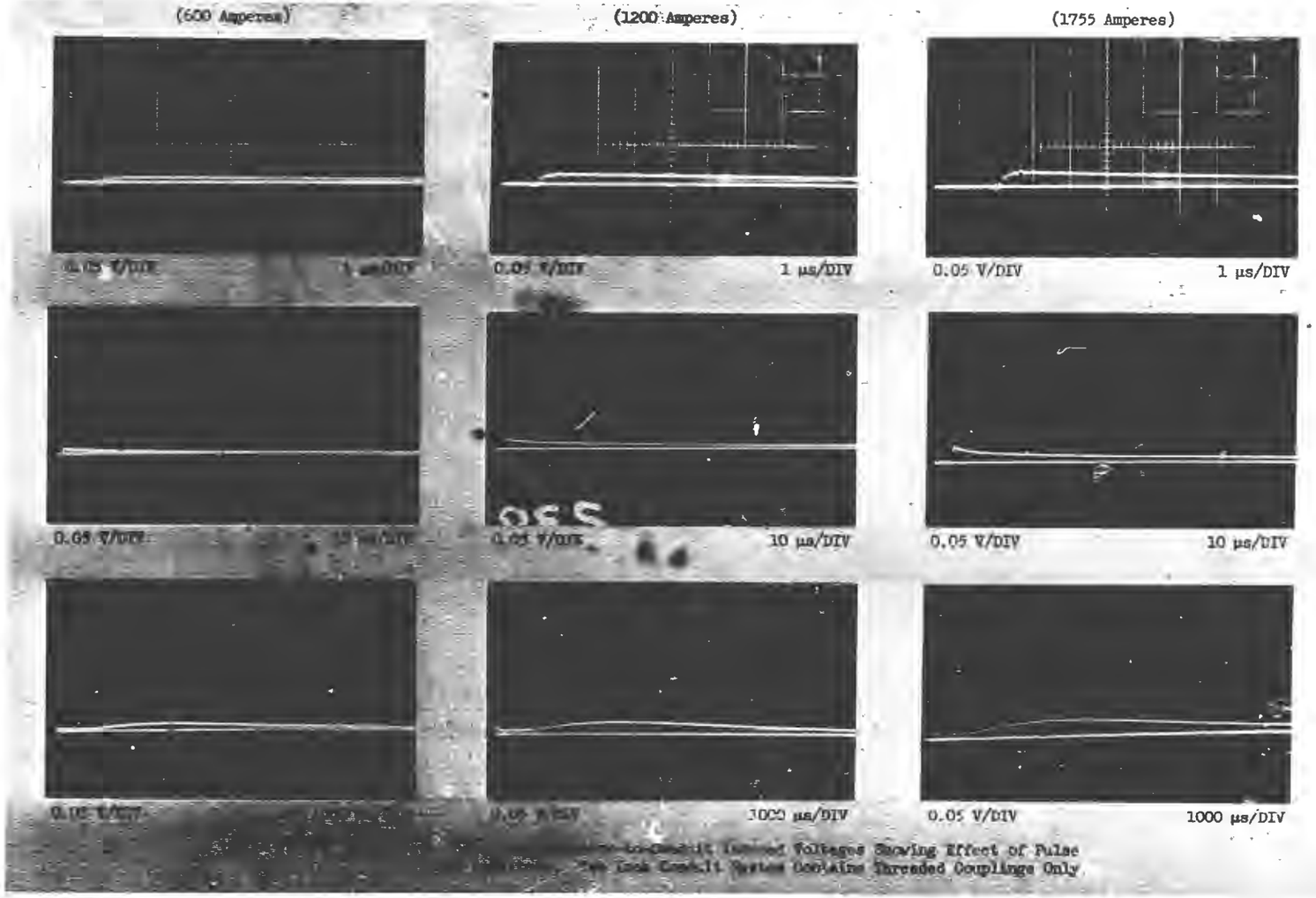
(600 Amperes)
(1200 Amperes)
(1755 Amperes)
0.05 V/DIV
1 μs/DIV
0.05 V/DIV
1 μs/DIV
0.05 V/DIV
1 μs/DIV
0.05 V/DIV
10 μs/DIV
0.05 V/DIV
10 μs/DIV
0.05 V/DIV
10 μs/DIV
0.05 V/DIV
1000 μs/DIV
0.05 V/DIV
1000 μs/DIV

- 50 -

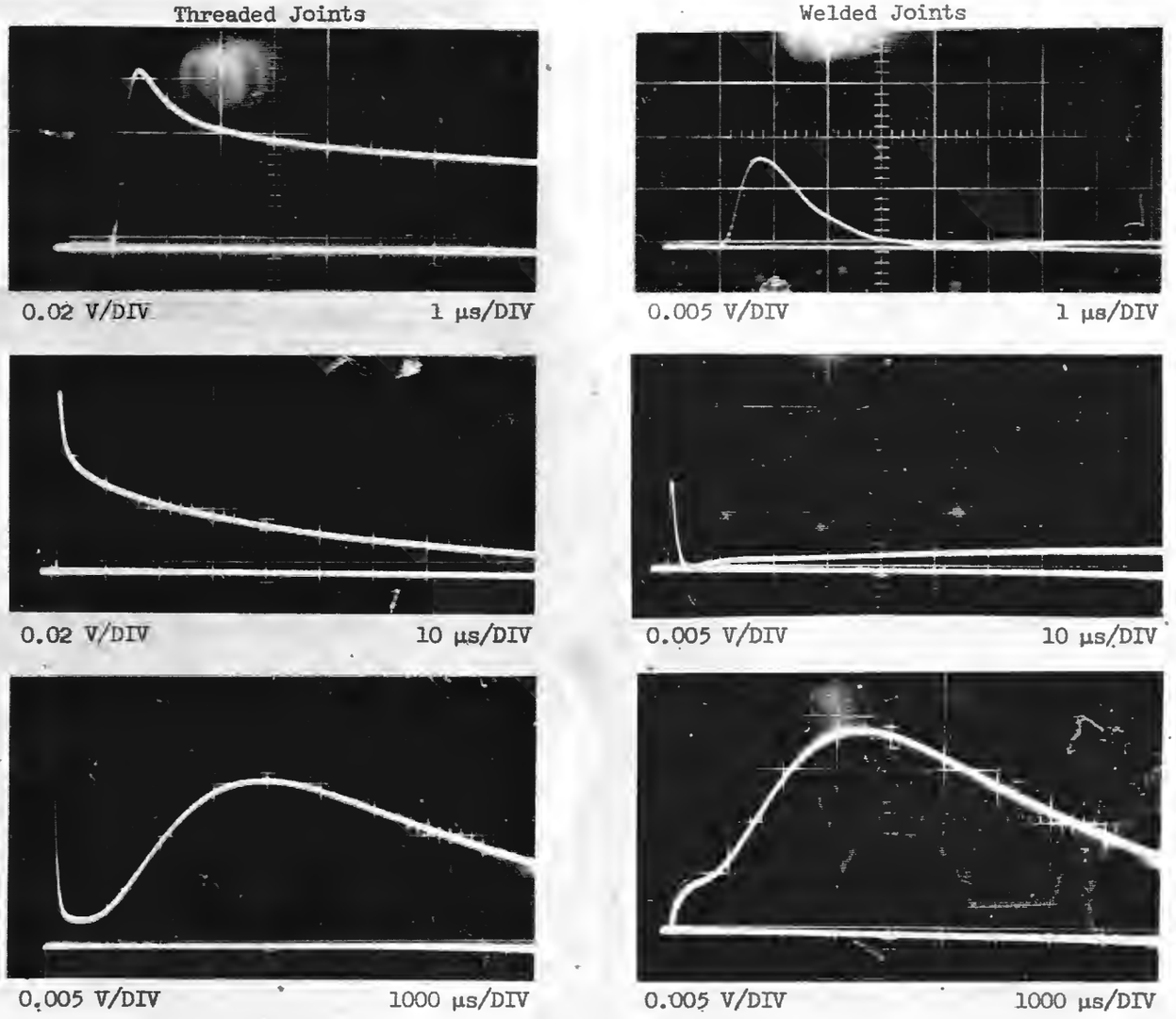

FIGURE 17 Wave Shapes of Conductor-to-Conduit Induced Voltages Showing Effect of Threaded or Welded Joints. Applied Pulse Current - 1755 amperes

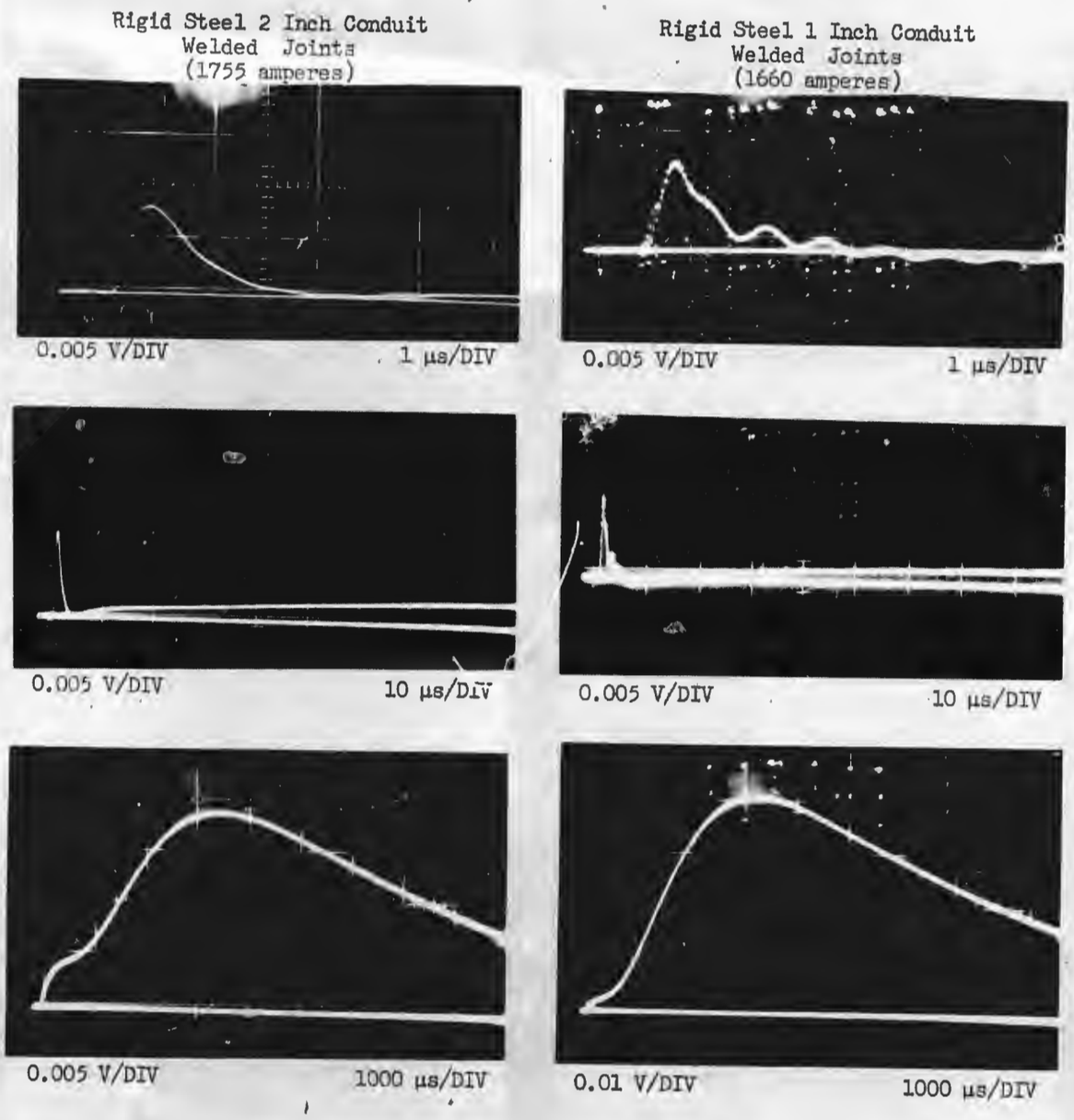

FIGURE 18 Wave Shapes of Conductor-to-Conduit Induced Voltages Showing Effect of Conduit Wall Thickness

Steel - 1755 amps Conduit Current

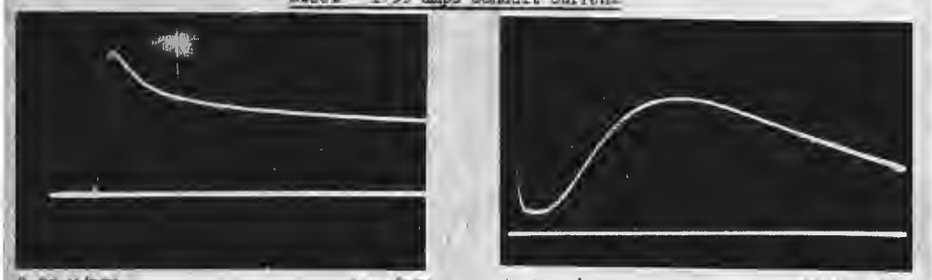

0.02 V/DIV 1 μs/DIV 0.005 V/DIV 1000 μs/DIV

Wrought Iron - 1420 amps Conduit Current

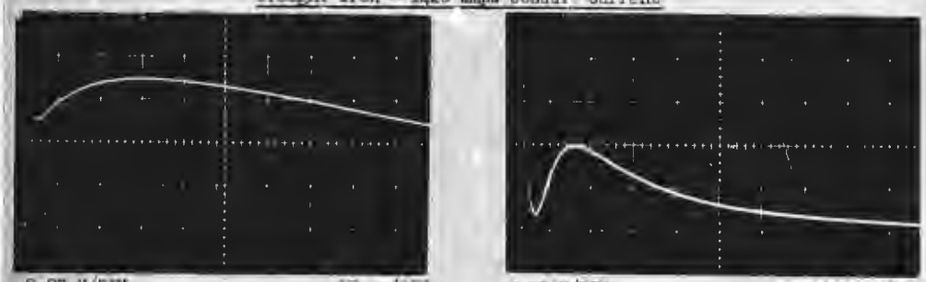

0.02 V/DIV 1 μs/DIV 0.02 V/DIV 1000 μs/DIV

A. Conductor-to-Conduit Induced Voltage

Steel - 1755 amps Conduit Current

0.005 V/DIV 1 μs/DIV 0.005 V/DIV 10 μs/DIV

Wrought Iron - 1420 amps Conduit Current

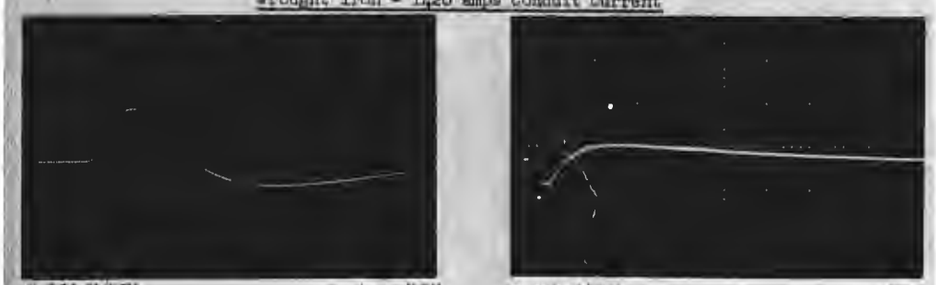

0.005 V/DIV 1 μs/DIV 0.005 V/DIV 10 μs/DIV

B. Conductor-to-Conductor Induced Voltage

FIGURE 19 Wave Shape of Induced Voltages on Conductors in Two Inch Conduit System Comparing Steel and Wrought Iron. Applied Pulse Current - 1755 amperes

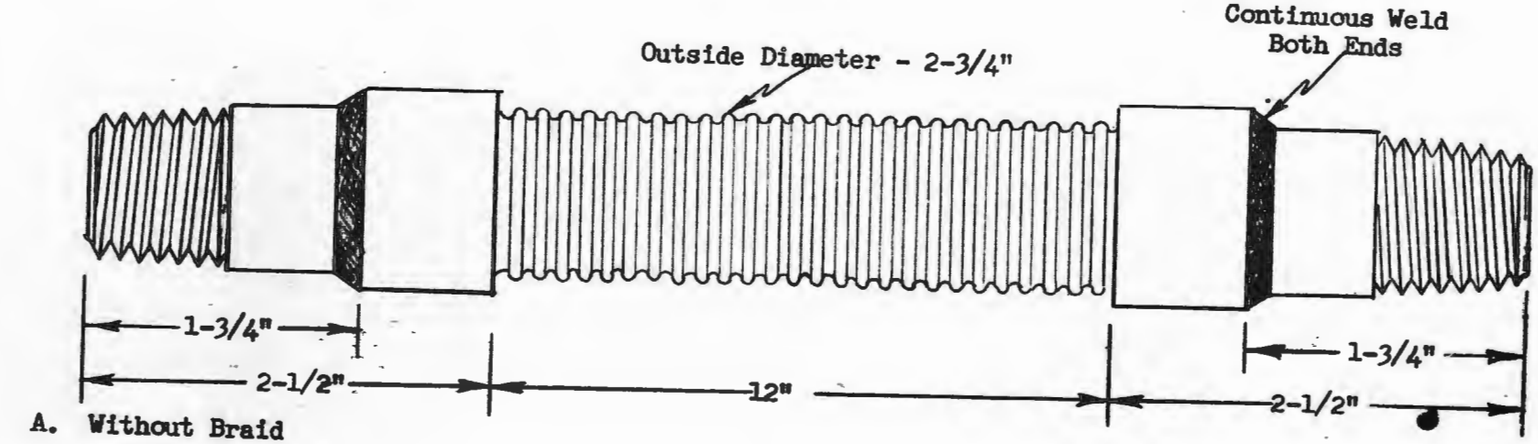

A. Without Braid

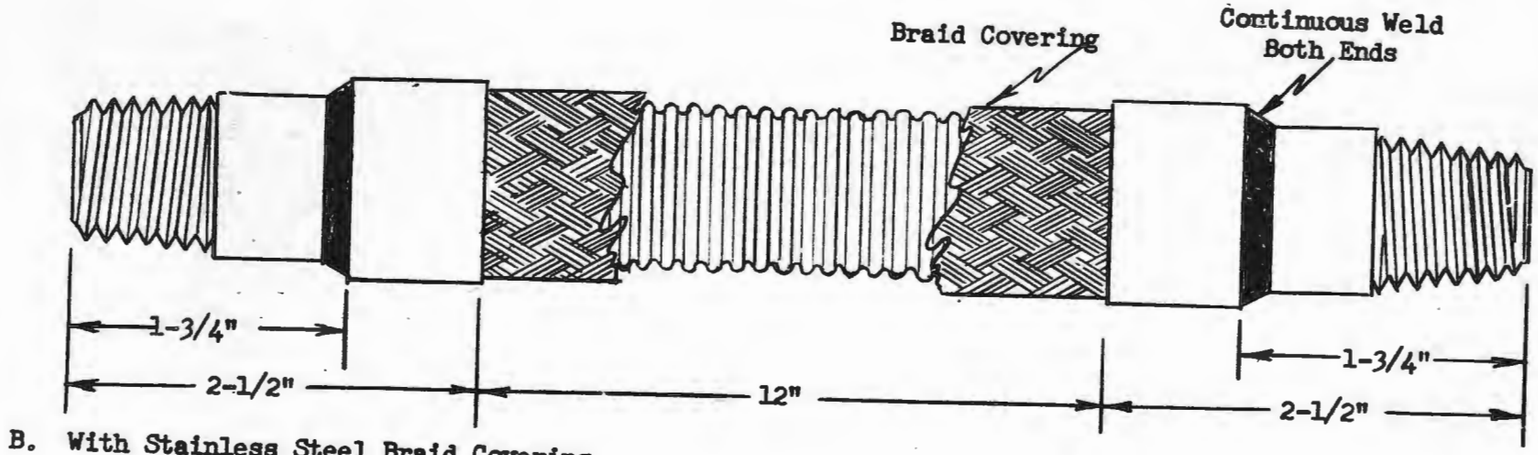

B. With Stainless Steel Braid Covering

FIGURE 20 Construction of Corrugated Flexible Tubing (Bellows)
(Drawing not to scale.)

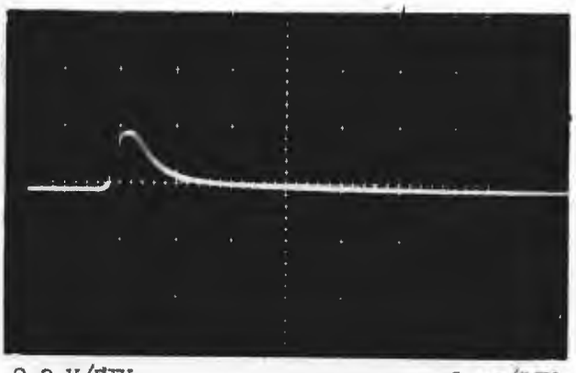

0.2 V/DIV 1 μs/DIV

A. Conductor-to-Conductor Voltage

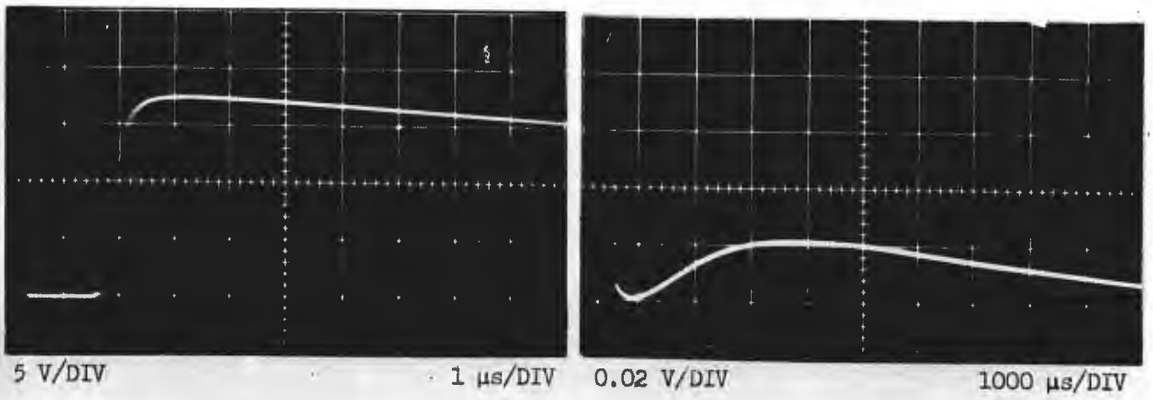

5 V/DIV 1 μs/DIV 0.02 V/DIV 1000 μs/DIV

B. Conductor-to-Conduit Voltage.

FIGURE 21 Conductor-to-Conductor and Conductor-to-Conduit Induced Voltages from 30 Foot Two Inch Rigid Conduit System Containing One Foot of Flexible, Corrugated Stainless Steel Tubing. Applied Pulse Current - 1420 amperes

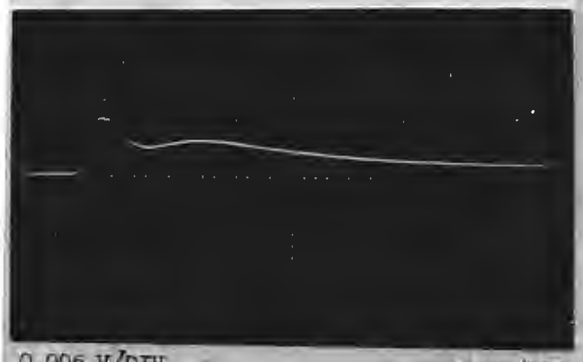

0.005 V/DIV 1 μs/DIV

A. Conductor-to-Conductor Voltage

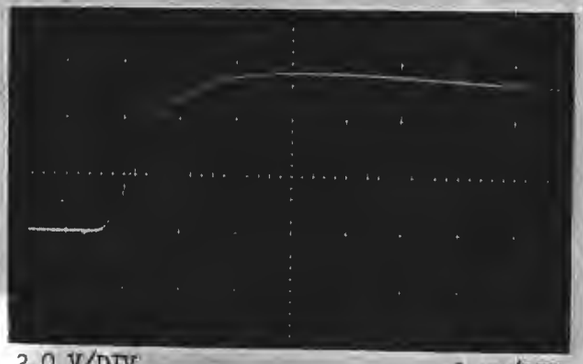

2.0 V/DIV 1 μs/DIV

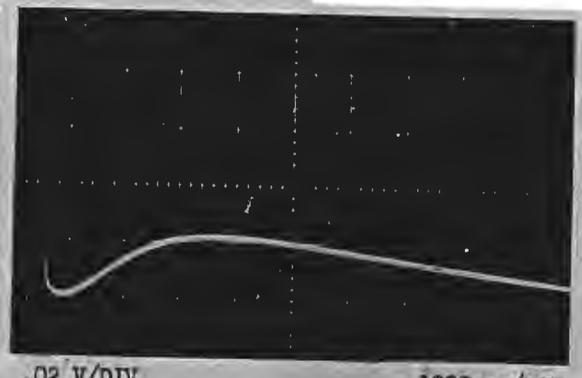

.02 V/DIV 1000 μs/DIV

B. Conductor-to-Conduit Voltage

FIGURE 22 Conductor-to-Conductor and Conductor-to-Conduit Induced Voltages from 30 Foot Two Inch Rigid Conduit System Containing One Foot of Flexible Corrugated Stainless Steel Tubing. Tubing has a Braided Stainless Steel Cover. Applied Pulse Current - 1755 amps

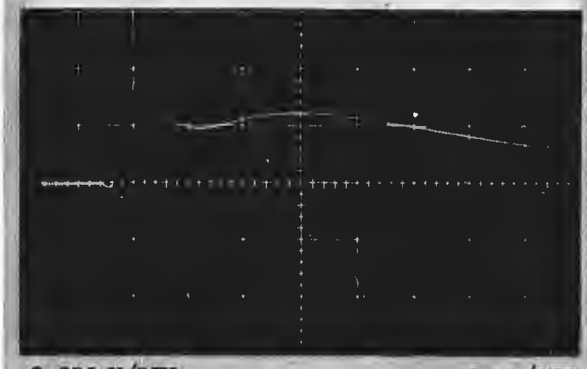

0.005 V/DIV 1 μs/DIV

A. Conductor-to-Conductor Voltage

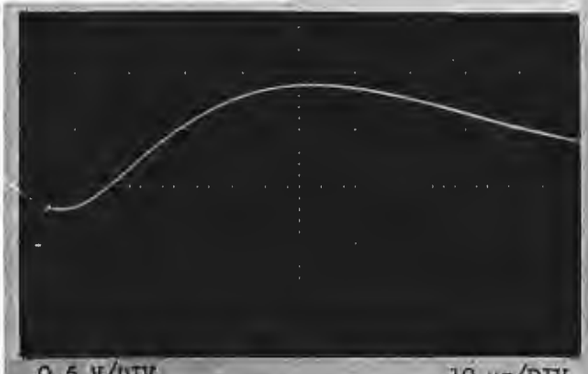

0.5 V/DIV 10 μs/DIV

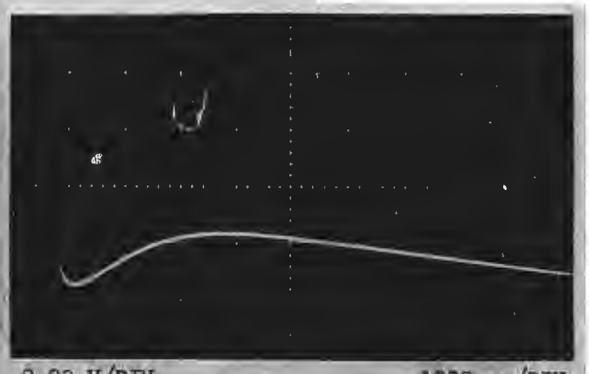

0.02 V/DIV 1000 μs/DIV

B. Conductor-to-Conduit Voltage

FIGURE 23 Conductor-to-Conductor and Conductor-to-Conduit Induced Voltages from 30 Foot Two Inch Rigid Conduit System Containing One Foot of Flexible Corrugated Carbon Steel Tubing. Applied Pulse Current - 1420 amperes

5 V/DIV 1.0 μs/DIV

A. Conductor-to-Conductor Voltage

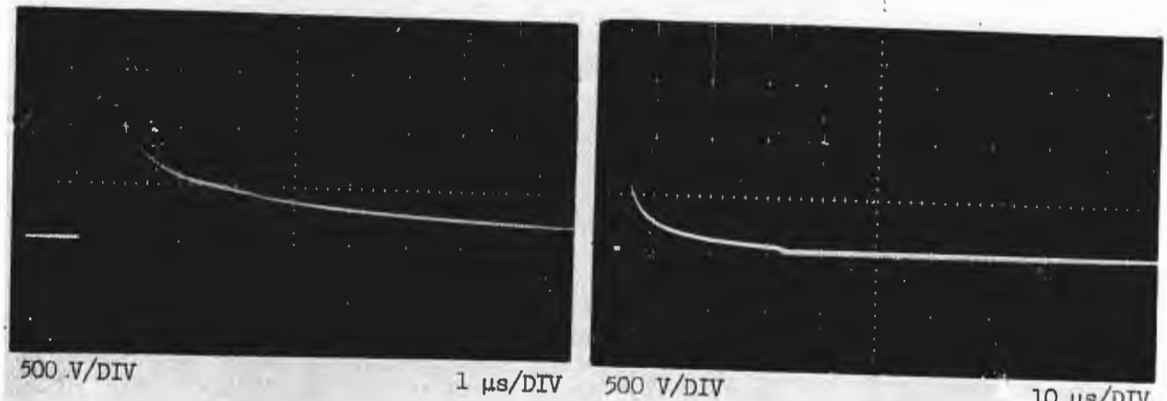

500 V/DIV 1 μs/DIV 500 V/DIV 10 μs/DIV

B. Conductor-to-Conduit Voltage

FIGURE 24 Conductor-to-Conductor and Conductor-to-Conduit Induced Voltages on Conductors in 25 Feet of Standard Grade Flexible Conduit. Applied Pulse Current - 1420 amperes

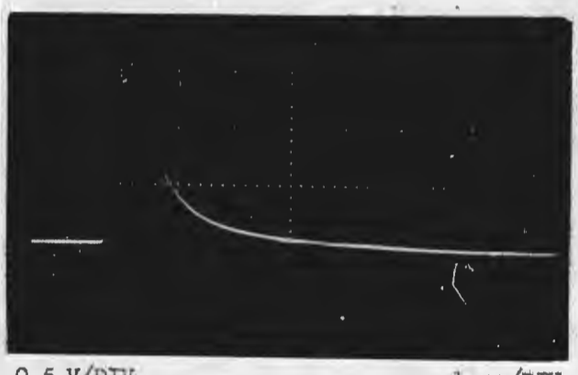

0.5 V/DIV 1 μs/DIV

A. Conductor-to-Conductor Voltage

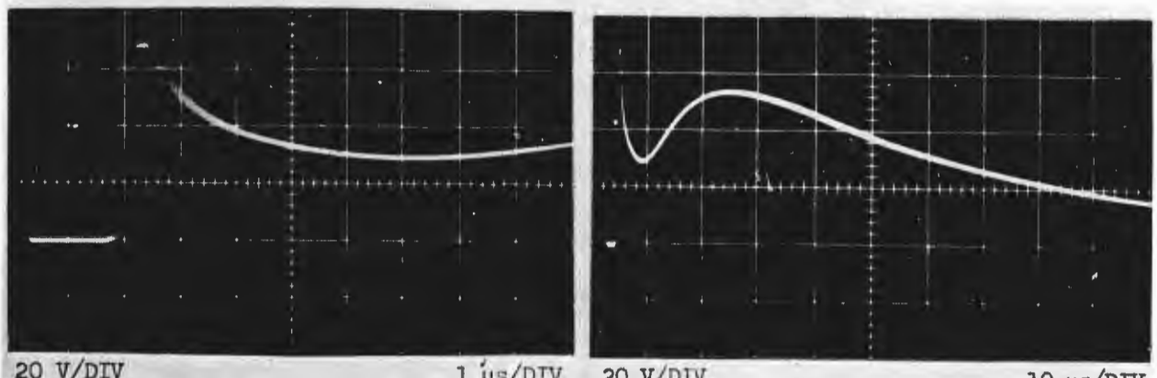

20 V/DIV 1 μs/DIV 20 V/DIV 10 μs/DIV

B. Conductor-to-Conduit Voltage

FIGURE 25 Conductor-to-Conductor and Conductor-to-Conduit Induced Voltages on Conductors in 25 Feet of Sealtite® Flexible Conduit. Applied Pulse Current - 1420 amperes

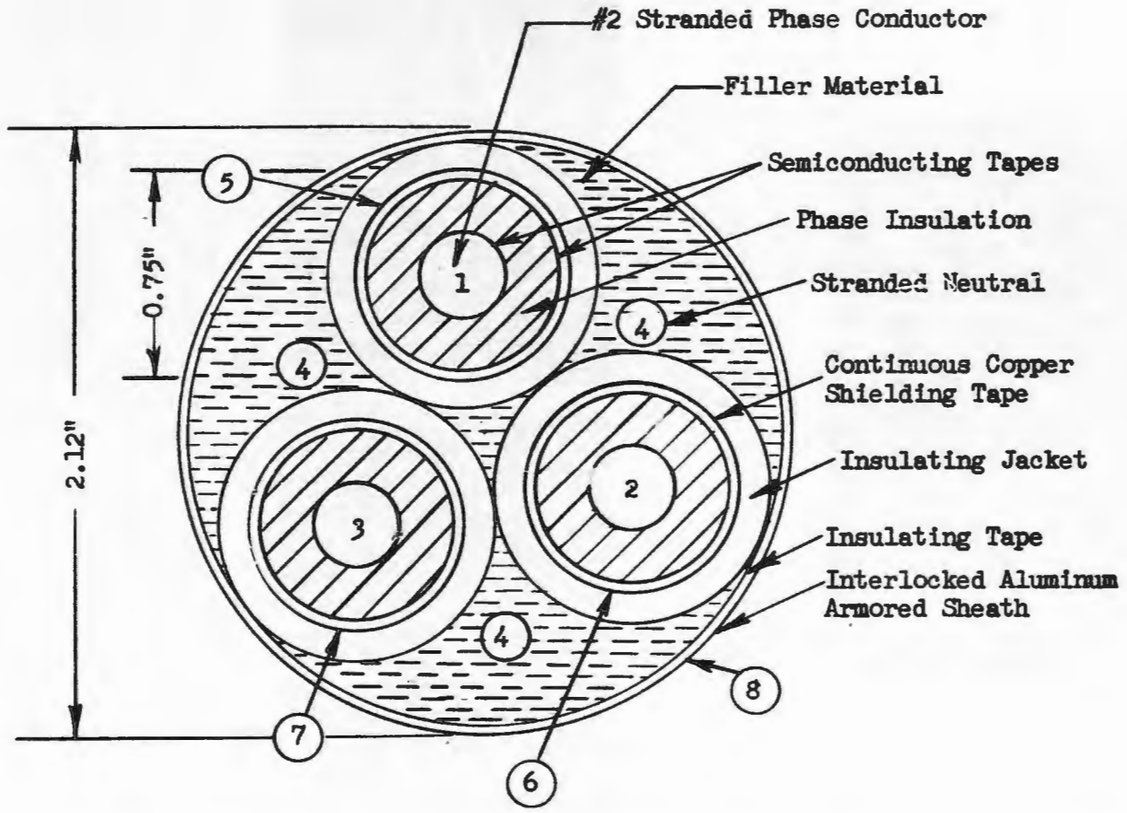

FIGURE 26 Cross Section of Armored, Shielded Power Cable Showing Elements and Test Conductor Designations as Given in Figure 27.

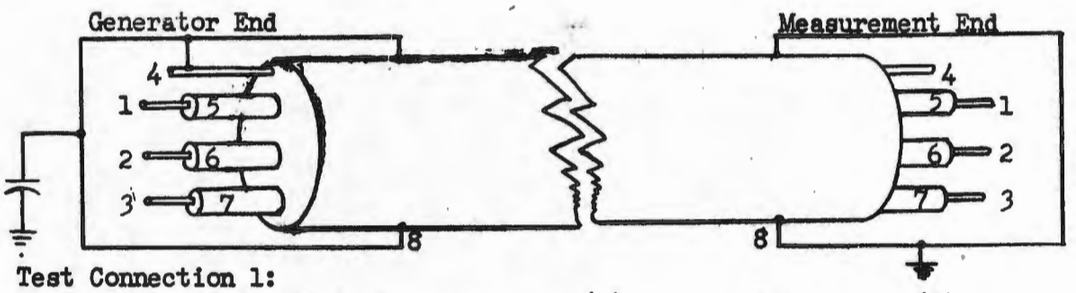

Test Connection 1:
Generator End - Neutral ground wire (4) connected to armor (8).
Measurement End - All conductors isolated.

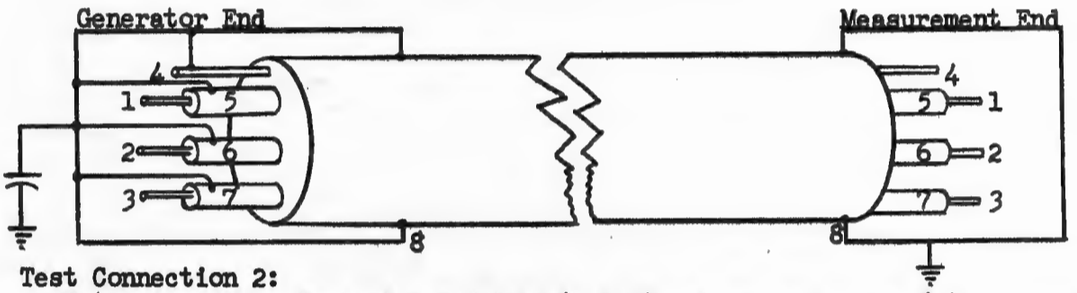

Test Connection 2:
Generator End - Conductor shields (5,6,7) and neutral wire (4) connected to armor (8).
Measurement End - Phase conductors (1,2,3), shields (5,6,7), and neutral wire (4) isolated.

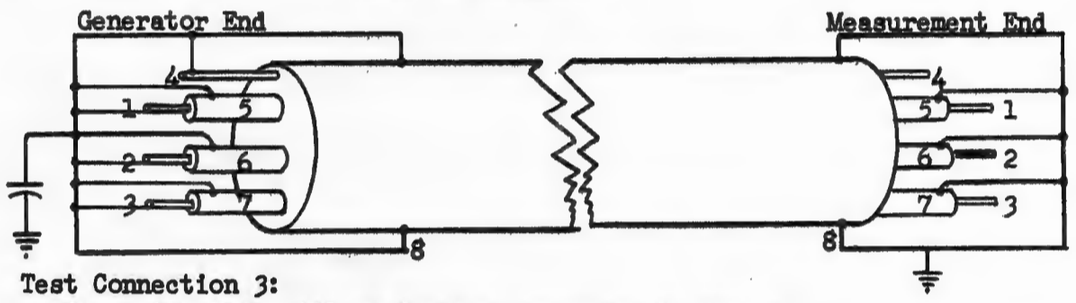

Test Connection 3:
Generator End - All conductors connected to armor.
Measurement End - Phase conductors (1,2,3) and neutral wire (4) isolated; shields (5,6,7) connected to armor (8).

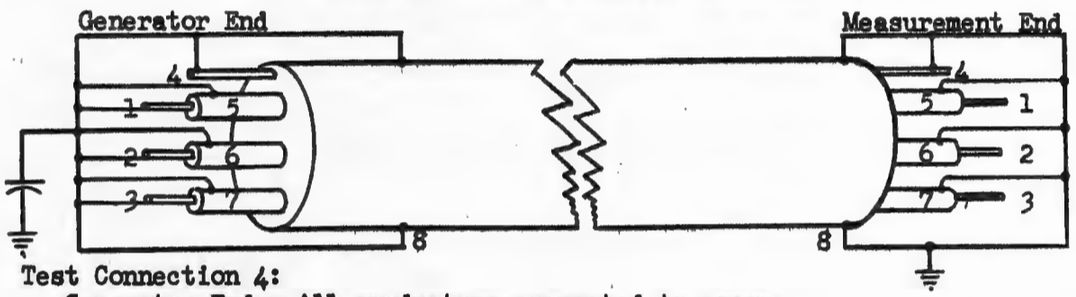

Test Connection 4:
Generator End - All conductors connected to armor.
Measurement End - Phase conductors (1,2,3) isolated; shields (5,6,7) and neutral wire (4) connected to armor (8).

FIGURE 27 Test Connections for Armored Power Cable Injected Current Tests

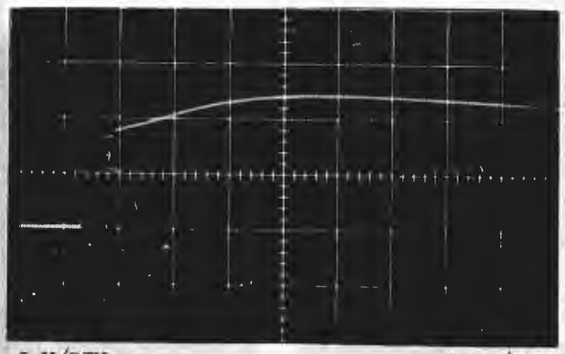

5 V/DIV 1 μs/DIV

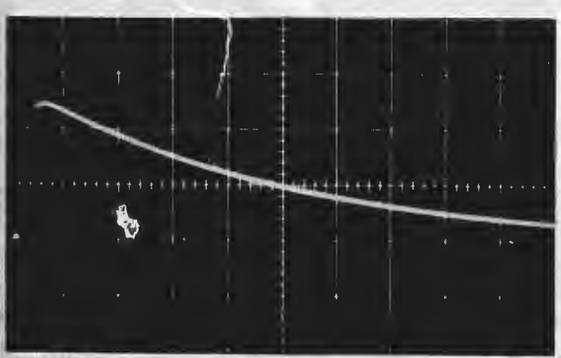

5 V/DIV 10 μs/DIV

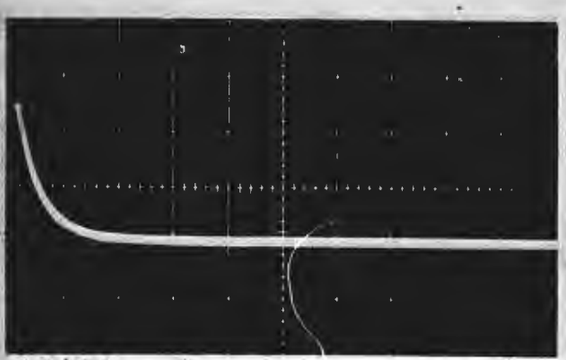

5 V/DIV 100 μs/DIV

FIGURE 28 Neutral Wires-to-Armor Induced Voltage (4-8) - Test Condition 1 Applied Pulse Current - 1420 Amperes

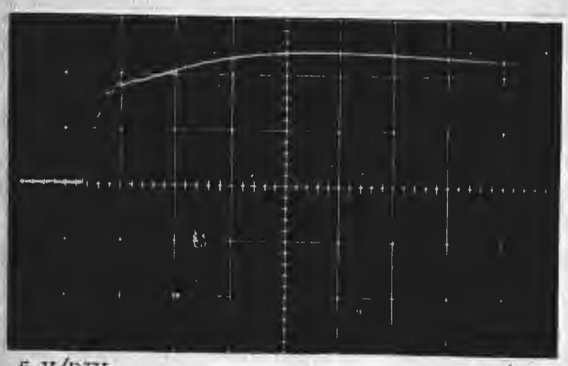

5 V/DIV 1 μs/DIV

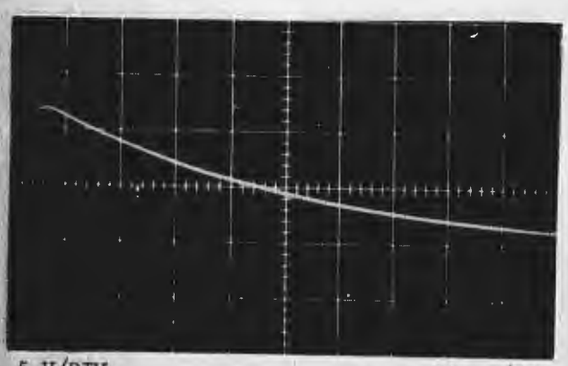

5 V/DIV 10 μs/DIV

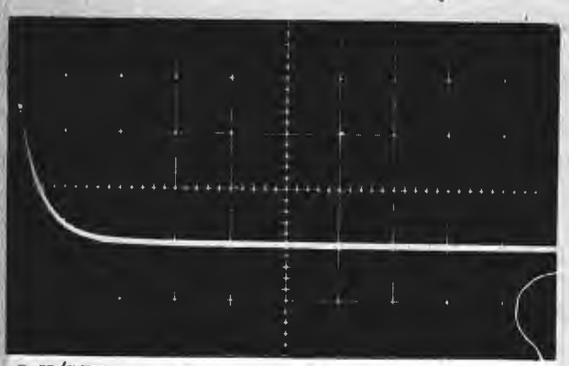

5 V/DIV 100 μs/DIV

FIGURE 29 Neutral Wire-to-Armor Induced Voltage (4-8) - Test Condition 2
Applied Pulse Current - 1420 Amperes

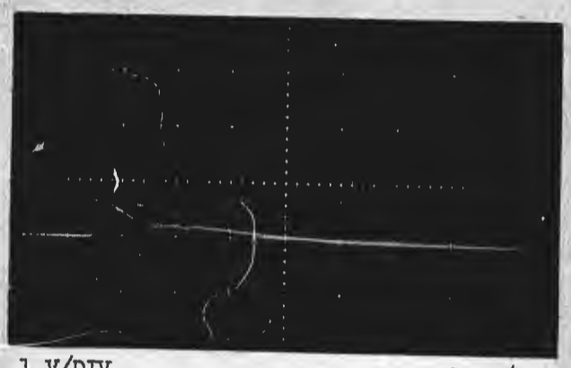

1 V/DIV 1 μs/DIV

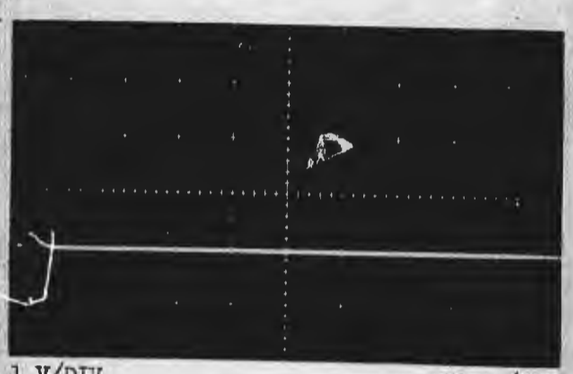

1 V/DIV 10 μs/DIV

FIGURE 30 Phase Conductor-to-Armor Induced Voltage (1-8) - Test Condition 2
Applied Pulse Current - 1420 Amperes

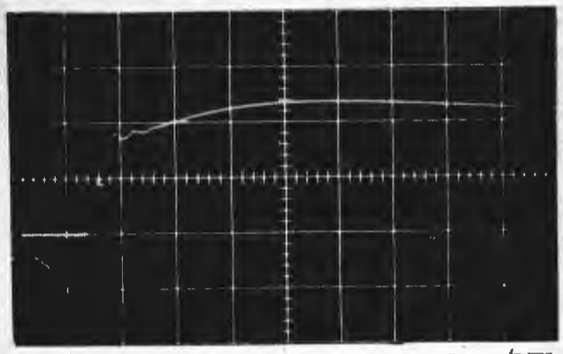

5 V/DIV 1 μs/DIV

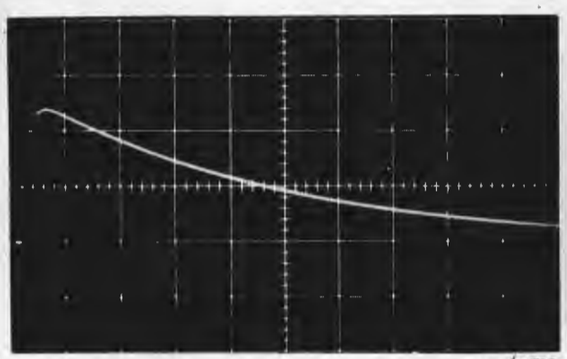

5 V/DIV 10 μs/DIV

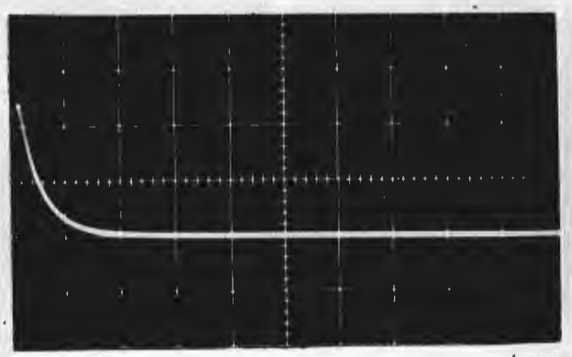

5 V/DIV 100 μs/DIV

FIGURE 31 Shield-to-Armor Induced Voltage (5-8) - Test Condition 2
Applied Pulse Current - 1420 Amperes

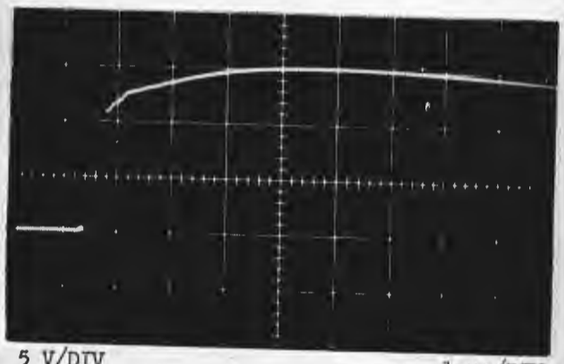

5 V/DIV 1 μs/DIV

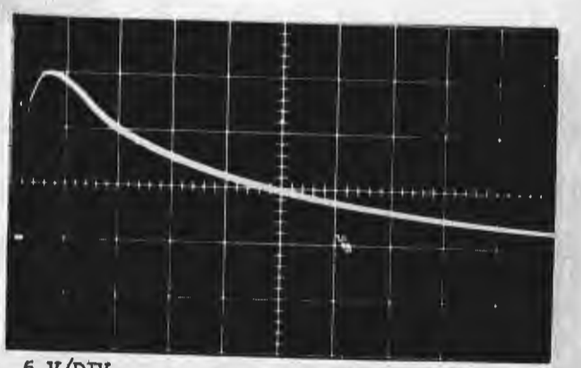

5 V/DIV 10 μs/DIV

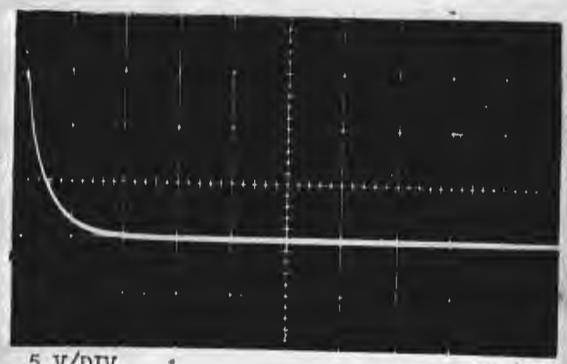

5 V/DIV 100 μs/DIV

FIGURE 32 Phase Conductor-to-Shield Induced Voltage (1 - 5) - Test Condition 2. Applied Pulse Current - 1420 Amperes

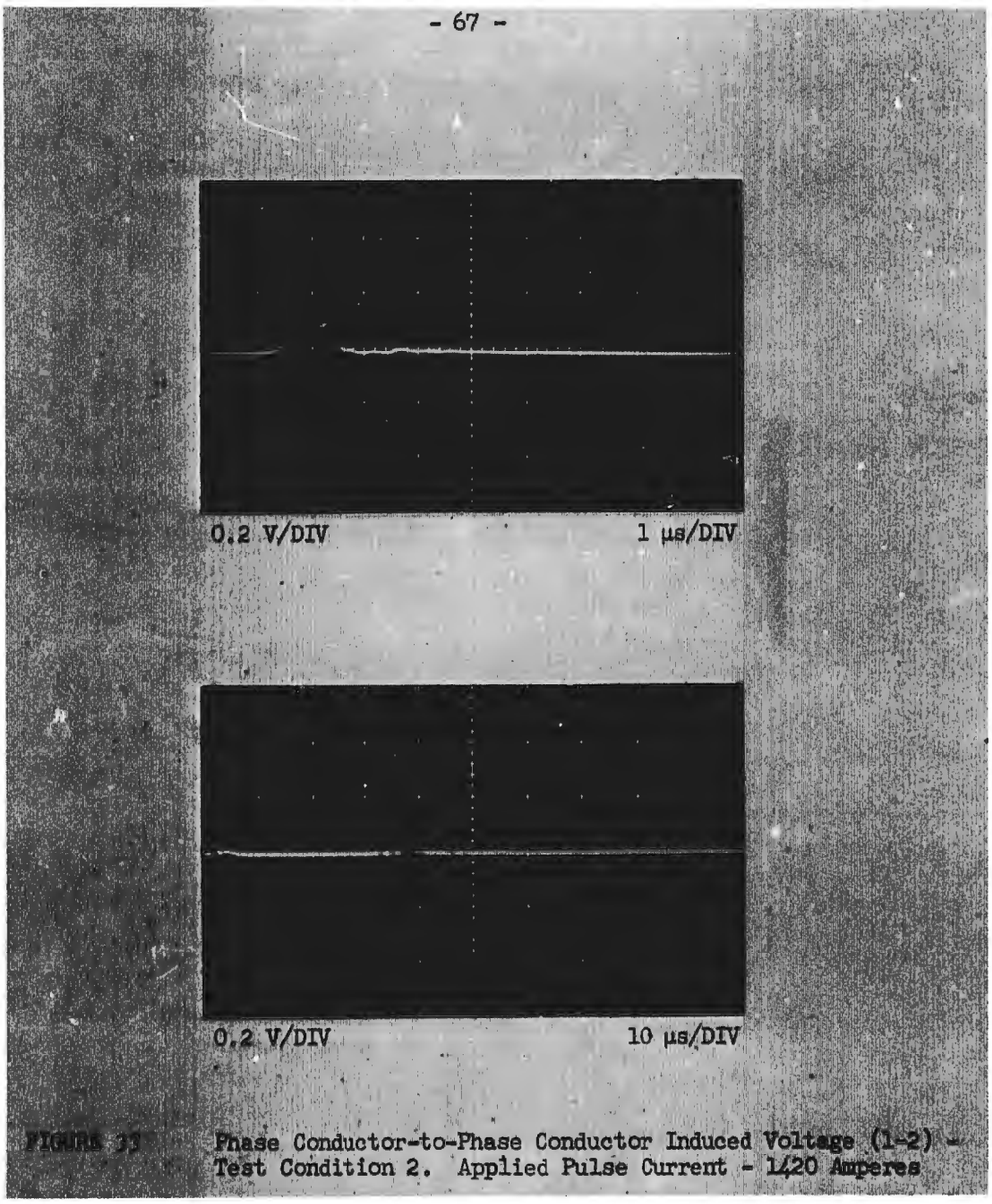

FIGURE 33 Phase Conductor-to-Phase Conductor Induced Voltage (1-2) - Test Condition 2. Applied Pulse Current - 1420 Amperes

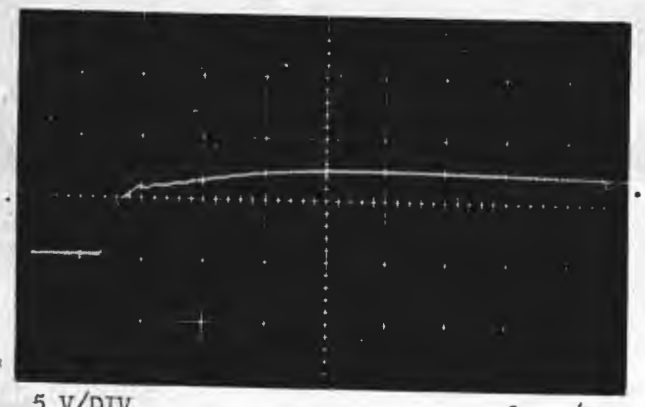

5 V/DIV 1 μs/DIV

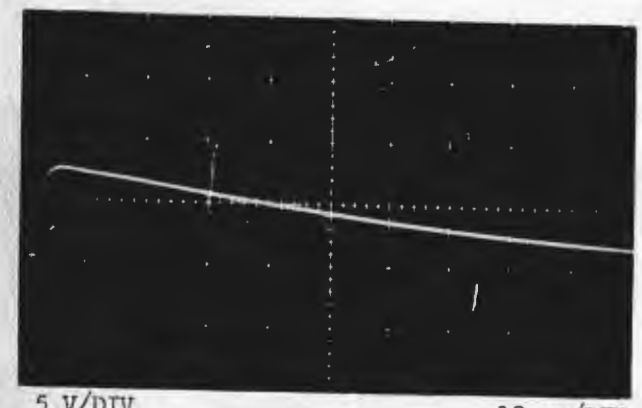

5 V/DIV 10 μs/DIV

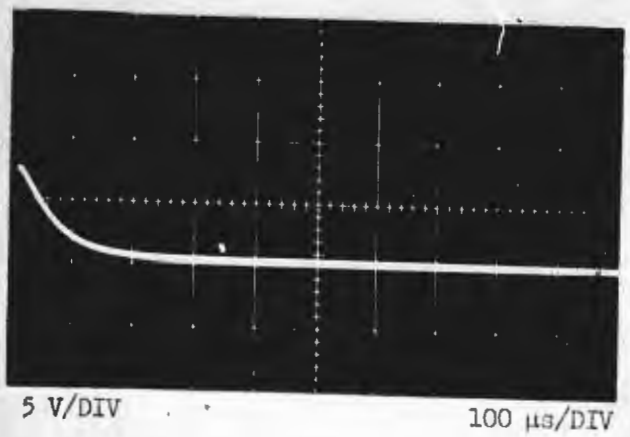

5 V/DIV 100 μs/DIV

FIGURE 34 Neutral Wire-to-Armor Induced Voltage (4-8) - Test Condition 3
Applied Pulse Current - 1420 Amperes

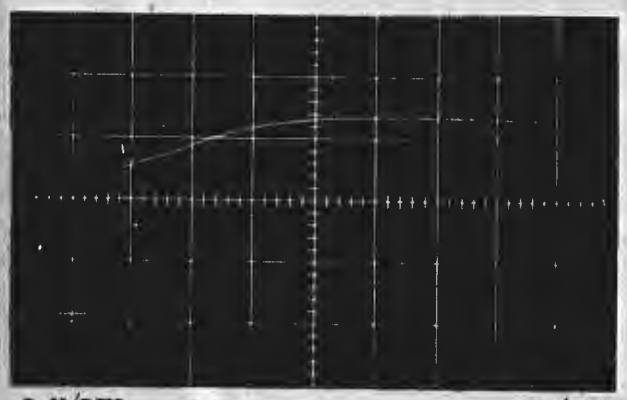

2 V/DIV 1 μs/DIV

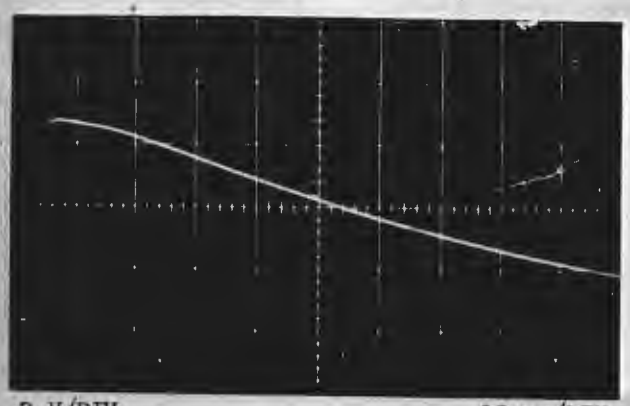

2 V/DIV 10 μs/DIV

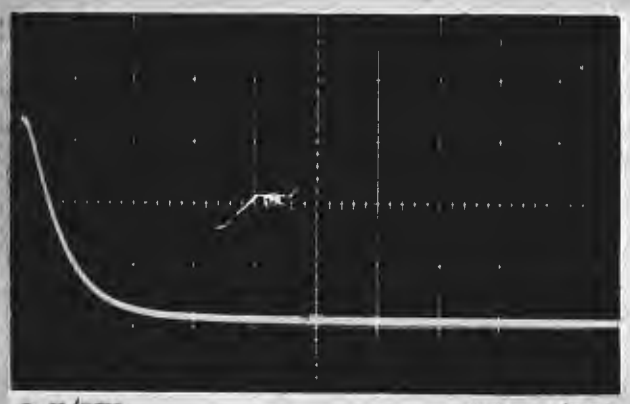

2 V/DIV 100 μs/DIV

FIGURE 35 Phase Conductor-to-Armor Induced Voltage (1 - 8) - Test Condition 3. Applied Pulse Current - 1420 Amperes

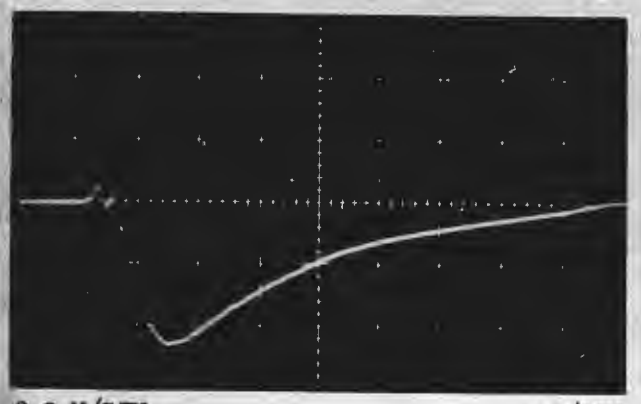

0.2 V/DIV 1 μs/DIV

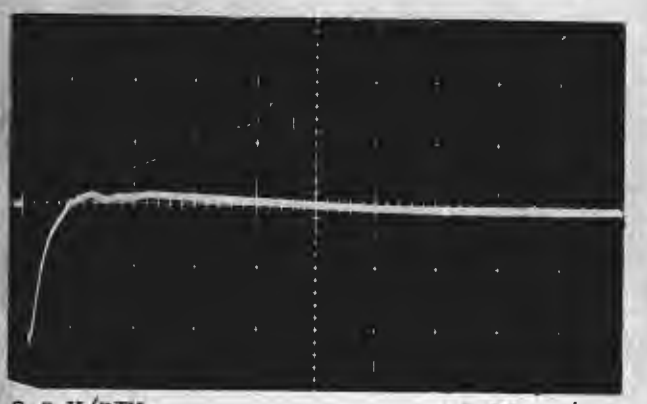

0.2 V/DIV 10 μs/DIV

FIGURE 36 Phase Conductor-to-Phase Conductor Induced Voltage (1-2) - Test Condition 3. Applied Pulse Current - 1420 Amperes

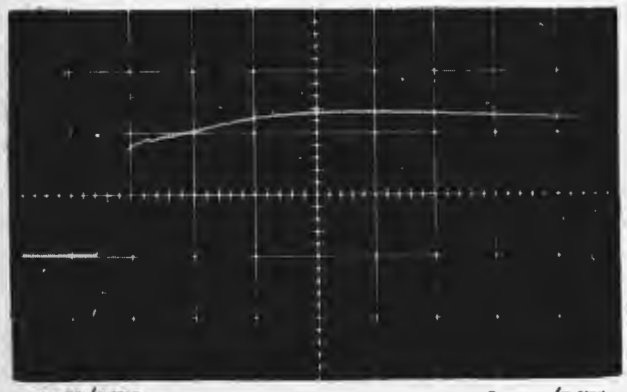

2 V/DIV 1 μs/DIV

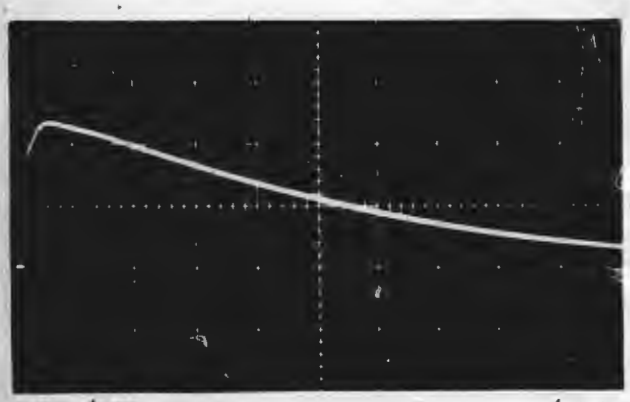

2 V/DIV 10 μs/DIV

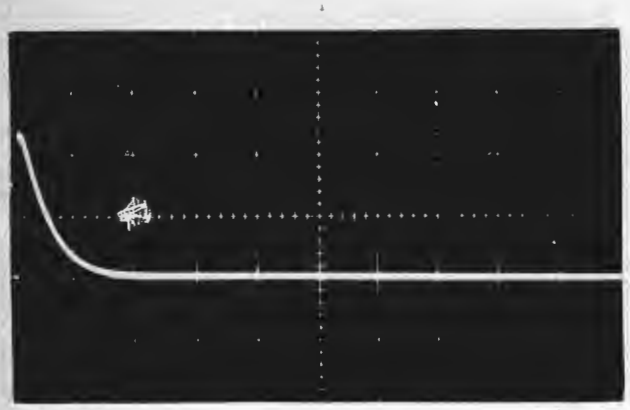

2 V/DIV 100 μs/DIV

FIGURE 37 Phase Conductor-to-Armor Induced Voltage (1-8)
Test Condition 4.
Applied Pulse Current - 1420 Amperes

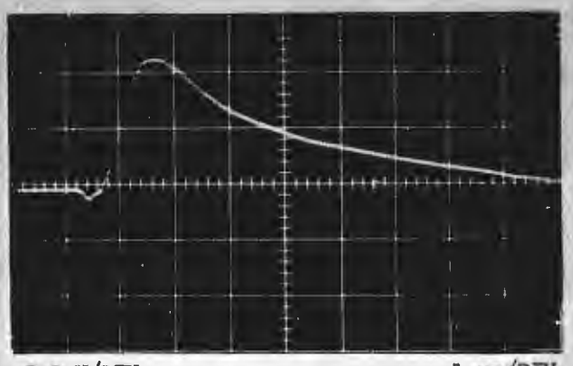

0.2 V/DIV 1 μs/DIV

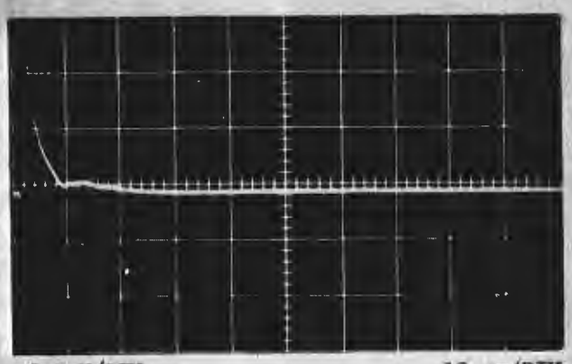

0.2 V/DIV 10 μs/DIV

FIGURE 38 Phase Conductor-to-Phase Conductor Induced Voltages (1-2) - Test Condition 4. Applied Current Pulse - 1420 Amperes

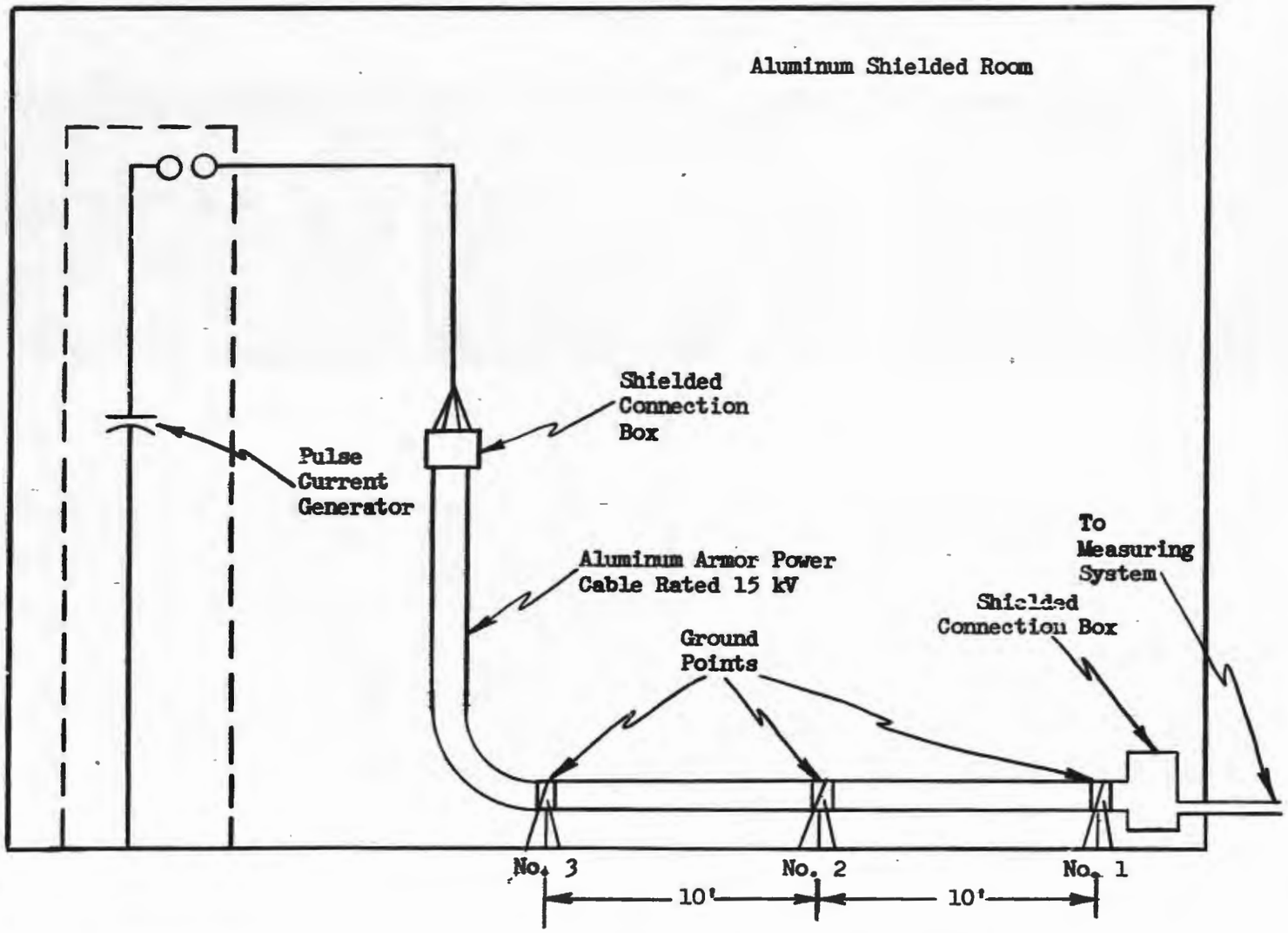

FIGURE 39 Cable Test Setup to Determine Effect of Ground Plane and Multiple Cable Armor Grounds

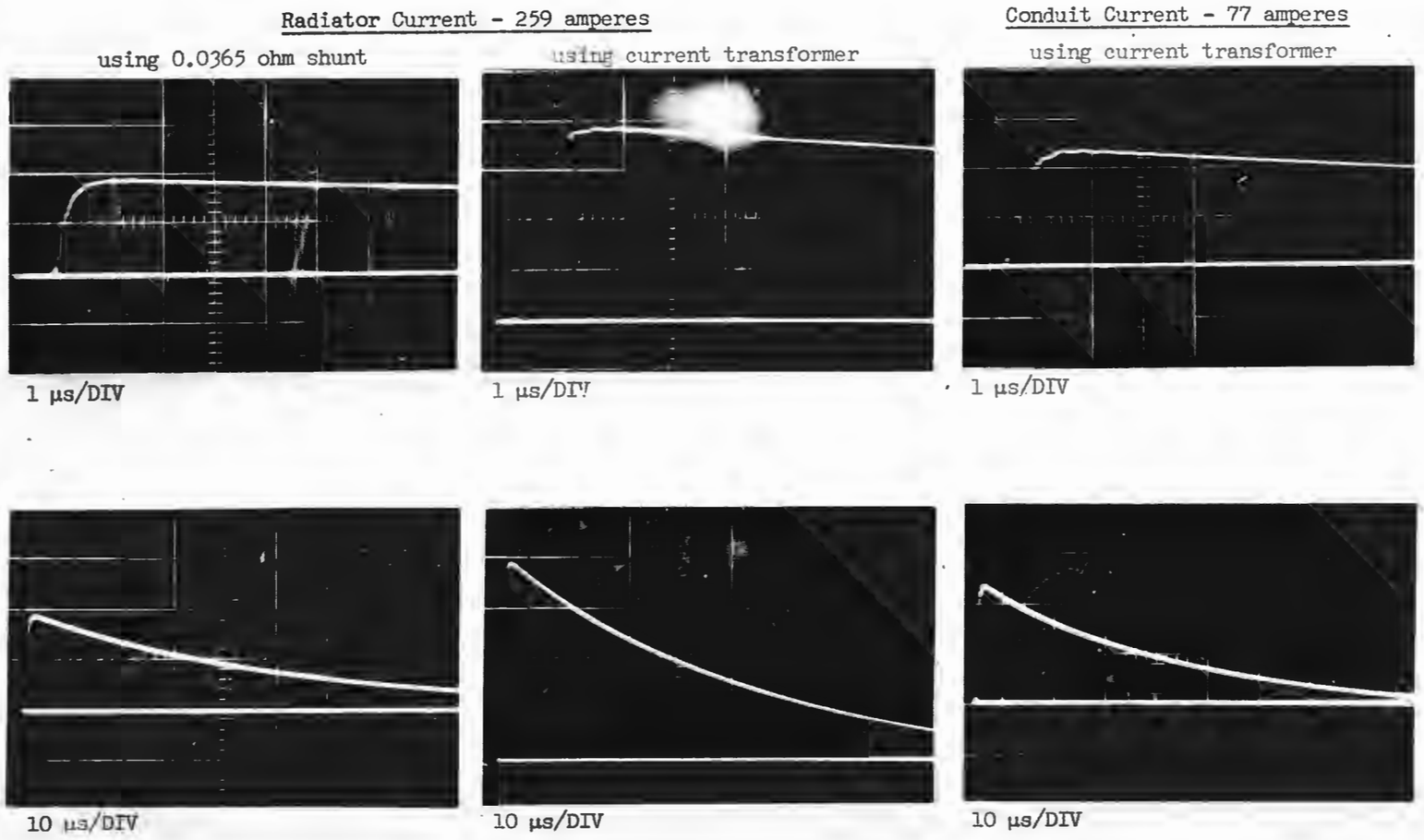

FIGURE 40 Comparison of the Wave Shapes of the Radiator Current and Current Induced on the Conduit Loop

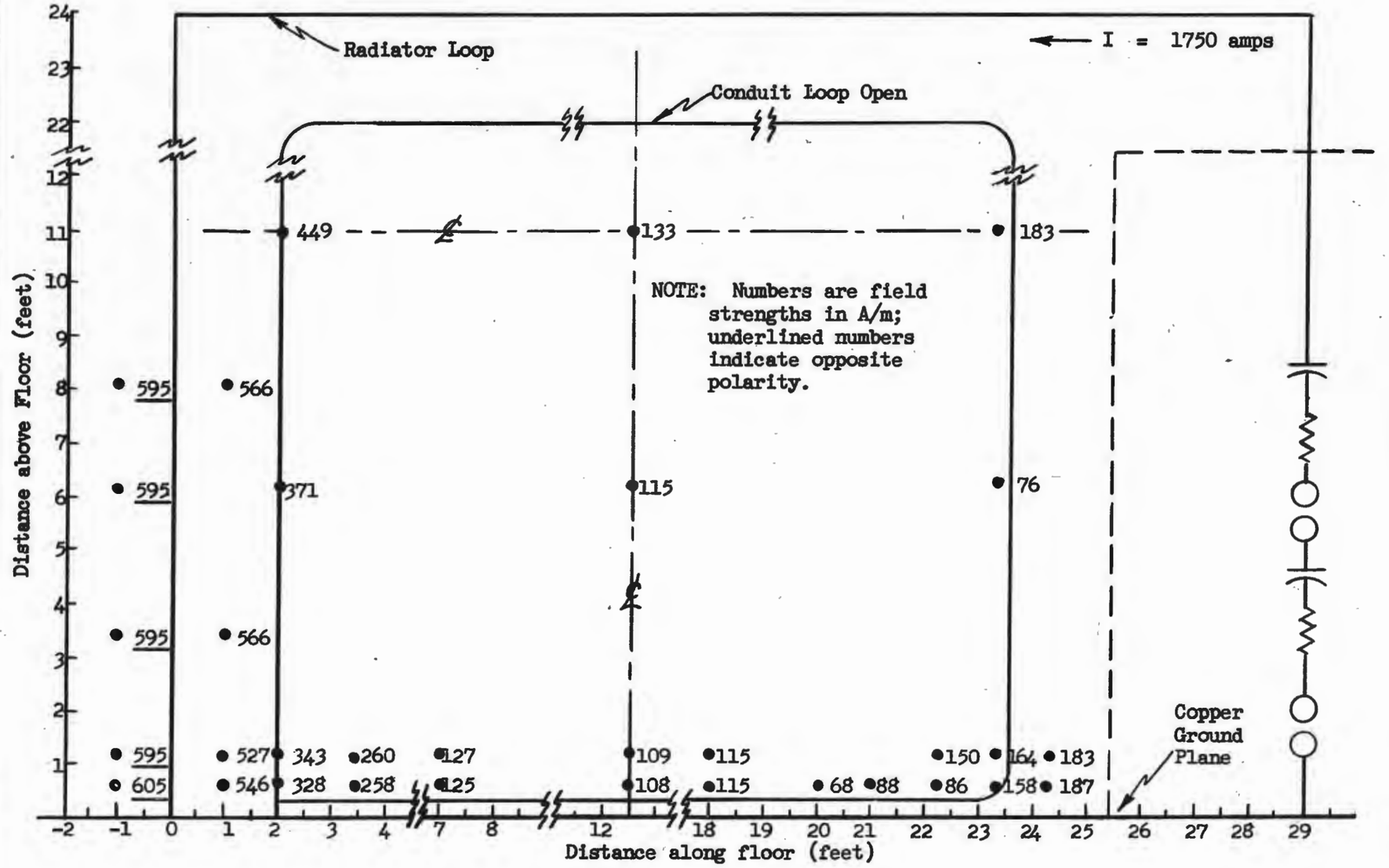

FIGURE 41 H-Field (A/m) for Conduit Loop Open

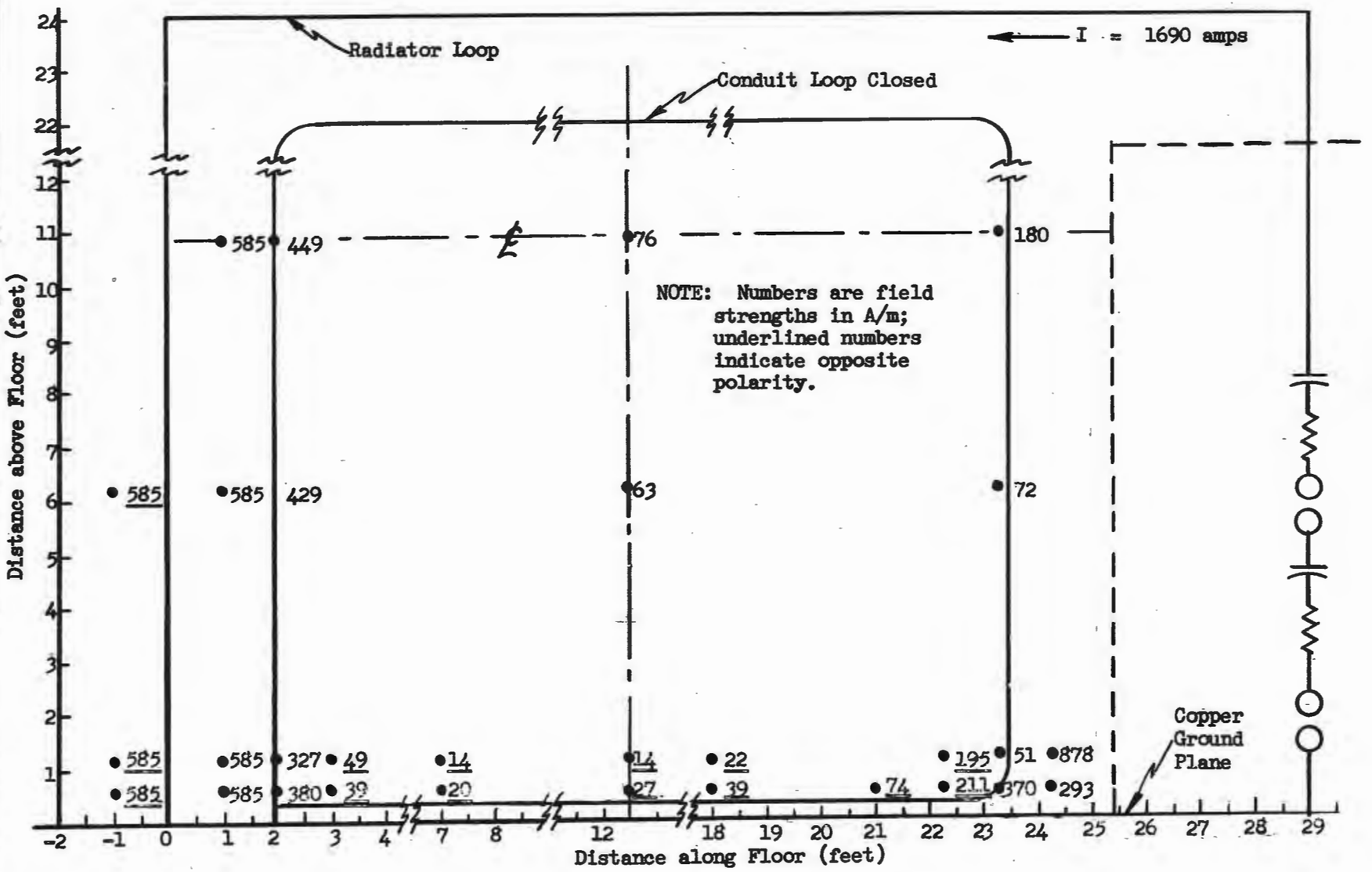

FIGURE 42 H-Field (A/m) for Conduit Loop Closed

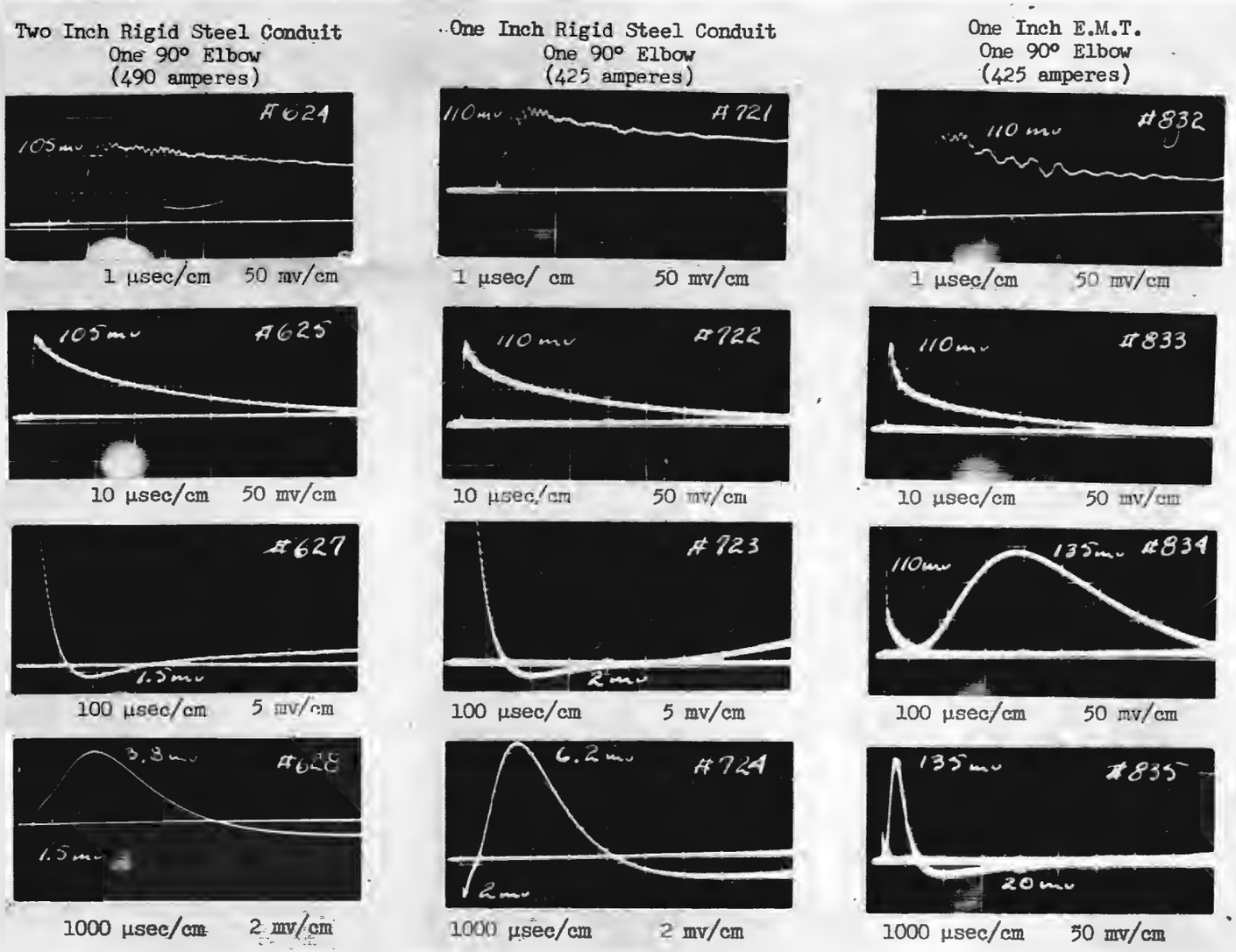

FIGURE 43 Comparison of Conductor-to-Conduit Induced Voltages in Bottom Half of Conduit Loop with Induced Current Flowing in the Conduit Loop

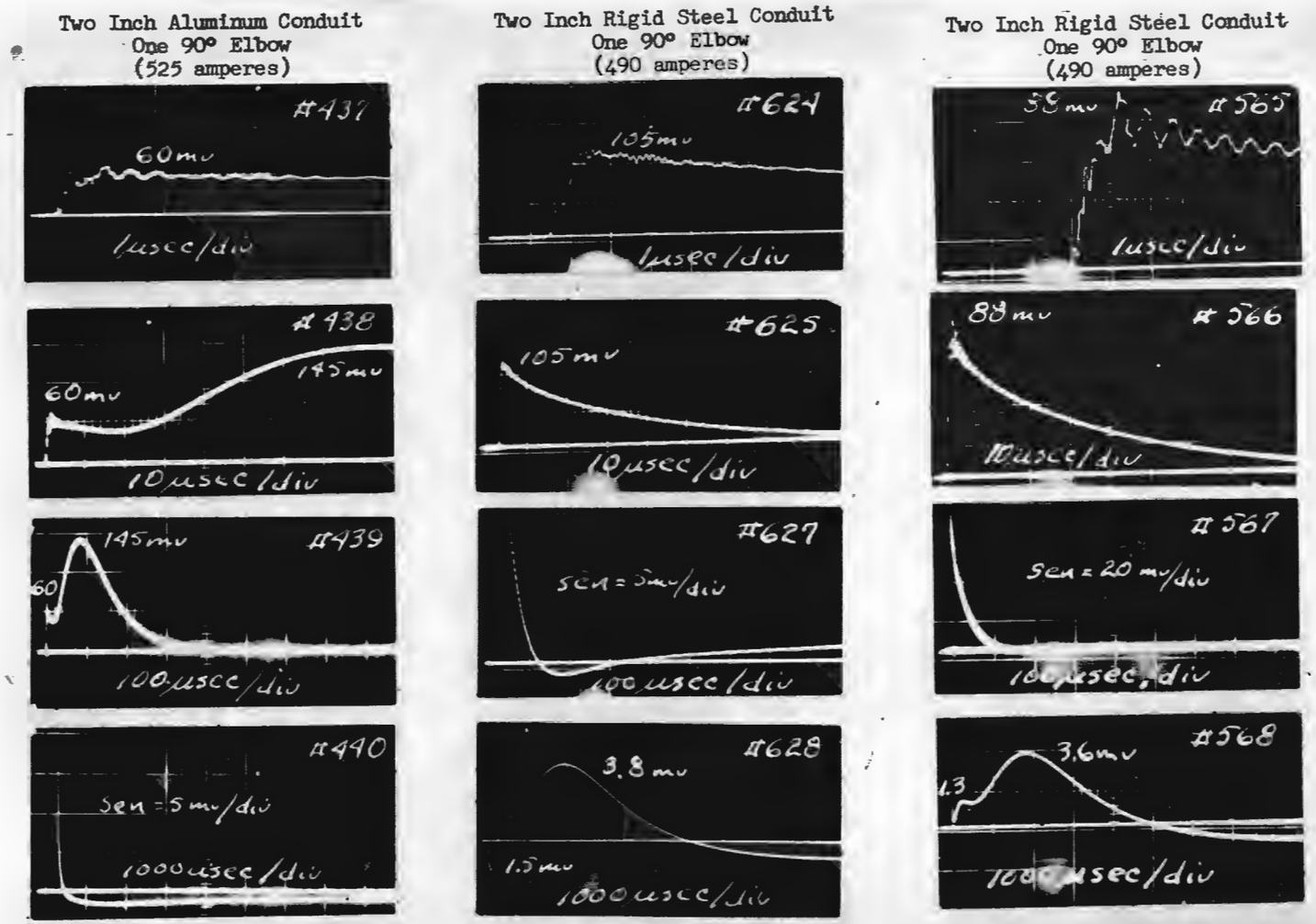

FIGURE 44 Comparison of Conductor-to-Conduit Induced Voltages in Bottom Half of Conduit Loop with Induced Current Flowing in the Conduit Loop

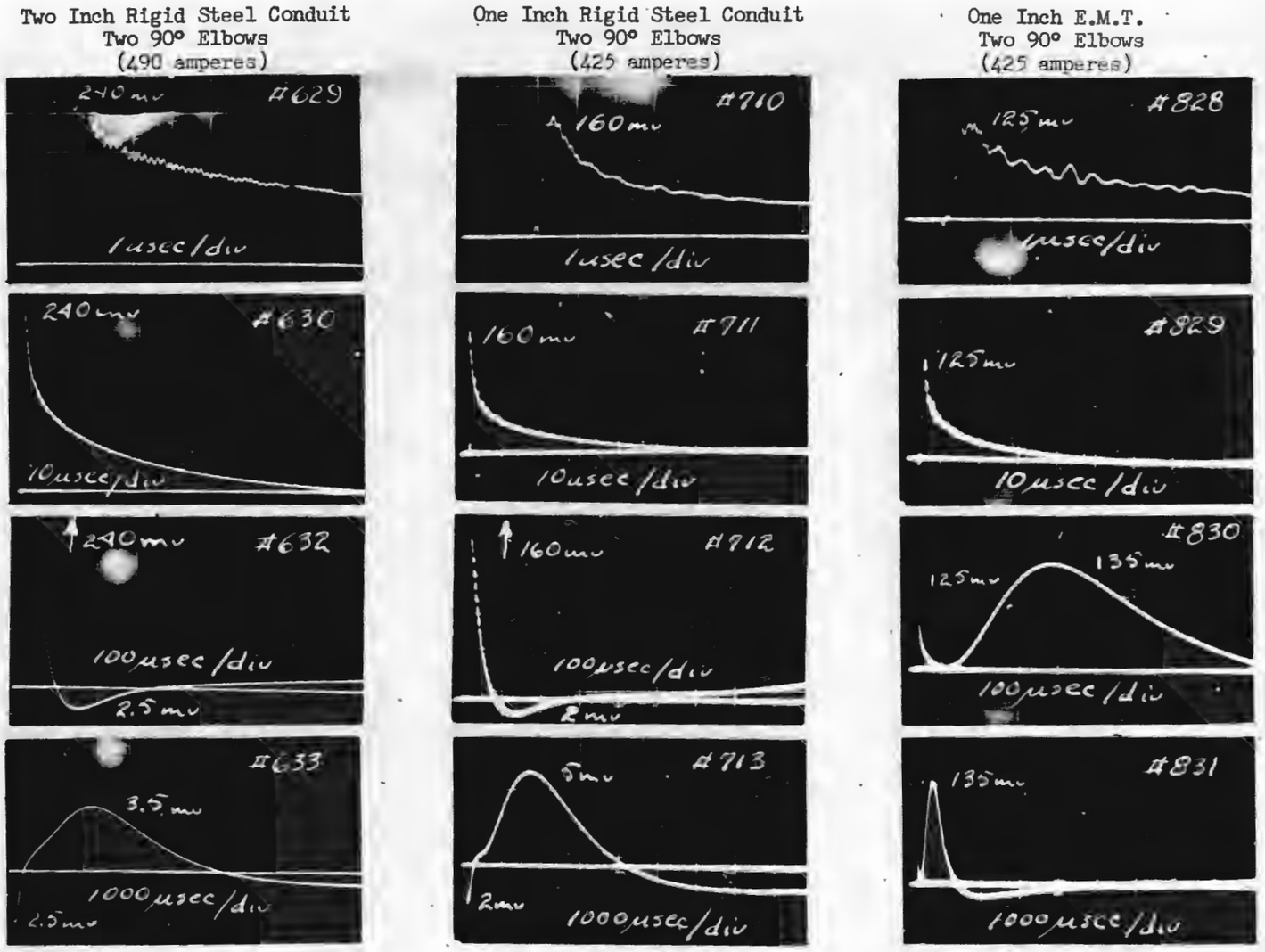

FIGURE 45 Comparison of Conductor-to-Conduit Induced Voltages in Top Half of Conduit Loop with Induced Current Flowing in the Conduit Loop

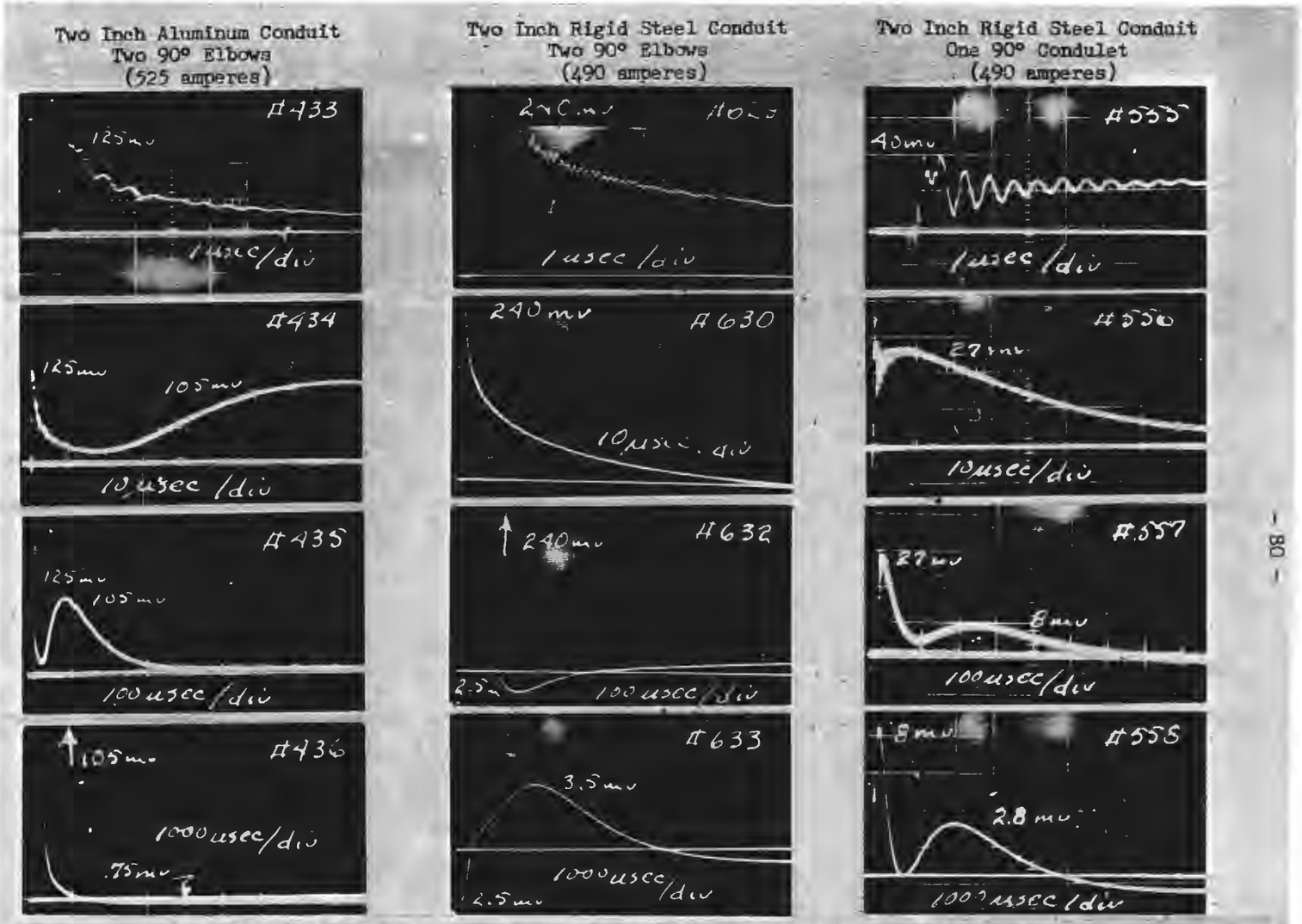

FIGURE 46 Comparison of Conductor-to-Conduit Induced Voltages in Top Half of Conduit Loop with Induced Current Flowing in the Conduit Loop

APPENDIX

Quasi Unit Function Current Wave Injection

During the injected current experiments on two inch rigid steel conduit, an induced voltage wave shape was measured which appeared as follows:

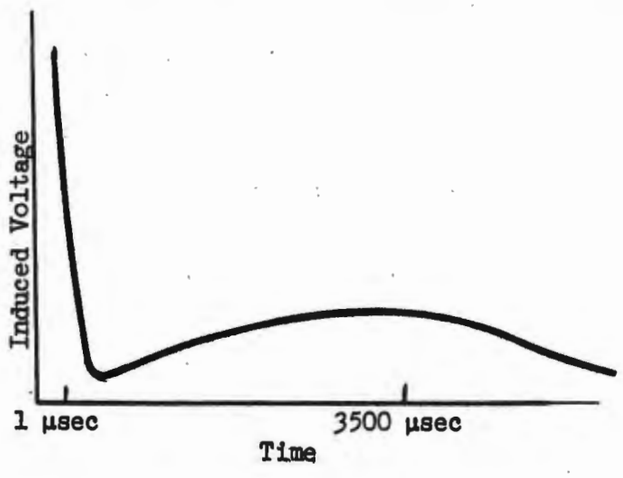

That is, two voltage peaks occurred, the first being produced by the magnetic flux leaking into the conduit and linking the conductor within at such places as joints, bends, etc. The second peak occurred at a time which was long compared to the time of occurrence of the applied current wave. This indicates that the conduit itself has a long time response characteristic.

To evaluate the response of the conduit by application of a quasi unit function, the 30 foot conduit system as shown in Figure 3b. of this report was set up. The generator was disconnected and a 12 volt battery through an external series resistance connected to the conduit. This generated an 80 x ∞ microsecond wave. The conductor within the conduit was electrically connected to the conduit at the battery end. Induced voltage measurements were made at the ground end of the conduit across a 75 Ω measuring impedance between conductor and ground. The applied current and induced voltage wave

shapes are shown in Figure A1. Note that the induced voltage at the time the applied current has reached crest is only 2.5% of its final value. The final IR induced voltage value is reached when the current density through the conduit wall becomes uniform which is after about 20 milliseconds. This is considerably greater than the 3.5 milliseconds measured for the injected current short time pulse conditions. This certainly suggests that the current density through the cylinder wall is far from uniform when the 3.5 millisecond pulse appears.

The crest value of the induced voltage reaches approximately 29 millivolts. Using the applied current of 15.8 amperes, the transfer impedance calculates to be 0.00184 ohm. The conduit system dc resistance measured 0.00218 ohm.

Theory is presented in the next section.

Theory

If a step function of current enters one end of a cylindrical conductor whose length is long compared to its diameter so that end effects can be neglected, the current will initially all be confined to the outer surface. As time goes on, the current will diffuse inward and eventually an equilibrium condition will be reached at which time the current density throughout the wall thickness of the cylinder will be uniform.

Likewise, the magnetic flux will initially all be external to the cylinder. As the current diffuses through the wall of the cylinder, a magnetic field will also diffuse through the cylinder. When equilibrium conditions have been reached, the magnetic flux density will vary linearly from zero at the inner surface to a maximum at the outer surface.

If a conductor is placed in the center of the cylinder and is connected to the ungrounded end of the cylinder, a voltage will be developed between that end and the ground end of the cylinder. As shown in Figure A2, this voltage may be found by integrating the electric potential along either the

path ABCD or ABCEF. If one integrates along the path ABCD, one finds the voltage V_{AD} to be initially zero. This is to be expected since the magnetic fields initially force all the current to flow on the exterior surface of the cylinder and, therefore, path ABCD encloses no flux. This is the phenomena of skin effect. The current density at the inner surface is thus, initially zero.

As the current diffuses into the cylinder wall, the current density at various times will probably appear about as shown in Figure A3. The current density is initially infinite and confined to an infinitesimally thin shell. For a final condition the current density will be uniform throughout the wall thickness. At any time the area under the current density curve must equal the total input current.

The current density at the inner wall will increase in the manner shown in Figure A4. Since the current density is assumed uniform over the length of the cylinder (end effects being negligible or ignored), the voltage V_{AD} will be,

$$V_{AD} = \int_0^{\ell} J_{r_1} \rho \, d\ell = J_{r_1} \rho \ell$$

where J_{r_1} = the current density at any time (t)

ρ = the resistivity of the cylindrical conductor

ℓ = the total length of the cylinder

The voltage (V_{AD}) wave shape will be the same as the wave shape of the current density at the inner wall surface.

For a final value of current density

$$J_{r_1} = \frac{I}{A}$$

where I = the total current

A = the cross-sectional area

The final value of V_{AD} then becomes

$$V_{AD} = J_f \rho \ell = \frac{I}{A} \cdot \frac{R \times A}{\ell} \cdot \ell = IR$$

If one evaluates V_{AD} by following the path ABCEF, the voltage induced by the flux buildup in the cylinder wall must be included. V_{ABCEF} is thus,

$$V_{AF} = J_{r_2} \rho \ell - \frac{d\phi}{dt}$$

The flux within the loop ABCEF will have the time history shown in Figure A5 and will reach a final limiting value. The time derivative of the flux $(\frac{d\phi}{dt})$ will start at infinity and decay to zero. The term $J_{r_2} \rho \ell$ will start at infinity (since J_{r_2} is initially infinite) and decay as the time history shown in Figure A6 to the limiting value

$$J = I/A$$

The net voltage is thus initially infinity minus infinity which for this case turns out to be zero. V_{AF}, which is the difference of the $J_{r_2} \rho \ell$ and $d\phi/dt$ terms will have the same wave form with respect to time as that of J_{r_1} of Figure A4.

The analytical expressions for this wave form have not yet been evaluated, but certain comments can be made. The wave form of the voltage V_{AD} in response to a step current excitation will be similar to an RC exponential charging curve or, more nearly, to a complementary error function (erfc) wave form.

According to Witt, the time constant of the buildup of voltage in a solid coaxial shunt will be approximately

$$T_m \approx \mu_o \delta^2/6 \rho$$

where δ = wall thickness in meters

ρ = resistivity in ohm-meters

μ_o = permeability of free space

The time constant thus varies with the square of the wall thickness of the cylinder, inversely with the resistivity of the material, and linearly with the permeability. Witt's derivation was for a nonmagnetic cylinder and, if the cylinder was of a magnetic material, the equation would be

$$T_m \approx \mu_r \mu_o \delta^2/6\rho$$

where μ_r = relative permeability (a dimensionless number)

Limitations of Theory

The theory given assumes the magnetic fields inside the inner wall of the cylinder to be zero. This can only occur when: 1) the cylinder is round, straight, and long enough so that end effects can be ignored, 2) there are no current carrying members inside the cylinder, and 3) there are no joints or holes through which magnetic flux can leak inside.

Corners, ends, and wiring fixtures obviously do not fall into this category. In practice bends should be made as smoothly and with as long a radius as possible. Long conduit runs in practice will fall into the category of being long enough to ignore end effects.

Current flow in conductors inside the conduit can probably be ignored since for any practical value of terminal impedance the current that might flow in the center conductor will be negligible compared to that flowing in the conduit. Only current injected onto the conductors from some other source than the IR (or IZ) drop along the conduit will be important and that is another problem entirely.

Flux leakage through poorly made joints or through poorly fitting covers is likely to override all bend, end, or conduit shape effects. With any kind of careful workmanship it would seem that induced voltages due to such flux leaks should not exceed the IR_{DC} drop along the conduit.

FIGURE A1. Comparison of Applied Quasi-Unit Function Current to 30 Foot Conduit System and Resulting Induced Conductor-to-Conduit Voltage on Conductor within Conduit. Applied Current Peak - 15.8 amperes

(Applied Current) (Conductor to Ground Voltage)

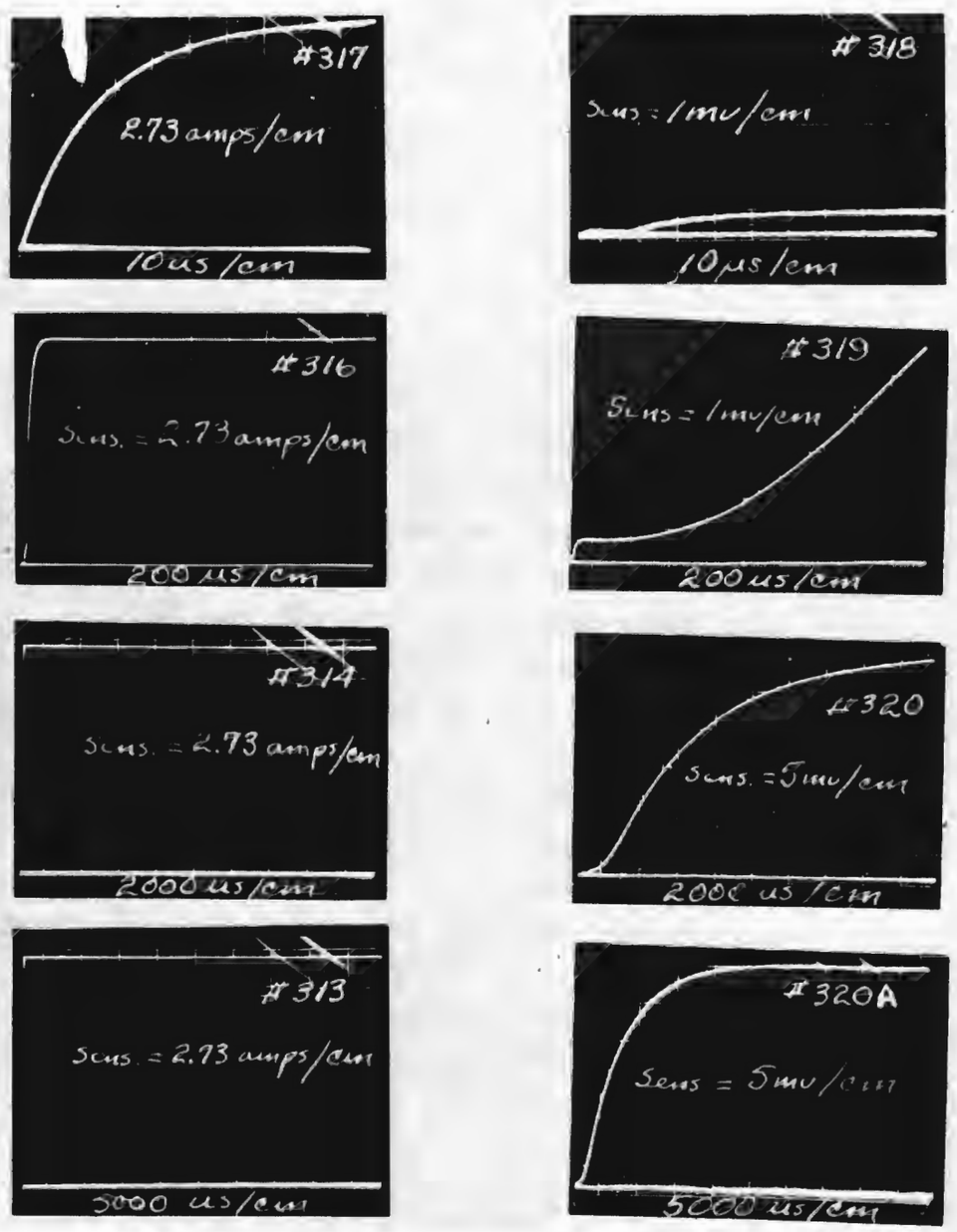

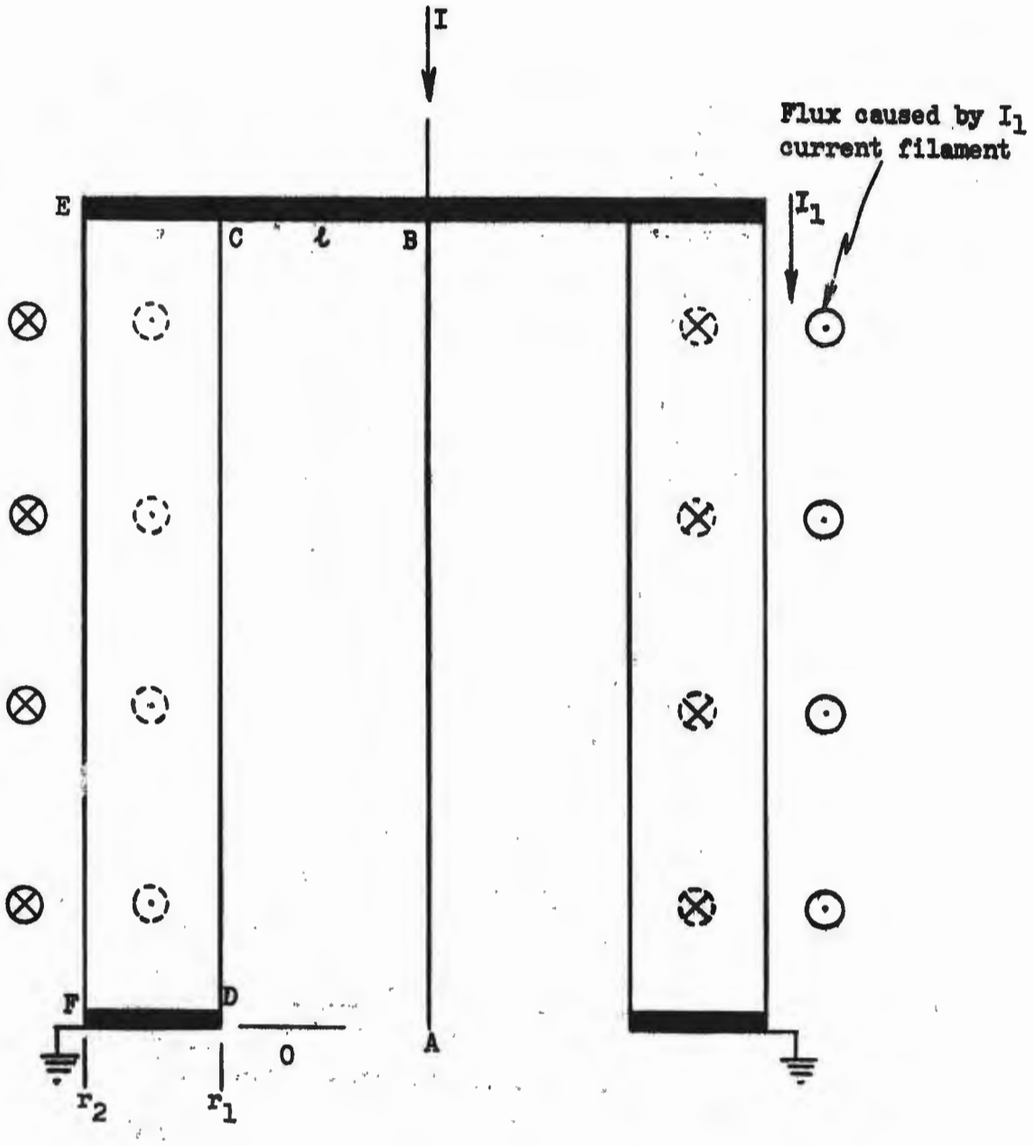

FIGURE A2. Idealized Conduit and Inner Conductor

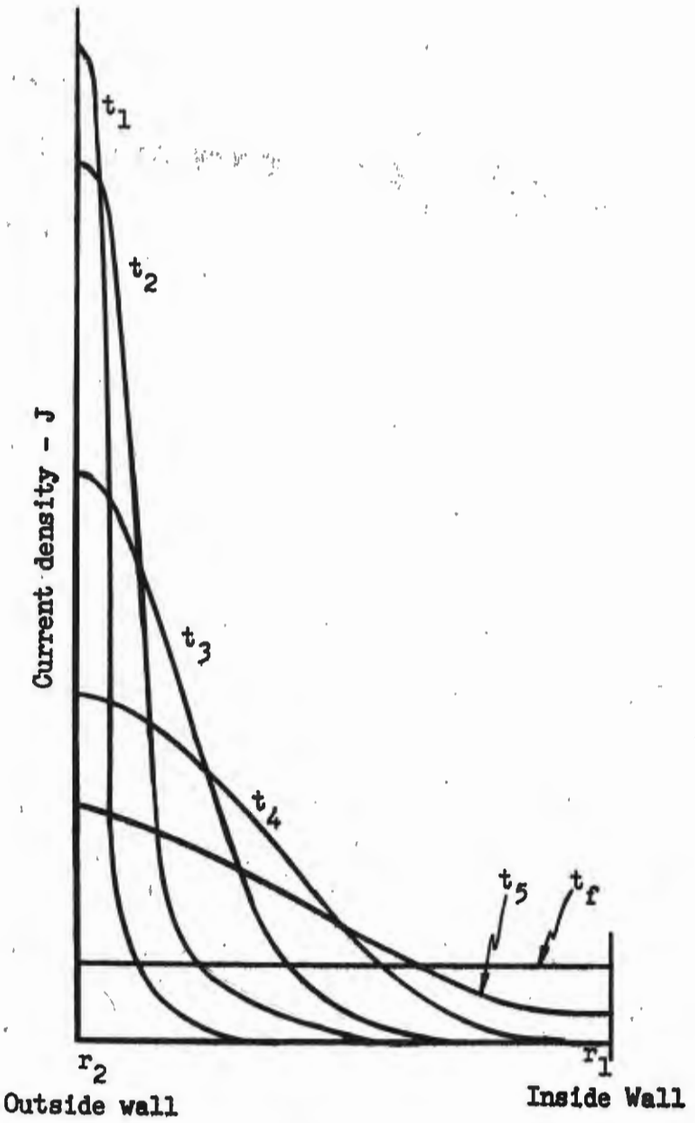

FIGURE A3. Probable Current Density in Cylinder Wall at Various Times

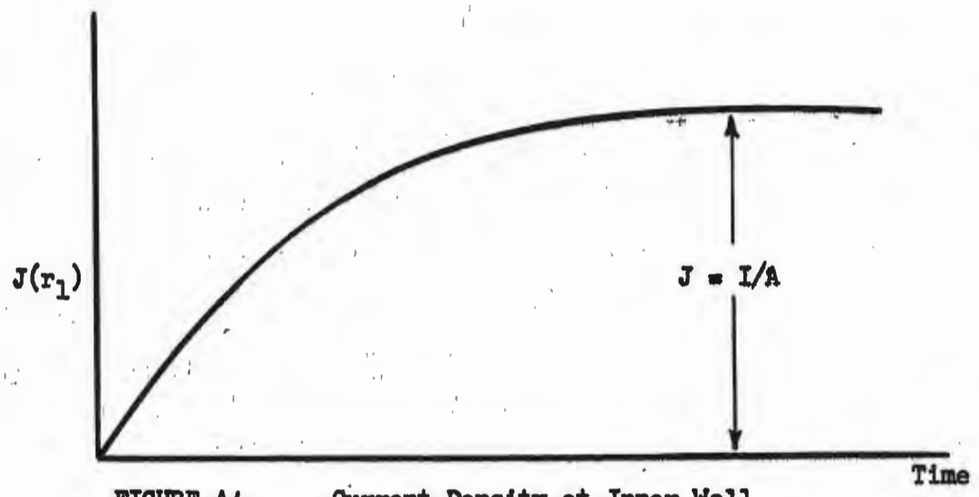

FIGURE A4. Current Density at Inner Wall

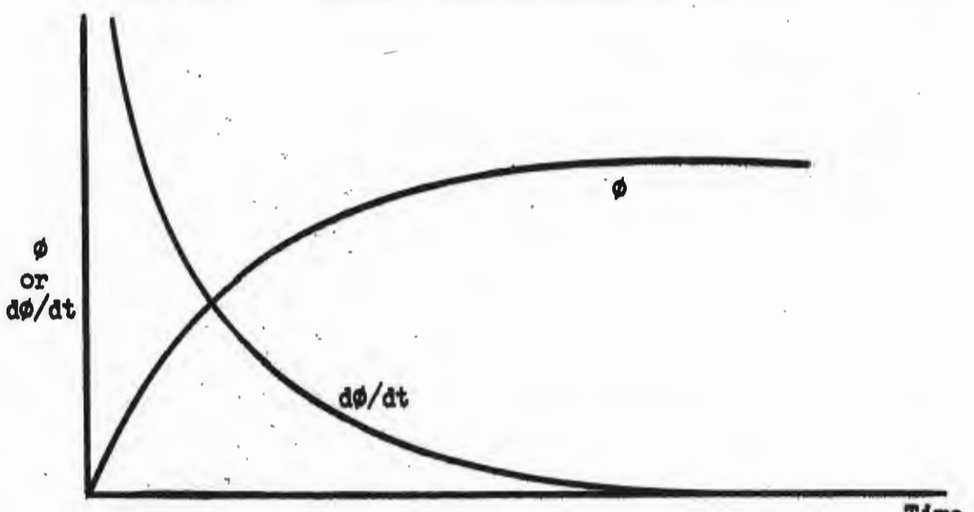

FIGURE A5. Flux within the Cylinder

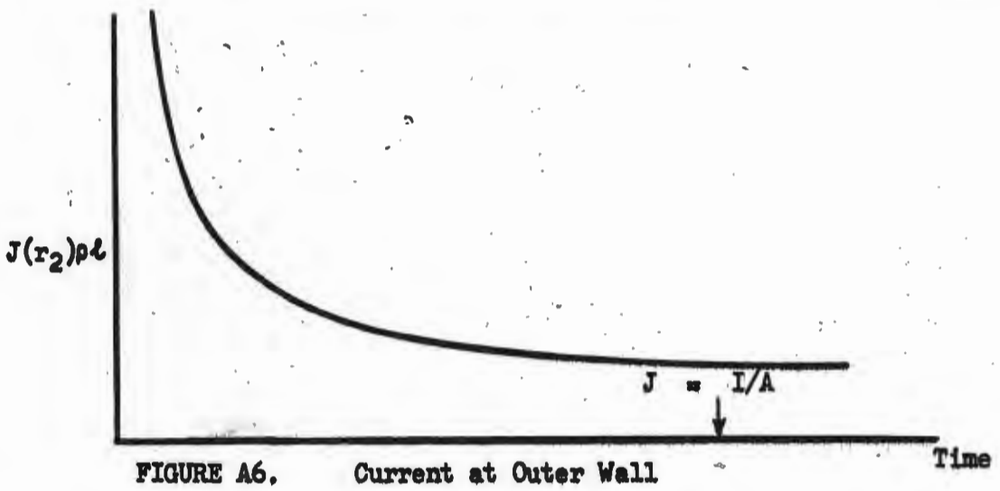

FIGURE A6. Current at Outer Wall

REFERENCES

1. Draft Copy, SURGE RESPONSE OF TYPICAL NIKE-X POWER SYSTEMS, 31 March 1967, I. B. Johnson, General Electric Company
2. Interim Summary Report, DEVELOPMENT OF DESIGN CRITERIA RELATING TO NEMP EFFECTS ON POWER SYSTEMS (U), 5 June 1965 - 5 September 1965 (SRD)
3. RESPONSE OF LOW RESISTANCE SHUNTS FOR IMPULSE CURRENTS, H. Witt, Electroteknik, 1960, pp. 45-47